Southern Plains Transportation Center
CYCLE 1

FINAL REPORT

2023–2024

USDOT BIL Regional UTC
Region 6

Next-Generation Permeable Pavement for Enhanced Durability and Functionality

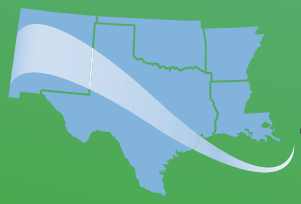

SOUTHERN PLAINS
TRANSPORTATION CENTER

Disclaimer

The contents of this report reflect the views of the authors, who are responsible for the facts and accuracy of the information presented herein. This document is disseminated under the sponsorship of the Department of Transportation University Transportation Centers Program, in the interest of information exchange. The U.S. Government assumes no liability for the contents or use thereof.

Technical Report Documentation Page

1. Report No. CY1-LSU-UARK-02	**2. Government Accession No.** [Leave blank]	**3. Recipient's Catalog No.** [Leave blank]
4. Title and Subtitle Next-Generation Permeable Pavement for Enhanced Durability and Functionality		**5. Report Date** 1/2025
		6. Performing Organization Code [Code]
7. Author(s) Dr. Mostafa A. Elseifi, https://orcid.org/0000-0003-2306-6873 Dr. Haitao Liao, https://orcid.org/0000-0003-1050-7086 Dr. Kofi S.S. Christie S M Tanvir Dr. José Carlos Azucena Nikesh Kumar		**8. Performing Organization Report No.** [Report No.] (Enter any/all unique alphanumeric report numbers assigned by the performing organization, if applicable.)
9. Performing Organization Name and Address Louisiana State University, Department of Civil and Environmental Engineering, Baton Rouge, LA 70803 University of Arkansas, Industrial Engineering Department, Fayetteville, AR 72701		**10. Work Unit No. (TRAIS)** [Leave blank]
		11. Contract or Grant No. 69A3552348306
12. Sponsoring Agency Name and Address Southern Plains Transportation Center 202 West Boyd St., Room 213B The University of Oklahoma Norman, OK 73019		**13. Type of Report and Period Covered** Final Report (09/23 – 1/25)
		14. Sponsoring Agency Code [Leave blank]

15. Supplementary Notes
Conducted in cooperation with the U.S. Department of Transportation as a part of University Transportation Centers (UTC) program.

16. Abstract
This study addresses the durability challenges of Open-Graded Friction Course (OGFC) by developing next-generation porous asphalt with improved mechanical, functional, and other properties. Modified OGFC mixes incorporating recycled waste materials, including steel slag, plastic waste, and reclaimed asphalt pavement (RAP), demonstrated enhanced performance and met key engineering criteria while reducing adverse impacts. Additional modifications, such as using highly modified asphalt (HiMA) and hydrated lime slurry, further improved resistance to raveling, cracking, and deformation. These enhancements ensured better durability and cost-effectiveness compared to conventional OGFC, contributing to extended pavement service life and reduced maintenance costs. OGFC's open-pore structure facilitates biodegradation of hydrocarbons like motor oil, making it effective for bioremediation and stormwater quality improvement. Unlike dense-graded asphalt, OGFC prevents hydrocarbon runoff contamination, offering strategic road construction solutions. The study also developed an AI-based design tool capable of predicting OGFC performance based on specified input variables, significantly reducing reliance on extensive laboratory testing. This user-friendly tool empowers engineers, especially in small communities, to make data-driven decisions, promoting durable and efficient road construction. Collectively, the study advances OGFC technology, aligning with optimal practices while ensuring economic viability and improved outcomes in Region 6.

17. Key Words [Open-graded friction course, recycled waste plastic, steel slag, reclaimed asphalt pavement, hydrated lime, highly modified asphalt binder]	**18. Distribution Statement** No restrictions. This publication is available at www.sptc.org and from the NTIS.

19. Security Classification (of this report) Unclassified	**20. Security Classification (of this page)** Unclassified	**21. No. of Pages** 89	**22. Price** N/A

Form DOT F 1700.7 (8-72) Reproduction of completed page authorized

NEXT-GENERATION PERMEABLE PAVEMENT FOR ENHANCED DURABILITY AND FUNCTIONALITY

Submitted by:
Dr. Mostafa A Elseifi
Dr. Haitao Liao
Dr. Kofi S.S. Christie
S M Tanvir
Dr. José Carlos Azucena
Nikesh Kumar

Affiliation:
Louisiana State University and the University of Arkansas

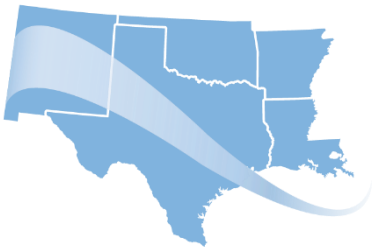

SOUTHERN PLAINS
TRANSPORTATION CENTER

Submitted to:
Southern Plains Transportation Center
The University of Oklahoma
Norman, OK

January 2025

Acknowledgments

The researchers of this study are appreciative of the financial support of the Southern Plains Transportation Center (SPTC). Furthermore, the authors would like to acknowledge the assistance of Sean Maher and Barry Moore of the Louisiana Department of Transportation and Development (LaDOTD).

Table of Contents

List of Tables

List of Figures

List of Equations

List of Abbreviations and Acronyms

AI	Artificial Intelligence
ANN	Artificial Neural Networks
AASHTO	American Association of State Highway and Transportation Officials
ASTM	American Society for Testing Materials
AV	Air Void
BBS	Bitumen Bond Strength
BOF	Basic Oxygen Furnace
CEI	Compaction Energy Index
DGHMA	Dense-Graded Hot-Mix Asphalt
EAF	Electric Arc Furnace
FDOT	Florida Department of Transportation
HDPE	High-Density Polyethylene
HiMA	Highly Modified Asphalt
HL	Hydrated Lime
HMA	Hot-Mix Asphalt
HWTT	Hamburg Wheel Tracking Test
ITS	Indirect Tensile Strength
LaDOTD	Louisiana Department of Transportation and Development
NCAT	National Center for Asphalt Technology
NMAS	Nominal Maximum Aggregate Size
OGFC	Open-Graded Friction Course
PAC	Porous Asphalt Concrete
RAP	Reclaimed Asphalt Pavement
RWP	Recycled Waste Plastic
SS	Steel Slag
TSR	Tensile Strength Ratio

Executive Summary

Porous asphalt pavement offers numerous benefits, such as improved visibility, enhanced wet-skid resistance, and reduced hydroplaning risk. Additionally, it has the potential to mitigate urban heat island effects and to improve stormwater quality by decreasing pollutants. However, the inferior durability of porous asphalt pavement poses a challenge for its widescale implementation. Durability issues of open-graded friction course (OGFC) include premature raveling, cracking, and stripping. Due to its inferior durability, OGFC deteriorates rapidly, necessitating its premature removal when these issues arise. Furthermore, voids are quickly filled by dust and debris, reducing long-term permeability and drainage benefits. On the other hand, managing large-scale industrial wastes such as plastic waste, reclaimed asphalt pavement (RAP), and steel slag is a major environmental concern. Recycling and reusing these waste materials in OGFC can significantly mitigate pollution, disposal issues, and reduce the environmental impacts of road construction.

The ultimate goal of this study is to develop and evaluate the next-generation of porous asphalt pavement by enhancing its desired mechanical, functional, and environmental properties. To achieve this objective, this study evaluated methods to improve OGFC durability and cost-effectiveness. Six OGFC mixes were tested, including a control mix with PG 76-22 binder and five modified OGFC mixes. Three of the modified mixes evaluated steel slag, recycled waste plastic, and reclaimed asphalt pavement (RAP) as partial replacements for the aggregate in the control mix. Additionally, one mix replaced the PG 76-22 binder with highly modified asphalt (HiMA) and another mix incorporated hydrated lime slurry as a modification. These mixes were evaluated for key performance indicators including permeability, resistance to cracking, moisture damage, rutting, and raveling. Binder bonding strength was also evaluated to assess adhesive strength of the different mixes.

Research activities also analyzed and quantified bio-remediation processes that may be used to hold and degrade oil and pollutant contaminants into less harmful forms through microbial degradation. Finally, based on the results of these laboratory tests, a cost-effectiveness analysis was conducted to determine the economic viability of implementing these modified OGFC mixes in practice. In addition, an artificial intelligence (AI)-based design tool was developed that may be used by mix designers and contractors to predict the performance of OGFC mixtures without the need for extensive laboratory testing.

Results demonstrated that the proposed modifications to OGFC mixtures significantly enhanced their performance and durability, ensuring better resistance to raveling, cracking, and deformation while maintaining the functional properties of the mix, such as permeability and drainage capacity. Furthermore, the modified OGFC mixes demonstrated superior cost-effectiveness compared to conventional mixes, offering a more durable and economically viable solution for road construction and maintenance. These improvements collectively contribute to extending the service life of pavements while reducing the frequency and costs associated with repairs and rehabilitation.

The incorporation of recycled waste materials, such as plastic waste, steel slag, and reclaimed asphalt pavement (RAP), into OGFC mixtures exhibited excellent laboratory performance, meeting key engineering criteria. Recycling and reusing these materials not only mitigate waste disposal challenges but also significantly reduce the environmental impact of road construction by diverting waste from landfills and decreasing the demand for virgin materials. This approach aligns with optimal construction practices, offering a dual benefit of environmental preservation and resource conservation.

This study confirmed OGFC's exceptional capacity to support biofilms, enabling its potential application in bioremediation. OGFC's open pore structure facilitates the degradation of hydrocarbons, such as motor oil, reducing contamination risks. In contrast, dense-graded asphalt's tight pore structure prevents oil penetration, increasing the likelihood of hydrocarbon runoff entering water streams and contaminating water supplies. Leveraging OGFC for biodegradation can significantly improve stormwater quality, making it a viable option for environmentally conscious road construction.

The development of an AI-based predictive tool allows engineers to estimate the performance of OGFC mixes, such as their durability and drainage properties, based on minimal input variables. This tool minimizes the need for extensive laboratory testing in the initial design phase, saving considerable time and financial resources. By simplifying the mix design process, this AI-driven approach empowers engineers, particularly in small communities, to make informed, data-supported decisions regarding pavement construction and maintenance. The tool is available as an executable file ready for use by any DOTs or researchers.

Chapter 1. Introduction

Porous Asphalt Concrete (PAC), also known as Open-Graded Friction Course (OGFC), is a special type of asphalt mix having a high air void content (between 18 and 24%) which offers some distinct benefits over most other traditional pavement surfaces, including significantly less rainwater accumulation on the pavement surface, enhanced visibility, improved wet skid resistance, reduced noise pollution from high speed vehicles and the elimination of the risk of hydroplaning (Chen et al. 2017; Watson et al. 2018; Abohamer et al. 2022). Additionally, it delivers minimized splash and spray from vehicles, and it can be utilized to reduce the impact of the urban heat island effect. Louisiana and Arkansas, which experience high rainfall and have a shallow groundwater table, could greatly benefit from the widespread adoption of OGFC, particularly if it delivers performance comparable to that of traditional dense-graded asphalt mixtures.

Despite all these advantages, there have been challenges in using OGFC as a surface course, mainly due to its shorter service life compared to conventional dense-graded asphalt mixes. The most critical problems of OGFC include premature durability (raveling and stripping) and clogging of voids by dirt, which result in lower durability and higher costs (Watson et al. 2018). Studies have shown that high air void (AV) content has a negative effect on OGFC durability (Abohamer et al. 2023). To ensure optimal performance of OGFC, it is necessary to develop appropriate solutions that address the current limitations.

Problem Statement

Porous asphalt pavement offers numerous benefits, such as improved visibility, enhanced wet-skid resistance, and reduced hydroplaning risk. Additionally, it has the potential to mitigate the urban heat island effect and to improve stormwater quality by decreasing pollutants. However, the inferior durability of porous asphalt pavement poses a challenge for its implementation. Durability issues of OGFC include premature raveling, cracking, and stripping. Due to its inferior durability, OGFC deteriorates rapidly, necessitating its premature removal when these issues arise. Furthermore, voids are quickly filled by dust and debris, reducing long-term permeability and drainage benefits. On the other hand, managing large-scale industrial wastes such as plastic waste, reclaimed asphalt pavement (RAP), and steel slag is a major environmental concern. Recycling and reusing these waste materials in OGFC can significantly mitigate pollution, disposal issues, and reduce the environmental impacts of road construction.

Research Objectives

The ultimate goal of this study is to develop and evaluate the next generation of porous asphalt pavement by enhancing its desired mechanical, functional, and environmental properties. The following objectives were achieved to improve the performance of porous asphalt pavement while addressing issues of the road infrastructure:

- Evaluate the effects of recycled plastic waste, reclaimed asphalt pavement, steel slag on OGFC mixture durability and functionality;
- Evaluate the effects of high-polymer modified asphalt binder and hydrated lime used as slurry on OGFC mixture performance;
- Evaluate production, cost, and constructability of OGFC mixes prepared with these additives.

- Analyze and quantify bio-remediation processes that may be used to hold and degrade oil and pollutant contaminants into less harmful forms through microbial degradation;
- Develop a computer tool to assist in the design of OGFC mixes.

Scope of Study

To achieve the goals of the research, several feasible alternatives were evaluated by modifying a state-approved and practically used OGFC mix, referred to as the Control Mix. The modifications included three mixes where the aggregate was partially replaced with steel slag, recycled waste plastic (RWP), and reclaimed asphalt pavement (RAP), respectively. Another mix was modified by replacing the PG 76-22 binder of the control mix with a highly modified asphalt (HiMA) and one mix used hydrated lime as a slurry in OGFC.

Modified mixes, in addition to the control mix, were assessed in the laboratory to measure the effects of the proposed modifications on their performance during three key stages: production, construction, and field performance. The selected laboratory test methods aimed at evaluating permeability, resistance to raveling, cracking, moisture damage, rutting, and binder adhesion strength.

A modular trickling-flow showerhead reactor was constructed to evaluate the retention of environmental contaminants and microbes within OGFC samples. The effects of OGFC on bio-remediation of contaminants were evaluated at varying concentrations and flowrates.

Finally, based on the results of these laboratory tests, a cost-effectiveness analysis was conducted to determine the economic viability of implementing these modified OGFC mixes in practice. In addition, an artificial intelligence (AI)-based design tool was developed, which may be used by mix designers and contractors to predict the performance of OGFC mixtures without the need for extensive laboratory testing.

Chapter 2. Literature Review

Benefits of OGFC and Its Application around the World

Due to the high content of air voids and large aggregate particle size, porous asphalt mixtures have high permeability and void saturation. This facilitates the ability of OGFC to channel water through the pavement structure. This also helps reduce the amount of water that stands on the pavement surface during wet weather, significantly improving the functional performance of OGFC compared to dense graded hot-mix asphalt (DGHMA) (Chen et al. 2017).

OGFC mixtures have unique characteristics that provide several advantages, which can be categorized into three main categories: (1) safety improvements, (2) driver benefits, and (3) environmental benefits. Porous asphalt mixtures are effective in reducing hydroplaning, even in conditions near saturation, which enhances safety on the road (Dell'Acqua et al. 2011). Studies conducted in India and the UK showed that using OGFC instead of DGHMA mixtures reduces splash and spray by 90 to 95%, thus improving visibility by 2.7 to 3.0 times (Nicholls 1999; Rungruangvirojn and Kanitpong 2010). Implementing OGFC has also shown its efficacy in enhancing pavement friction during unfavorable weather conditions. This results in decreased splashing and spraying from neighboring vehicles and reduced glare from approaching headlights in rainy weather. Moreover, it improves the visibility of pavement markings, thereby enhancing safety (Gu et al. 2018). Multiple studies have suggested that using OGFC mixture offers several benefits to the drivers. First, it allows for higher average speeds and traffic capacity. Second, it results in smoother pavement. Finally, it contributes to reduced fuel consumption.

Research has confirmed that OGFC plays a pivotal role in curbing vehicular accidents during wet weather, leading to a decline in the economic costs associated with these incidents. A study conducted by Shimeno et al. in Japan found that using OGFC significantly reduced the fatality rate during rainy weather by 4.6% as compared to the commonly used DGHMA (Shimeno et al. 2010). Another study conducted in 213 rain accident-prone sites nationwide in Japan showed that incorporating porous asphalt mixtures as surface layers decreased vehicle accidents by 85% (Takahashi 2013). When using OGFC mix, Louisiana observed a 100% reduction in fatalities and a 76% reduction in accidents (Rand 2004). Similarly, the city of San Antonio, Texas, reported a 51% reduction in major accidents on days with precipitation (King et al. 2013).

Traffic noise can be a nuisance to homes built near roads and negatively impact the quality of life. Most highway noise is caused by the interaction between tires and pavement, especially at speeds above 72 km/h (Donavan 2007). OGFC mixture has a high interconnected air voids content, which helps absorb sound energy generated from the tire-pavement interface. A study conducted by Bernhard et al. indicated that OGFC reduces the noise generated by tire/pavement by 3 to 6 dBA. This reduction is equivalent to diminishing the traffic volume by 50% or comparable to the construction of a noise barrier wall (Bernhard et al. 2005). Shimeno et al. also showed in their study conducted in Japan that the noise level on the road was approximately 3 dB lower in pavements using OGFC than DGHMA (Shimeno et al. 2010). The Netherlands utilizes porous asphalt mixtures in over 80% of their main road infrastructure network to efficiently control traffic-related noise (Van der Zwan 2011).

OGFC offers an additional environmental advantage of improved water runoff quality. Studies have shown that the amount of total suspended solids and lead present in water runoff from

OGFC mixture decreased by roughly 90% compared to water runoff generated by conventional Hot-Mix Asphalt (HMA) (Mitchell 2000; Eck et al. 2010).

Characteristics of OGFC Asphalt Mixtures

Selection of Materials, Gradation, and Binder Performance

OGFC mixtures have an open-graded aggregate structure, resulting in a coarser gradation than DGHMA. According to NCHRP 1-55, open graded aggregate gradation is required to achieve the high air voids content in OGFC mixture. This gradation is majorly comprised of coarse aggregate that allows the mixture to maintain stone on stone contact and form a stone skeleton. Although specifications do not specify aggregate minerology, properties and type of aggregate are critical in forming the stone skeleton. While the coarse aggregate ensures stone-on-stone contact, the fine aggregate and stabilizing agent help in maintaining the mix's stability and cohesion (Watson et al. 2018).

The gradation of aggregate in OGFC mixes also plays a critical role in determining their structural and functional performance. While using a high proportion of coarse aggregate influences the porosity of OGFC, minimizing the proportion of fine aggregate promotes better contact between the stones, prevents coarse aggregate particles from separating, and ensures that air voids are not compressed. The nominal maximum aggregate size (NMAS) is defined as "one sieve size larger than the first sieve to retain more than 10 percent of the material." In a study conducted by Hasan et al., the effects of aggregate gradation on the performance of OGFC were evaluated. The study investigated three different OGFC mixes with varying NMAS sizes; 14 mm, 20 mm, and 25 mm. The performance of each mix was evaluated based on the Cantabro test and ITS test. Results showed that as the NMAS size increased, a higher AV content was observed in the mix. Additionally, it was observed that the Cantabro loss value increased with the increase of AV content in the specimens (Hasan et al. 2013). A summary of the current aggregate property requirements is provided in Table 1, which compares the standards outlined in ASTM D7064 with those in AASHTO PP 77.

When determining the binder content for OGFC mixes, three properties are typically taken into consideration: binder draindown, durability, and air void content. The maximum limit of binder content (BC) in OGFC is determined by the potential of binder draindown, which helps prevent bleeding and short-term raveling. To ensure long-term durability, the Cantabro abrasion test (AASHTO TP 108) is commonly used to determine the minimum binder content required. Cantabro abrasion test is also used as a standard method to evaluate the durability of OGFC mix. Cantabro specimens are categorized as either unaged, aged or moisture-conditioned before testing. According to ASTM D 7064, unaged specimens should have a maximum stone loss of less than 20% and aged specimens should have a maximum stone loss of less than 30% (Watson et al. 2018).

Once the upper and lower limits of binder content have been established from the draindown potential and Cantabro abrasion test, the binder content is selected to meet the minimum air voids requirement, which usually ranges from 18 to 24% in the United States.

Table 1. Aggregate Requirement for OGFC Mix (Watson et al. 2018)

Aggregate Type	Test Description	Method	ASTM Min	ASTM Max	AASHTO Min	AASHTO Max
Coarse	Los Angeles Abrasion, % Loss	AASHTO T 96	-	30	-	30
Coarse	Flat or Elongated, % (5 to 1)	ASTM D 4791	-	10	-	10
Coarse	Soundness (5 cycles) - Sodium Sulphate	AASHTO T 104	-	-	-	10
Coarse	Soundness (5 cycles) - Magnesium Sulphate	AASHTO T 104	-	-	-	15
Coarse	Uncompacted Voids	AASHTO T 326 (Method A)	-	-	45	-
Fine	Soundness (5 cycles) - Sodium Sulphate	AASHTO T 104	-	-	-	10
Fine	Soundness (5 cycles) - Magnesium Sulphate	AASHTO T 104	-	-	-	15
Fine	Uncompacted Voids	AASHTO T 304 (Method A)	40	-	45	-
Fine	Sand Equivalency	AASHTO T 176	45	-	50	-

Durability Issues and Proposed Solutions

Although OGFC has been used for its multiple benefits since the 1970s, its performance has varied significantly due to the difference in materials selection, design, construction, maintenance, and especially durability. Concerns about its durability and service life have caused its usage to decrease recently. A survey conducted by the National Center for Asphalt Technology in 2015 revealed that only half of the responding agencies (40 states and Puerto Rico) utilized OGFC mixture. The widespread use of OGFC is hindered by issues related to durability and functionality, including raveling, clogging, and winter maintenance (Fay and Akin 2014; Zhang and Leng 2017).

The primary types of failure encountered by OGFC are rutting, raveling, cracking, and moisture damage. Wu et al. discussed these distress types while emphasizing the durability and functionality of OGFC. The rutting potential of OGFC is typically assessed using the loaded wheel test (Wu et al. 2020). The rutting mechanisms generally fall into three categories: (1) loss of materials, (2) densification, and (3) lateral plastic flow. For DGHMA, the rutting test is conducted at a temperature of 64°C, following the procedures outlined in AASHTO TP 63-09. The targeted air void content for DGHMA is 7 ± 1%. The thickness of the OGFC layer significantly influences its rutting performance, and gradations with a larger proportion of coarse aggregate generally exhibit superior rutting resistance. The Hamburg wheel-tracking test (HWTT) is used for the determination of asphalt mixture resistance to permanent deformation. In Louisiana specifications, the rutting performance criterion for OGFC with PG 76-22 is a maximum rutting depth of 0.50 in. (12.50 mm) after 5,000 passes. However, according to NCHRP 1-55, OGFC maximum rut depth after 20,000 passes should not exceed 0.50 in. (12.50 mm) (Watson et al. 2018).

According to NCHRP project 1-55 report, raveling is defined as the loss of aggregate at the pavement surface caused by repeated abrasion from traffic, exacerbated by moisture. This distress is associated with deficient asphalt binder film thickness and loss of adhesion at the binder-aggregate interface due to both excessive aging and moisture damage. To resist asphalt aging and raveling damage, preventive maintenance such as fog seal application should be employed to extend the pavement's service life. Moisture damage is majorly caused due to the presence of unique pore structure in OGFC, and micro-cracks can form under the combined effects of traffic loading and environmental factors. Water infiltrates these micro-cracks during freeze-thaw cycles, leading to adhesive failure at the binder-aggregate interface. As water expands within these cracks during freezing, it causes failure in the stone-to-stone contact regions after repeated frost-thaw cycles. Moisture damage is often accompanied by other distresses, such as raveling and aging, exacerbating their severity and extent. Moisture susceptibility is typically evaluated using parameters such as indirect tensile strength (ITS) and tensile strength ratio (TSR). TSR refers to the ratio of the average ITS of the wet-conditioned subset to the average ITS of the dry-conditioned subset, tested at a temperature of 25 ± 1°C. AASHTO PP 77 criterion specifies a retained tensile strength of 0.70, while ASTM D7064 standard requires a minimum TSR value of 0.80 (Watson et al. 2018).

In Alabama, OGFC pavements displayed premature distress, like raveling after six or seven years of service. As a result, Alabama Department of Transportation (ALDOT) restricted using OGFC as it failed prematurely (Xie et al. 2019). The durability of OGFC is influenced by the materials used, design, construction procedure, and maintenance programs. In addition, OGFC lifespan is also affected by traffic loading and environmental factors such as water, oxygen, ultraviolet radiation, etc. According to a study by Chen et al., the durability of OGFC deteriorates rapidly due to a reduction in effective air void, called clogging (Chen et al. 2017). There are two types of clogging: particle-related and deformation-related. Particle-related clogging occurs when contaminants such as dust, debris, tire wear particles, and other pollutants accumulate within the pores or voids of an OGFC mix. Deformation-related clogging refers to a reduction in the OGFC mixture's air voids content due to the accumulation of permanent or rutting deformation (Abdullah et al. 1998).

OGFC mixtures are also prone to draindown, but adding fibers or ground tire rubber (GTR) and using warm mix asphalt (WMA) can help prevent this issue. Draindown can be managed through testing and by avoiding extended storage time in the silo. It is important for the asphalt plant to carefully regulate and monitor the addition of fibers, hydrated lime, and other additives. OGFC has higher air voids than dense-graded mixtures, so over-compaction must be avoided. On the other hand, under-compaction of OGFC can worsen durability issues like raveling. Compaction is usually conducted using static steel wheel rollers. Because OGFC mixtures are thin layers, maintaining consistent temperature and balanced paving operations are important during the construction phase. Consistent temperature and paving speed help reduce the risk of under-compaction of OGFC. Additionally, proper tack coat application ensures bonding between the OGFC and the underlying layer of the pavement (Gilliland et al. 2022).

Monitoring multiple factors that contribute to the strength and durability of OGFC is critical. These factors include the gradation of the aggregate, the amount of asphalt utilized, the degree of aging, and the thickness of the layer. To ensure adequate durability of OGFC surfaces, testing various mixtures is essential by modifying these factors. Two factors that have a significant impact on the overall durability of OGFC are aggregate gradation and layer thickness. According to Aschenbrener et al., the durability and long-term functionality of OGFC pavement depend largely on its permeability. This is because the number of interconnected voids present in the pavement has a direct impact on its in-place permeability. In particular, the

quantity, size, orientation, and interconnectivity of air voids serve as critical indicators of a pavement's permeability characteristics (Aschenbrener 1995).

Abohamer et al. conducted several tests including the Cantabro test, Hamburg wheel-tracking test, Texas overlay test, Modified Lottman, and boil tests to evaluate the durability, permanent deformation, cracking, and moisture-damage resistance of OGFC mixes. Their results indicated that using WMA technologies improved OGFC durability and performance (Abohamer et al. 2022). Polymer and rubber-modified binders enhanced bonding with aggregate, reduced draindown, and improved moisture resistance, leading to better OGFC properties and longer service life. Punith et al. found that using plastic fibers such as cellulose and synthetic fibers reduced the draindown effect, which improved OGFC pavement durability (Punith et al. 2011). Based on the study conducted by Song et al., the appropriate choice of tack coat type and application rate can effectively enhance the bonding between OGFC layers and the underlying layers, resulting in a monolithic system that can improve the durability of OGFC (Song et al. 2015). The aforementioned studies show that OGFC mixes have extensive benefits, making them a promising pavement material for the future. However, further research is needed to promote better understanding of the material, durability, and behavior.

Use of Recycled Waste Plastic in Asphalt Mixtures

The significant amount of plastic waste currently being produced has raised concerns about its safe recycling and reuse. This is especially worrying as plastic particles have the potential to be toxic and easily enter the food chain. Regrettably, only a small fraction of plastic waste is currently being recycled in countries such as the United States and Australia. However, the plastic recycling rate in the United States has fallen to 5 to 6% in 2021, down from 8.7% in 2018, while plastic waste generation continues to increase, as reported by the Environmental Protection Agency (EPA) (Volcovici 2022). One promising solution to reduce plastic waste is to incorporate it into construction, particularly for road applications. This can be achieved by modifying the asphalt mixture with recycled waste plastic (RWP), which majorly consists of aggregate and asphalt binder, effectively lowering the final cost of the mixture. Moreover, substituting waste plastics for virgin polymers can significantly reduce costs. Apart from the economic benefits, there is a growing societal concern about the use of plastic waste, particularly since China's 2018 ban on importing recyclable waste from developed countries (Walker 2017). Therefore, it is imperative to adopt optimal strategies.

The utilization of recycled waste plastics in asphalt modification has been a topic of interest for researchers since the 1990s. Various plastic types, including high-density polyethylene (HDPE), low-density polyethylene (LDPE), polypropylene (PP), polyethylene terephthalate (PET), ethylene–vinyl acetate (EVA), polyvinyl chloride (PVC), polyethylene (PE), and polyethylene terephthalate (PTP), have been subject to investigation, with findings revealing that the inclusion of plastic waste in asphalt may enhance performance criteria such as rutting resistance, fatigue resistance, and stiffness. However, the literature presents conflicting results due to variations in samples, inadequate mixing conditions, insufficient temperature control, and experimental inaccuracies.

Considering the method used to introduce waste plastic into the mixture is essential. Researchers have classified these methods into dry and wet processes (Heydari et al. 2021). In the dry process, heated binder is added to a mixture of hot aggregate and plastic, which is more suitable for rigid plastic with high melting points. In contrast, in the wet process, plastic is mixed with hot binder, which is then combined with the aggregate. This technique is more fitting for plastics with low melting points. To achieve a uniform and well-dispersed asphalt binder, plastic

must be finely powdered or well-shredded before blending with the binder at high temperature and mixing speed. Several studies have been conducted to evaluate the performance of modified samples prepared using both dry and wet processes.

A study conducted by Hassani et al. investigated the possibility of using recycled waste plastic as a substitute for a portion of the aggregate in asphalt mixtures. The research revealed that the Marshall stability and Marshall quotient of the samples were similar to those of the control samples, meeting practical use requirements (Hassani et al. 2005). A study by Radeef et al. developed an enhanced dry process of asphalt mixture modification where waste plastic accounts for 20% of the weight of the asphalt binder (Radeef et al. 2021). The purpose of the study was to improve the consistency of the dry mixing process of RWP. The study compared the control asphalt mixture to two RWP modified asphalt mixtures prepared using a conventional dry process (PMIX-C) and a modified dry process (PMIX-E). PMIX-C involved a single step of mixing plastic with heated aggregate before adding the binder, whereas PMIX-E involved a more detailed process with initial plastic coating of coarse aggregate followed by partial asphalt binder integration to enhance plastic digestion and coating. Crushed granite aggregate with a nominal maximum size of 14mm was used. The RWP was derived from polymer-based waste material (low-density polyethylene) and was in the form of shredded plastic bags ranging between 5 to 10mm. The researchers evaluated the moisture damage, resilient modulus, creep deformation, and rutting performance of the mixes. The enhanced dry process developed in this study showed significant improvement in asphalt performance, particularly with the addition of 20% RWP to the weight of the asphalt binder. In Figure 1, the results of the ITS and TSR test for unconditioned and wet-conditioned mixtures are illustrated.

The results shown in Figure 1 indicate that the ITS values in dry conditions at the end of the loading test were higher for PMIX E and the control mixture compared to wet conditions. However, PMIX-E displayed higher values of TSR and ITS in both dry and wet conditions, by about 6%, 8%, and 12%, respectively. This observation suggests that PMIX-E was less susceptible to moisture damage due to the influence of the plastic coat on the aggregate surface, which prevented water diffusion between the aggregate and the asphalt binder. In contrast, for PMIX-C, the presence of non-molten plastic waste particles increased the air voids content, leading to a less satisfactory performance against moisture damage.

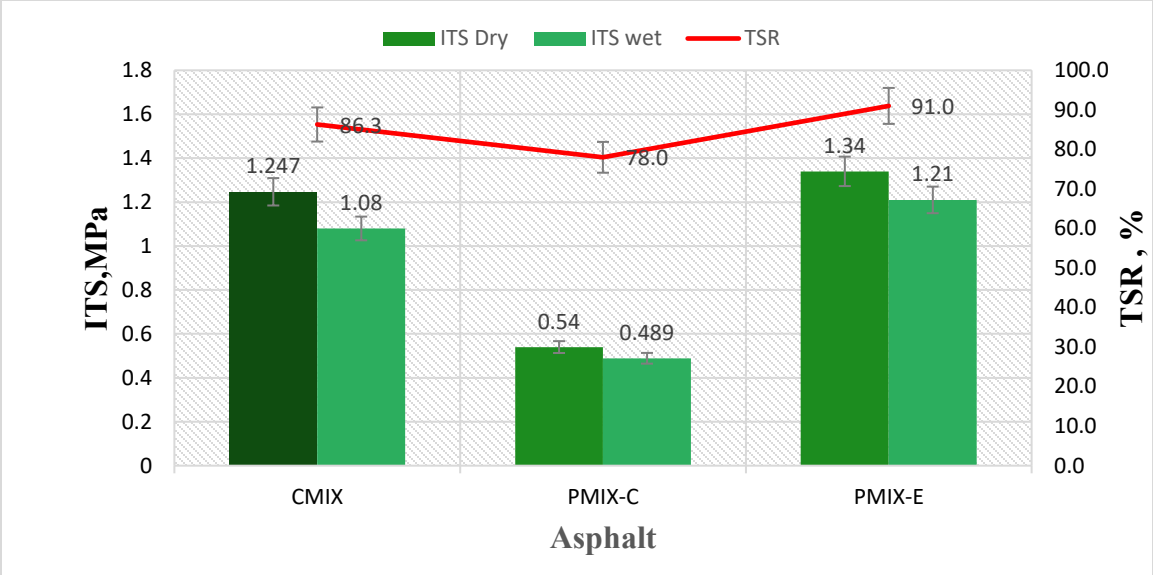

Figure 1. TSR and Tensile Strength Value of the Control, PMIX-C and PMIX-E Mixtures (Radeef et al. 2021)

Plastic particles were found to increase the available area to be covered by the asphalt film, resulting in insufficient asphalt aggregate coating. A high air void content also allowed water to infiltrate the macro-pores and wash away the asphalt binder film that coated the aggregate. PMIX-E outperformed PMIX-C and the control mixtures, demonstrating low vulnerability to moisture damage and strong resistance to both elastic and permanent deformation. The plastic-coated aggregate surface acted as a barrier, preventing water intrusion between the asphalt and aggregate, thereby minimizing stripping. The modified asphalt around the coated aggregate enhanced the adhesive and cohesive properties of the mixtures, leading to up to a 35% improvement in resistance to permanent deformation. Similarly, under dynamic loads, incorporating RWP using the modified method also enhanced the rutting resistance of the control mixture by up to 60%.

Rahman and Wahab's research showed that integrating recycled waste plastic into modified asphalt mixture as a partial replacement for fine aggregate (sieve size ranging from 2.36 to 1.18mm) can enhance the mixture's permanent deformation properties (Rahman and Wahab 2013). The study focused on assessing the optimal quality and impact of using recycled PET obtained from used plastic bottles by determining the permanent deformation and stiffness behavior of modified asphalt mixtures. Modified asphalt mixtures produced for this research had the concentrated content of recycled PET pallets between 5 and 25% of the asphalt mixture's weight. The test samples underwent a Repeated Load Axial Test (RLAT) with a 100 kN axial load applied for 1800 cycles to measure the permanent deformation of the modified asphalt mixture. Additionally, an Indirect Tensile Stiffness Modulus Test (ITSM) was conducted to evaluate the stiffness of the modified asphalt mixture. Figure 2 presents the results of the Repeated Load Axial Test (RLAT) to determine the permanent deformation of the modified asphalt mixture.

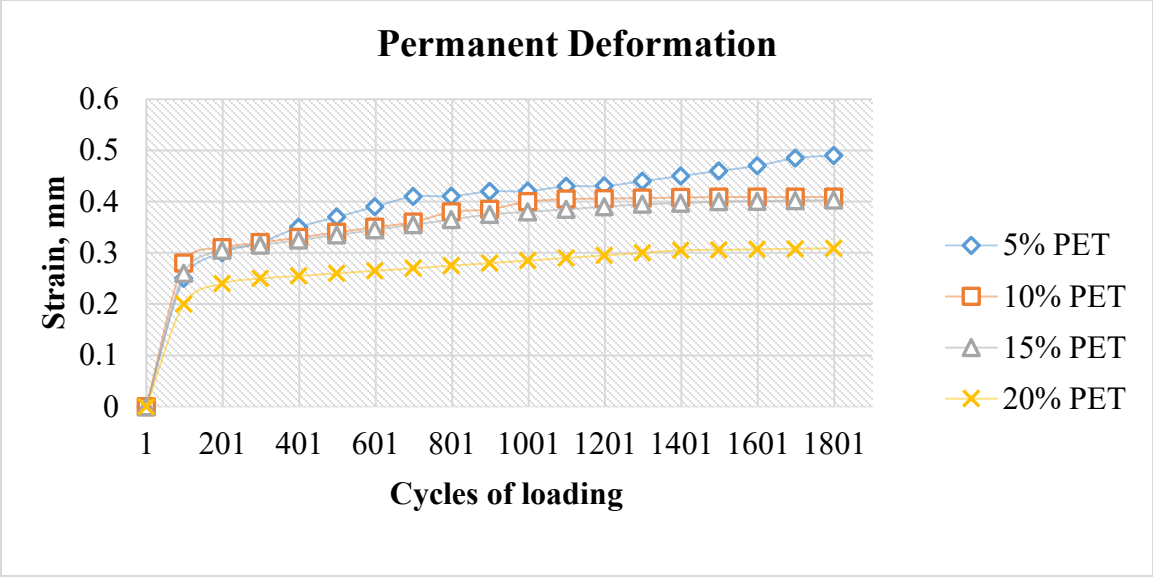

Figure 2. Permanent Deformation Properties of Control Sample and PET Modified Asphalt Mixtures (Rahman and Wahab 2013)

From the results illustrated in Figure 2, it can be observed that utilizing PET-modified asphalt enhanced the asphalt mixture's permanent deformation resistance. This study indicated that the least amount of permanent deformation was observed when the asphalt mixture incorporated a 20% recycled PET replacement. Moreover, PET-modified asphalt experienced only half of the permanent deformation of non-modified asphalt after 1,800 cycles. According to these results, recycled PET had shown a significant recovery after 1,800 cycles, when subjected to a loading time of 1 hour at a temperature of 30ºC. The study concluded that the PET-modified asphalt mixture is capable of withstanding road failures while improving the overall performance and service life of the road. The study also concluded that using a 20% PET-modified asphalt mixture is a feasible solution for constructing road pavements, considering its environmental and economic benefits. However, this study also showed that the stiffness of the mixture is reduced when compared to an unmodified asphalt mixture.

A study conducted by Genet et al. demonstrated that the incorporation of 6.5% of waste low-density polyethylene (LDPE) plastic into an asphalt mix resulted in a 33.7% higher stability value compared to the non-modified version (Genet et al. 2021). As per Mazouz and Merbouh's research, modification of HMA with LDPE resulted in a pronounced improvement in both stiffness and creep deformation resistance. The study highlighted that optimal thermo-mechanical performance can be achieved with a 5% LDPE blend. Furthermore, this ratio led to a reduction in overall deformation by 51% and 13% at 20°C and 50°C temperatures, respectively (Mazouz and Merbouh 2019).

Elnaml et al. reported that the addition of 3% HDPE to asphalt mixtures met the cracking threshold requirements set by the Louisiana Department of Transportation and Development (LaDOTD) for high-traffic volume roads (Elnaml et al. 2023). Their study aimed to investigate the performance of asphalt mixture containing post-consumer recycled plastic waste materials, specifically high-density polyethylene (HDPE), and compared its performance with two conventional mixtures. Mixtures 1 and 2 included SBS-modified asphalt binders PG 76-22 and PG70-22, respectively, as specified by LaDOTD. The third asphalt mixture contained PG 67-22

and 3% HDPE by weight of the asphalt binder. Asphalt binders' high and intermediate temperature performance grading, bending beam rheometer (BBR) test, and multiple stress creep recovery (MSCR) test were conducted on the studied modified asphalt binders to characterize the rheological properties. The mechanical test methods on the asphalt mixtures included stiffness, permanent deformation (LWT rutting test), moisture damage (moisture induced stress tester), fracture and fatigue resistance (semi-circular bending), and durability (Cantabro test).

The test results showed that the asphalt binder modified with HDPE plastic waste material graded as PG 70-22 exhibited similar rheological properties as SBS-modified PG 70-22 asphalt binder. The asphalt mixture with HDPE exhibited greater stiffness than conventional mixtures. In terms of permanent deformation, the modified mixture provided comparable rutting resistance to traditional mixtures, meeting LaDOTD's maximum threshold of 6 mm for level 2 traffic (ESALs > 3 million). Adding recycled HDPE plastic waste to the asphalt improved both moisture and cracking resistance compared to conventional mixtures. Long-term field cracking predictions from AASHTOWare Pavement ME software (v.1.1.6) indicated that the pavement structure with an HDPE-modified wearing course layer demonstrated statistically similar cracking resistance to that of conventional asphalt. These findings suggest that incorporating recycled plastic waste in asphalt modification is a viable approach for optimal pavement technologies, offering environmental and economic advantages.

Use of Recycled Waste Plastic in OGFC

OGFC mixtures containing reclaimed polyethylene (PE) fibers sourced from low-density polyethylene (LDPE) tote bags exhibited enhanced tensile strength, greater resistance to permanent deformation, fatigue-induced damage, and moisture susceptibility compared to mixtures prepared without fibers. Based on the findings of Kar et al., the OGFC mixture that was modified with 6% waste polyethylene (by weight of the mixture) met the key requirements for draindown, Cantabro loss, and moisture susceptibility tests. The research suggests that incorporating waste polyethylene can significantly enhance the performance of OGFC (Kar et al. 2024).

Based on the research conducted by Al-Busaltan et al., the introduction of Recycled Low-Density Polyethylene (R-LDP) into OGFC was effective in improving OGFC mixture properties to meet the required specifications (Al-Busaltan et al. 2020). The study aimed to minimize costs and maximize durability. It investigated the effect of using recycled R-LDP as an asphalt modifier on the performance of OGFC asphalt mixtures. The study evaluated changes in mixture air voids, porosity, draindown, permeability, rut depth, moisture damage, and abrasion loss to evaluate the effect of RWP. Although the results showed that R-LDP modification increased mixture air voids, porosity, and permeability by 15, 10, and 40%, respectively, these properties fell within the required ranges by the specifications (ASTM D7064 and D7064M). Furthermore, R-LDP modification noticeably contributed to reducing rut depth, moisture damage, and abrasion loss (both unaged and aged) by 31, 20, and 40%, respectively. Figure 3 shows the final rut depths (RD) obtained from the wheel track test on both a reference asphalt mixture and a R-LDP modified asphalt mixture.

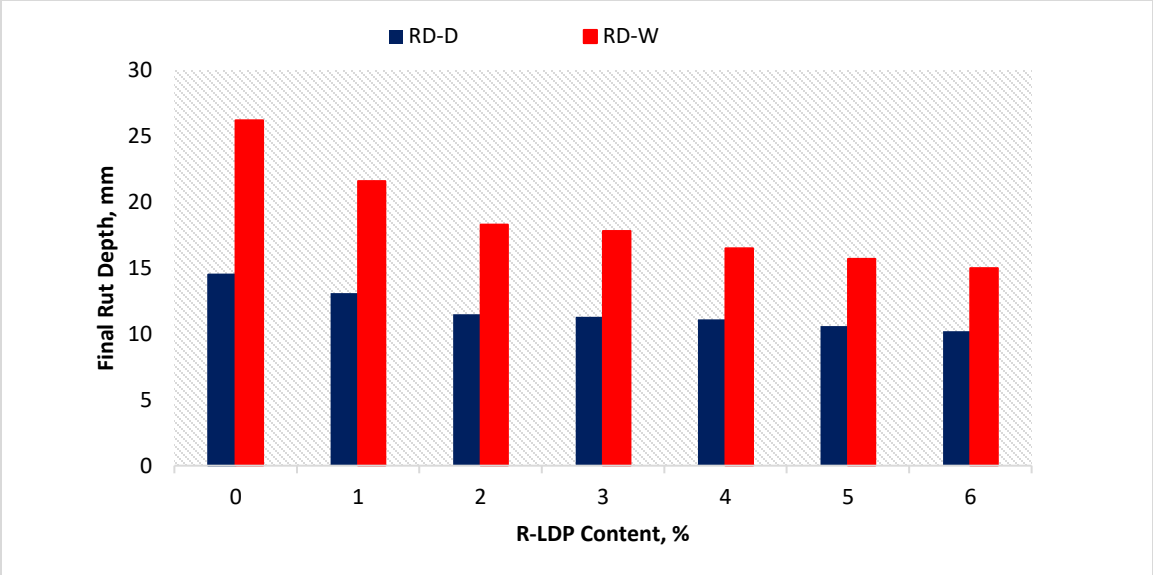

Figure 3. Variation in Final Rut Depth for Different Levels of R-LDP Contents in OGFC Mixtures for Dry and Wet Conditions (Al-Busaltan et al. 2020)

Rutting test results presented in Figure 3 indicate that the OGFC mixture's resistance to permanent deformation was directly proportional to the level of modification. The higher the dosage of the R-LDP additive, the lower the potential for rutting in the OGFC mixtures. However, the strengthening effect of R-LDP on the OGFC mixture decreased as the dosage level increased. It is also evident from the comparison of the results under dry and wet conditions that the OGFC mixtures in this study were sensitive to moisture. The rut depth of the reference mix (RM) was nearly twice as high under wet conditions compared to dry conditions. Even though the use of R-LDP reduced the water susceptibility of the OGFC mixtures under dry conditions, its impact was more significant for the samples under wet conditions. Therefore, it can be concluded that using R-LDP not only improves the mixture's resistance to repeated loading but also significantly mitigates the OGFC mixture's susceptibility to moisture damage. Additionally, this study showed that the modification significantly decreased abrasion loss (both unaged and aged) and practically eliminated the issue of draindown. Overall, incorporating R-LDP proved effective in improving OGFC mixture properties to an acceptable level required by most specifications. Hence, the inclusion of R-LDP proved to be a highly effective means of enhancing OGFC mixture properties, meeting required performance according to most specifications.

Use of Reclaimed Asphalt Pavement in Asphalt Mixtures

According to FHWA, reclaimed asphalt pavement (RAP) is a term used for pavement materials that contain asphalt and aggregate, which have been recycled and/or reprocessed. These materials are generated when asphalt pavements are removed for reconstruction, resurfacing, or to obtain access to buried utilities. RAP consists of aggregate coated by asphalt cement that is extracted from damaged existing road surfaces (FHWA 2016). Since the 1930s, RAP has been utilized to curtail road construction expenses and mitigate problems associated with asphalt disposal, as well as to conserve natural resources. According to the Federal Highway Administration, a staggering 40 million tons of RAP are recycled each year, making it the most commonly recycled material in the United States (FHWA 2011). The use of RAP in asphalt pavements offers both economic and environmental advantages. By reducing the need for virgin

materials, minimizing construction waste, and optimizing natural resources, RAP promotes optimization in the industry through a cycle of reuse. The methods to ensure adequate pavement performance despite the aged and stiff binder include using rejuvenating or softening additives, a softer virgin binder grade, and increasing the total mixture binder content (Copeland 2011).

Hajj et al. conducted a study to assess how the source and content of RAP affected the properties of HMA in terms of moisture sensitivity, resistance to rutting, fatigue cracking, and thermal cracking (Hajj et al. 2009). The study used three sources of RAP, one source of virgin aggregate, and one source of virgin asphalt binder to create HMA mixes with two target asphalt binder grades. The three RAPs used in this study were chosen from three different local sources in Reno, Nevada. The study examined two types of mixes: a PG64-22/Type 2C and a PG64-28/Type 2C. Each mix was assessed at three RAP contents of 0, 15, and 30% using the three different RAP sources. The performance of the control and RAP mixes was assessed in terms of their resistance to moisture damage, rutting, fatigue, and thermal cracking. The findings of the experimental program are summarized in Table 2 for different mixes prepared with different RAP contents.

Table 2. Comparison of Asphalt Mixes with Varying RAP Contents (Hajj et al. 2009)

Binder Grade	RAP Source	RAP Content (%)	Moisture Resistance	Rutting Resistance	Fatigue Resistance	Thermal Cracking Resistance
PG 64-22	I	15	Pass	Worse	Better	Same
PG 64-22	I	30	Pass	Worse	Worse	Better
PG 64-22	II	15	Pass	Better	Same	Better
PG 64-22	II	30	Pass	Worse	Worse	Better
PG 64-22	III	15	Pass	Better	Better	Same
PG 64-22	III	30	Pass	Better	Better	Better
PG 64-28	I	15	Fail	Same	Worse	Better
PG 64-28	I	30	Pass	Same	Worse	Better
PG 64-28	II	15	Pass	Same	Worse	Better
PG 64-28	II	30	Pass	Same	Worse	Better
PG 64-28	III	15	Pass	Same	Worse	Better
PG 64-28	III	30	Pass	Same	Worse	Better

From the data presented in Table 2, the study found that overall, adding RAP to a mixture led to acceptable moisture resistance. In most cases, the mixture with added RAP showed equivalent or better resistance to rutting compared to the control mix (0% RAP). Depending on the RAP source and content, adding RAP to a mixture with an unmodified target asphalt binder either improved or worsened fatigue resistance. However, adding RAP to a mixture with a polymer-modified asphalt binder consistently led to worse fatigue resistance, regardless of the RAP source and content. Lastly, adding RAP to a mix resulted in similar or better resistance to thermal cracking compared to the virgin mix.

Al-Shabani and Obaid showed in their experiment that using RAP and polymer-modified asphalt binder significantly improved the performance of asphalt mixtures by enhancing their durability and resistance to cracking, as well as reducing moisture damage (Al-Shabani and Obaid 2023). For their research, Al-Shabani et al. established a standard reference mix for comparison and other mixtures with different quantities of RAP at various percentages. The Marshall test for stability and the indirect tensile strength test were performed in their experiment to evaluate the mechanical properties of the mixtures. Figure 4 (a and b) shows the Marshall stability of the

mixes and the tensile strength ratio. These mixes contained RAP at a percentage of 15, 30, and 45% of the mixture by weight of the aggregate.

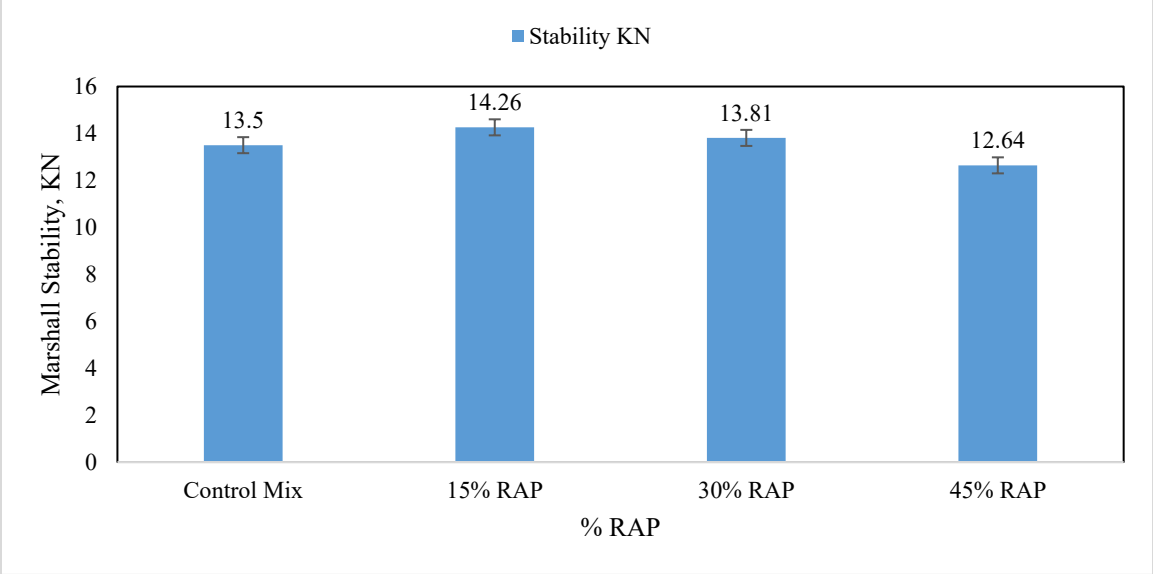

(a)

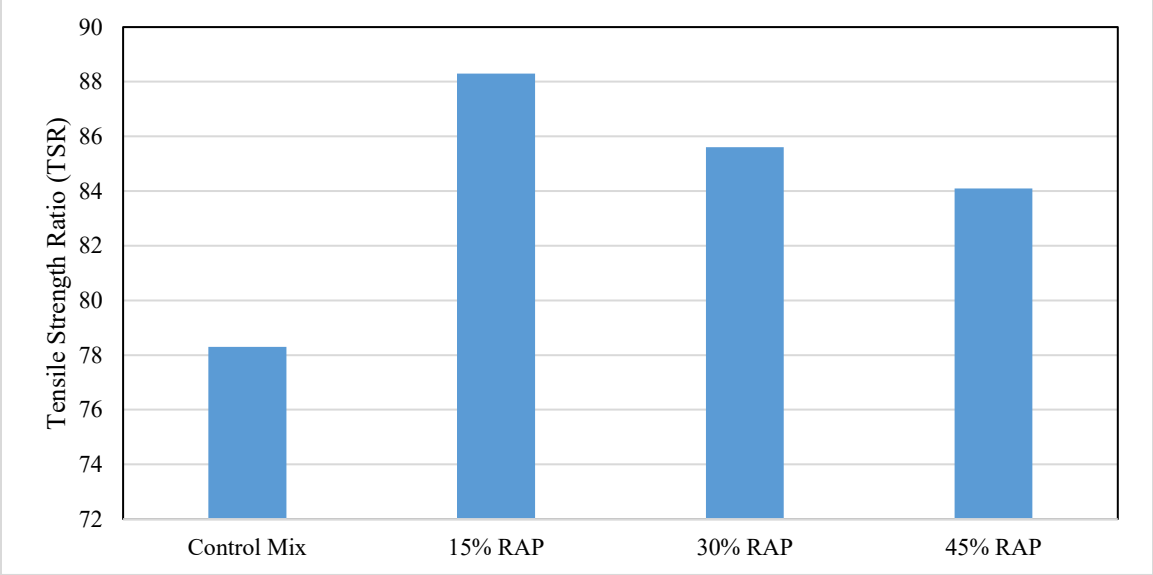

(b)

Figure 4. The Impact of RAP Content on (a) the Marshall Stability of HMA and (b) TSR (Al-Shabani and Obaid 2023)

The results in Figure 4 show that the optimal RAP ratio for achieving the highest stability and TSR is 15%. It can also be seen from the figures that, compared to the control mix, the addition of RAP to the mixture improved both the stability and resistance to moisture susceptibility of the mixtures in most cases. This is because RAP contains an aged asphalt binder that has undergone oxidative hardening, which makes it stiffer. Incorporating RAP into HMA enhances

the mix's overall stability by increasing its stiffness and lowering its vulnerability to rutting and deformation. Additionally, the more porous surface created by RAP improves drainage, minimizing water retention within the pavement structure and reducing the risk of early deterioration. The study concluded that using RAP contributes to the mix by decreasing the need for virgin materials.

Studies conducted by Anusha et al. have demonstrated a promising strategy for reducing the cost of asphalt mix by incorporating RAP as a replacement for traditional aggregate, and it was found in their research that RAP can be used as a substitute for up to 30% of the conventional aggregate in open graded mixes (Anusha et al. 2019). To assess whether RAP can be used effectively in open graded mixes, various tests were carried out, including the rutting test, as well as the indirect tensile test and fatigue test. Figure 5 presents the results obtained from the rutting test in their experiment.

Results presented in Figure 5 illustrate that for the mixture with 30% replacement of the aggregate with RAP, the rutting depth was found to be 5.1 mm, which was reached after 10,000 passes. In comparison, the conventional mix required 8,000 passes to reach the same depth. This indicates that the mixtures containing 30% RAP had higher resistance against rutting compared to conventional mix.

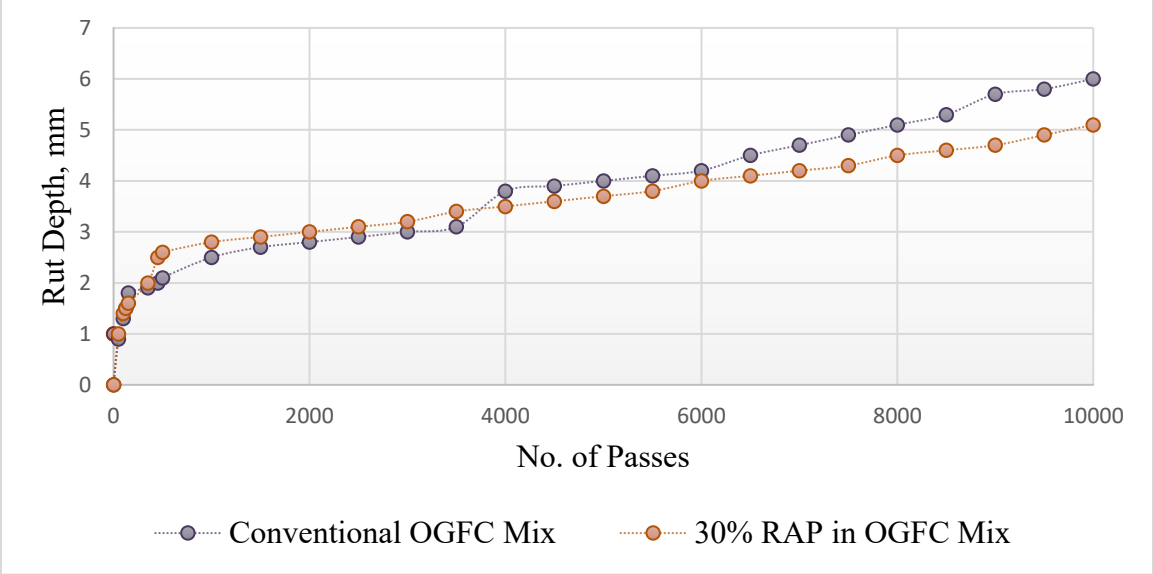

Figure 5. Rut Depth versus Number of Passes (Anusha et al. 2019)

On the other hand, some studies have indicated that the use of aged RAP can lead to more brittle mixtures and lower cracking resistance. As a result, these mixtures are more susceptible to cracking under lower temperatures and repeated loading (You et al. 2011; Mensching et al. 2014). Nevertheless, the enhanced rigidity of the recycled material may prove beneficial in high-temperature scenarios, leading to pavements that exhibit superior resistance to rutting (Zhang et al. 2020).

Use of Steel Slag in Asphalt Mixtures

Steel slag is a by-product of the steel manufacturing process, which is generated when molten steel is separated from impurities in steel-making furnaces. Every year, 50 million tons of steel slag is produced worldwide, with 12 million tons produced in Europe (Motz and Geiseler 2001). In the United States, around 7.7 to 8.3 million tons of steel slag are produced each year. The most common applications for steel slag in the United States are as a granular base or as an aggregate material in construction projects. The steel industry's rapid development in the last century has resulted in a significant increase in steel slag by-products. This has created a growing demand for effective recycling, especially in civil engineering and road construction.

Steel slag is a dense, robust, and durable material that may serve as an excellent aggregate for HMA and in different pavement layers, such as surface layers, unbound granular base, and subbase. Its exceptional resistance to friction and abrasion makes it a top choice for industrial roads, intersections, embankments, engineered fills, and parking areas that demand optimal wear resistance. Compared to conventional aggregate, steel slag aggregate has high abrasion and polishing resistance, improved skid resistance, and the ability to retain its properties throughout the pavement's life (Crisman et al. 2019). When added to hot mix asphalt, steel slag's shape and rough texture improve the bonding with binder, leading to high stability and resistance to cracking and stripping (Airey et al. 2004; Wu et al. 2007).

Airey et al. experimented with the Basic Oxygen Steel (BOS) slag and Blast Furnace Slag (BFS) as secondary aggregate to check their feasibility as feasible alternatives of aggregate for asphalt mixture production (Airey et al. 2004). The permanent deformation results for the control and slag dense base asphalt mixture (DBM) and stone mastic asphalt (SMA) are presented in Table 3 demonstrating the total strain (%) after 3,600 cycles and average strain rate (microstrain/cycle) between 1,800 and 3,600 cycles.

Based on the results presented in Table 3, it can be observed that the steel slag mixture (DBM Slag) exhibited the least amount of total strain and strain rate in comparison to both the limestone control mixture (DBM Control) and gritstone control mixture (SMA Control) with regard to relative permanent deformation performance. Furthermore, the performance of all the secondary aggregate mixtures remained consistent after undergoing moisture conditioning. The enhanced rutting resistance of the steel slag + BFS mixtures is due to the rough, porous surface texture of the BOS and BF slags, which promotes better aggregate interlocking and improves resistance to permanent deformation.

Table 3. Permanent Deformation Parameters for Slag Asphalt Mixtures (Airey et al. 2004)

Mixture	Unconditioned Total Strain (%)	Unconditioned Strain Rate (με/cycle)	Moisture Conditioned Total Strain (%)	Moisture Conditioned Strain Rate (με/cycle)
DBM Control	0.63	0.37	0.48	0.17
DBM Slag	0.45	0.34	0.46	0.23
SMA Control	0.83	0.32	1.09	0.45

Ahmedzade and Sengoz conducted a study on the effects of using steel slag as a coarse aggregate in HMA (Ahmedzade and Sengoz 2009). They reported that incorporating steel slag improved the desired mechanical properties and electrical conductivity of the asphalt mixtures. Four distinct asphalt mixtures consisting of either limestone (LS) or steel slag (SS) as coarse

aggregate and two types of asphalt cement, AC-5 and AC-10, were used in their experiment. Test specimens from these mixtures were prepared and subjected to a series of tests, such as Marshall stability, indirect tensile stiffness modulus, creep stiffness, and indirect tensile strength, to evaluate their mechanical properties. Table 4 illustrates the findings of the Marshall stability test.

Table 4. Marshall Design Results (Ahmedzade and Sengoz 2009)

Property	AC-10/LS	AC-5/LS	AC-10/SS	AC-5/SS
Optimum binder content (%)	5.0	4.85	5.8	5.2
Aggregate bulk specific gravity (g/cm³)	2.634	2.634	2.760	2.760
Mix bulk specific gravity (g/cm³)	2.392	2.385	2.455	2.466
Air void (%)	2.53	2.97	2.93	3.0
Voids in mineral aggregate (%)	13.51	13.65	15.92	15.05
Marshall stability (kN)	17.46	16.50	20.19	19.54
Flow (mm)	2.97	2.86	2.32	2.29
Marshall Quotient (MQ) (kN/mm)	5.88	5.77	8.70	8.53

Based on the results presented in Table 4, mixtures containing steel slag exhibited superior Marshall stability and reduced flow values when compared to control mixtures. These factors are critical in Marshall tests, which determine the asphalt concrete's ability to withstand shoving, rutting, and gradual subgrade movements without cracking. These results also show that using steel slag coarse aggregate in asphalt concrete samples results in higher Marshall quotient (MQ) values than control mixtures, indicating better resistance to permanent deformation and shear stresses.

This study's test results also showed that asphalt mixtures containing steel slag coarse aggregate exhibited higher stiffness modulus values compared to the control mix. These mixtures also showed substantially higher creep stiffness, suggesting better resistance to rutting. Furthermore, the steel slag mixtures demonstrated better cohesive strength than those with limestone aggregate. The study concluded that using steel slag as a coarse aggregate in asphalt mixtures improved resistance against moisture damage and moisture-induced rutting. Additionally, the electrical conductivity of mixtures with steel slag coarse aggregate was found to be greater than that of the control mixtures. This improved electrical conductivity allows for the use of these mixtures in creating conductive asphalt concrete for applications such as deicing of parking garages, sidewalks, driveways, highway bridges, and airport runways. In summary, the investigation results highlight the excellent engineering properties and good electrical conductivity of steel slag mixtures.

Asi et al. assessed the effectiveness of steel slag aggregate by conducting indirect tensile strength, resilient modulus, rutting resistance, fatigue life, and creep modulus tests on control and modified samples (Asi et al. 2007). Their findings indicated that replacing up to 75% of the limestone coarse aggregate with steel slag aggregate improved the mechanical properties of the asphalt concrete mixes. In this experiment, different percentages of steel slag aggregate (SSA) were used to replace the limestone coarse aggregate. The percentages used to replace aggregate with steel slag were 0, 25, 50, 75, and 100%. The effectiveness of the SSA was evaluated based on the improvement in various properties of the AC samples, such as indirect tensile strength, resilient modulus, rutting resistance, fatigue life, creep modulus, and stripping resistance etc. Figure 6 presents the average Indirect Tensile Strength (ITS) values obtained from the experiment conducted by Asi et al. for different asphalt mixes.

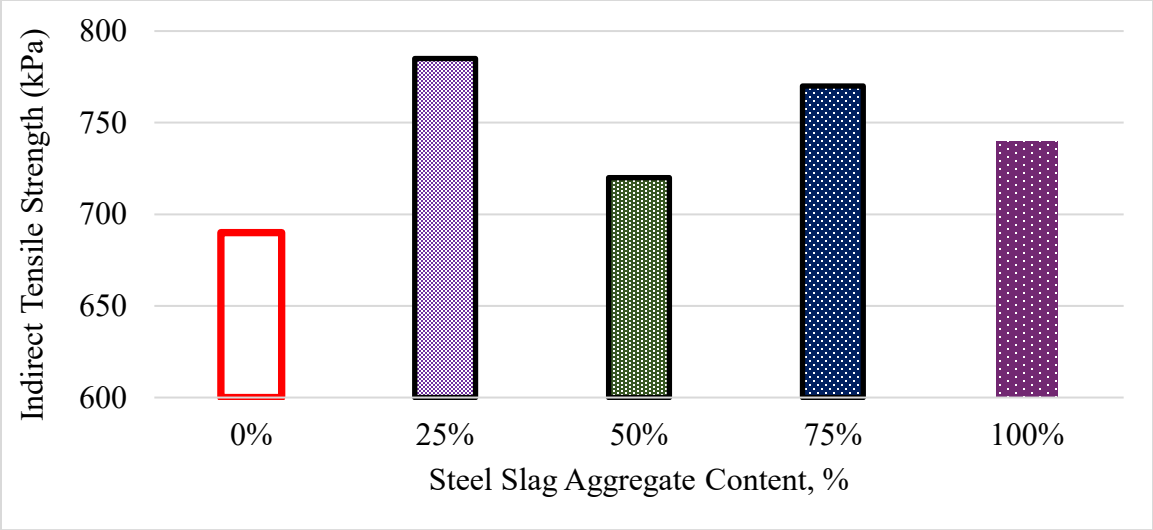

Figure 6. Indirect Tensile Strength for Various Steel Slag Content at 25°C (Asi et al. 2007)

Results presented in Figure 6 indicate that the addition of SSA to the asphalt mixes enhanced their ITS compared to the control mix. According to Asi et al., this improvement can be attributed to the enhanced aggregate structure of the SSA. However, the results also indicate that the optimal replacement level for steel slag aggregate was 25% in this experiment.

Based on the research of Hassan et al., an increase in steel slag content corresponds to an increase in the optimal binder content. Additionally, the use of coarse slag aggregate surpasses that of fine slag aggregate when it comes to meeting the requirements for the Marshall Mix design. Results from field testing have shown that steel slag asphalt offers superior deformation resistance compared to the control mix, all while maintaining favorable moisture susceptibility and binder aging (Hassan et al. 2021).

In a study conducted by Pathak et al., steel slag has been found to improve the frictional resistance of OGFC mixes as well. Additionally, the use of steel slag in OGFC mixes has shown improved design and moisture resistance parameters as compared to the control mixes that do not contain steel slag. For enhanced safety in regions with hilly topography and high rainfall, it is recommended to replace 50% of coarse aggregate with basic oxygen furnace (BOF) steel slag in OGFC mixes (Pathak et al. 2020). In another research, Pattanaik et al. also found that replacing up to 75% of the control mixture aggregate with Electric Arc Furnace (EAF) steel slag in OGFC mixtures improved rutting and fatigue performances (Pattanaik et al. 2019). The utilization of steel slag aggregate in HMA may have certain drawbacks including potential volume expansion, increased binder content, and overall high cost due to its dense nature. This results in lower volume of asphalt for the same unit weight of conventional aggregate, as well as increased transportation costs (Yildirim and Prezzi 2011).

Volume expansion caused by the hydration of its free lime or magnesia components is one of the major problems associated with steel slag. This can negatively impact the performance of the asphalt mixture incorporating steel slag, especially when the levels of free lime or magnesia are high (Knellar et al. 1994). According to Coomarasamy et al., steel slag-asphalt mixes tend to fail in moist environments due to the formation of calcium-rich deposits, primarily calcium carbonate, on the surface and interface. This negatively impacts interfacial bonding and can result in excessive expansion of the slag, ultimately leading to cracking of the mixture

(Coomarasamy et al. 1995). Kandahl et al. have suggested that steel slag should only replace either the fine or coarse aggregate fraction in paving mixes, but not both. This is because hot mix asphalt that contains 100% steel slag is vulnerable to high void space and bulking problems, which are caused due to the angular shape of steel slag aggregate. Mixes that have high void space (100% steel slag aggregate) are also susceptible to over-asphalting during production and subsequent flushing due to in-service traffic compaction (Kandahl et al. 1982).

Use of Hydrated Lime in Asphalt Mixtures

Hydrated lime has been a commonly used mineral filler in asphalt mixtures due to its numerous benefits. Its ability to maintain proper adhesion between the aggregate and the asphalt binder makes it a popular choice as an antistripping agent. Additionally, by acting as an active filler, it reduces chemical aging of binder and stiffens the mastic at high temperature more effectively than typical mineral fillers. Using hydrated lime, the binder can be strengthened even at room temperature due to its tiny features and expansive surface area. These characteristics contribute significantly to the longevity of asphalt mixture, proving hydrated lime's reputation as an effective additive. Hydrated lime also enhances the resistance to moisture damage, increases the stiffness of the asphalt mixtures to resist rutting and low-temperature fractural growth, and improves the overall toughness of the mixture (Lesueur et al. 2012).
Aljbouri and Albayati conducted a study on the effects of hydrated lime on the durability of hot mix asphalt (Aljbouri and Albayati 2024). They incorporated hydrated lime into an asphalt mixture using both a dry method (on the aggregate) and a wet addition method (to the binder). Different percentages were tested for each method (1, 2, and 3% of the weight of aggregate for the dry method and 0.5, 1, and 1.5% by weight of asphalt binder for the wet method). The results of the TSR (Tensile Strength Ratio) test from this study is presented in Figure 7.

Figure 7 shows that the addition of hydrated lime to the asphalt mixture improved the tensile strength for both the dry and wet methods. According to the study, the values of TSR for both mixture types increased, with the greatest increase occurring with the wet method at a hydrated lime content of 1.5%. Additionally, the TSR increased by 11.7% compared to the control mix. The study also showed that the value of TSR for the dry method at 3% lime was higher by 20.2% than the control mix. The inclusion of calcium in the lime material strengthened the bond between the aggregate. According to the authors, the surface texture and film of the asphalt binder may have undergone a chemical reaction that improved the resistance to moisture damage.

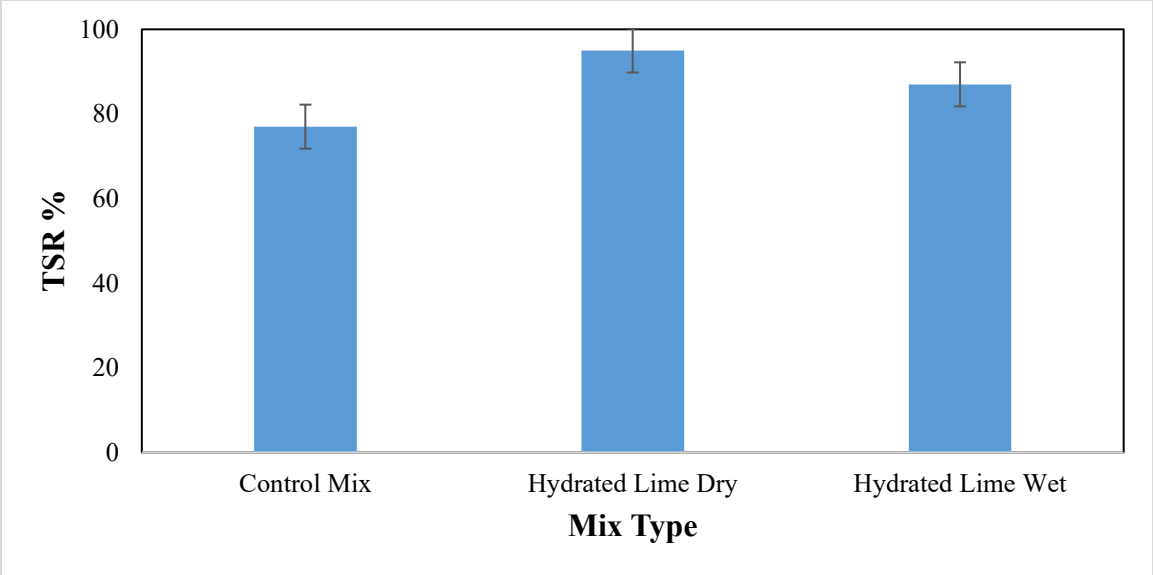

Figure 7. Effect of Hydrated Lime on TSR (Aljbouri and Albayati 2024)

Kabir's research focused on the impact of adding hydrated lime on the mechanical properties of HMA (Kabir 2008). As part of his research, he tested the addition of hydrated lime into asphalt in two ways - as a slurry with the aggregate/asphalt binder mixture in one set, and as a dry blend with the asphalt binder in another. The conventional mixture (control mixture) did not contain any hydrated lime. All three sets of samples included two polymer-modified asphalt binder that meet Louisiana's specifications for PG 76-22M, PG 70-22M, and a neat PG 64-22 asphalt. This study involved comparing the mean rut depth of various mixtures using the LWT test. To ensure precision, two samples were analyzed for each mixture and the average rut depth was recorded. The rut depth was monitored for 20,000 passes, but if it exceeded 20.0 mm before completion, the test was stopped. Mixtures with a rut depth of less than 6.0 mm after 20,000 passes were considered to pass the LWT test. The results from this study are illustrated in Figure 8.

Figure 8 illustrates that the three mixtures of the 64 HMA group - 64CO, 64LS, and 64LM - failed as they experienced rut depths greater than 6.0 mm. In this context, CO, LS, and LM stand for control, slurry or paste, and dry or no-paste, respectively. On the other hand, the results also indicate that all the other mixtures (70 HMA and 76 HMA group) performed adequately and passed the minimum rut depth requirement of 6.0 mm. The study found that adding hydrated lime generally increased the stiffness of HMA mixtures, which improved the resistance to permanent deformation in asphalt pavements. Specifically, mixtures containing PG 64-22 asphalt showed significantly improved resistance to rutting with the addition of hydrated lime, but the improvement in fatigue endurance was less significant.

The addition of hydrated lime made the asphalt binders slightly stiffer, helping them resist permanent deformation by reducing shear strain under load. The study also showed that adding hydrated lime, whether in paste or no-paste form, improved the indirect tensile strength of all HMA mixtures at 25°C and 40°C, regardless of aging criteria. However, adding hydrated lime reduced the strain and toughness index of most mixtures, although the values were still well above the minimum required criteria for sufficient fatigue resistance. Furthermore, there was a slight reduction in age hardening for mixtures containing hydrated lime in combination with

polymer-modified asphalt binder. Overall, the study clearly demonstrated that the introduction of hydrated lime enhanced the performance of HMA mixtures.

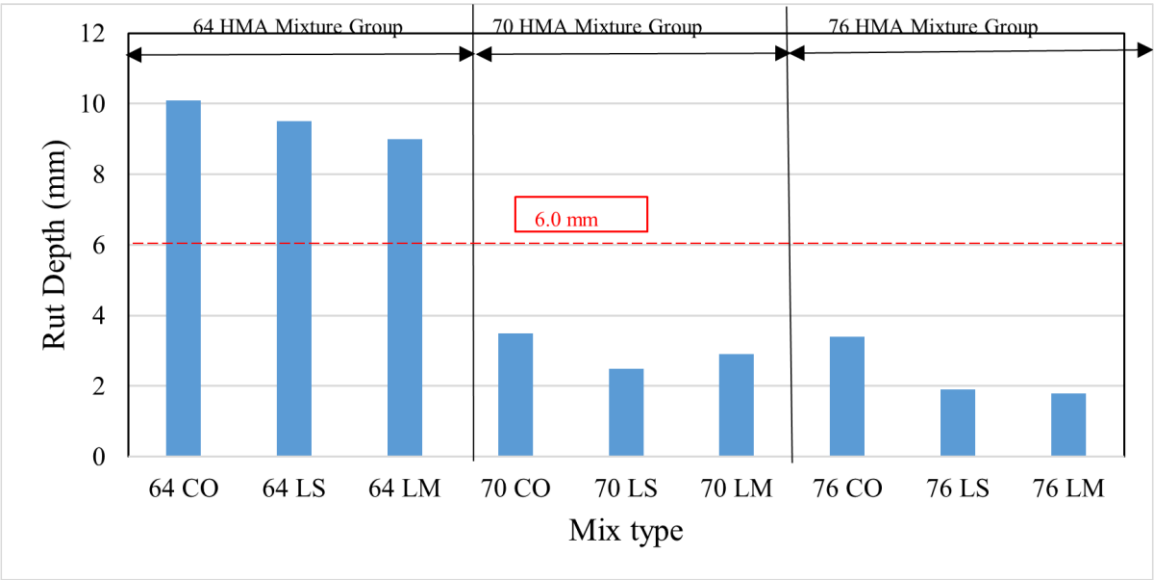

Figure 8. Effect of Hydrated Lime and Mixture Type on the Terminal Rut Depth (Kabir 2008)

A study conducted by Preti et al. indicated that using high surface area hydrated lime as a filler in OGFC asphalt mixtures can improve fracture performance compared to the traditional approach (Preti et al. 2020). According to Mohammad and Altinsoy's research, adding hydrated lime as a mineral filler to asphalt concrete mixture improved its permanent deformation characteristic and fatigue endurance. This improvement was most noticeable at higher testing temperatures, regardless of whether the mixture contained a polymer modified binder or not (Mohammad and Altinsoy 2002).

Highly Modified Asphalt (HiMA) Binder in OGFC Mix

Highly modified asphalt (HiMA) is a high polymer content asphalt binder that is used to enhance elasticity and stiffness as compared to traditional polymer-modified asphalt. HiMA mixtures consist of an asphalt binder typically modified with 7 to 8% polymer, usually styrene-butadiene-styrene (SBS). This amount of polymer is more than twice the amount used in conventional polymer-modified binders, which is typically around 3% by weight of the binder (Vargas-Nordcbeck and Musselman 2021). Based on the research conducted by the Florida Department of Transportation (FDOT), conventional modified asphalt binders have a binder-polymer structure comprising of asphalt binder with a dispersed swollen polymer phase that enhances binder properties. It was observed that as the polymer content increases, the structure shifts to a swollen polymer with a dispersed asphalt phase. This transformation causes the resulting binder to exhibit rubber-like behavior, thereby improving resistance to cracking and performance against rutting (Habbouche et al. 2019).

According to the 2021 FHWA report by Vargas-Nordcbeck and Musselman (2021), based on the results obtained from experimental test sections constructed at the National Center for

Asphalt Technology (NCAT) test track in Auburn, Alabama, FDOT adopted the use of HiMA to improve rutting performance. HiMA was initially used to address severe rutting in high-stress locations subject to heavy axle loads and slow-moving traffic. HiMA was then employed to reduce reflective cracking and raveling in certain pavement types.

In 2018, an experiment was carried out by FDOT to assess the performance of HiMA binder. Three Superpave asphalt mixtures with similar gradations were utilized to examine the impact of polymer and binder content. One mixture contained a PG 76-22 polymer-modified binder, another used HiMA binder with the same effective binder content, and the third one also used HiMA binder but with an additional 0.5% binder content. The study involved three different structural sections, each consisting of three test lanes that were milled and resurfaced with two identical 1.5-in. lifts of each mixture for rutting resistance evaluation. Additionally, three test pits were resurfaced with two 1.5-in. lifts of each mixture placed directly on the prepared base layer for evaluating fatigue cracking resistance. Accelerated loading was conducted using a heavy vehicle simulator (HVS), which is electrically powered, fully automated, and mobile. A laser profiler was used to obtain the rut measurements, while the fatigue resistance was assessed using strain gauges located at the bottom of the asphalt pavement. The relationship between the rut depth and the number of HVS passes, as obtained from the laser profiler, is depicted in Figure 9.

Test results shown in Figure 9 indicated that after 100,000 HVS passes, rutting in the HiMA sections was nearly half of that observed in the control section. Similarly, the HiMA sections displayed 20 to 40% lower strains than the control section over the recorded temperature range. It was also noted that the additional 0.5% binder in the HiMA mixture did not significantly increase rutting resistance compared to the HiMA mixture at the optimum binder content. According to FDOT, the results demonstrated that the HiMA binders enhanced the rutting and fatigue cracking performance of the asphalt mixtures. FDOT also suggested HiMA mixtures enhance structural capacity, potentially enabling a reduction in pavement thickness without compromising performance (Kwon et al. 2018).

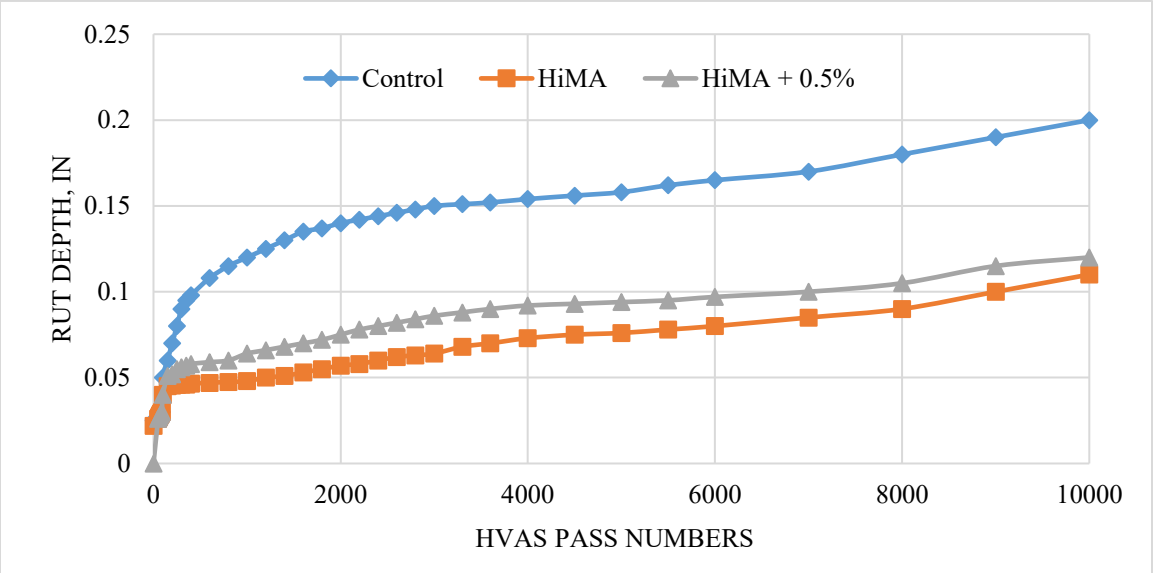

Figure 9. Average Rut Depth Progression in the Florida Study (Kwon et al. 2018)

NCAT's results on HiMA performance also led the Accelerated Pavement Load Facility (APLF) in Ohio to run an experiment to explore whether the improved stiffness of HiMA could support a thinner perpetual pavement design (Khoury et al. 2016). In the indoor APLF, four test lanes of perpetual pavement were built including highly modified asphalt (HiMA). The pavement was heated and tested at temperatures of 21.1 and 37.8°C with controlled humidity and subgrade moisture. Each lane was then subjected to 10,000 passes of a wide-base single tire load of 40 kN at each temperature. To measure surface rutting across the four test sections, a rolling wheel profilometer was used. Rutting was measured at the beginning of each run and after 100, 300, 1000, 3000, and 10,000 passes using the profilometer to measure surface height and rutting. The data on rutting profile, including the maximum depth of rutting at each stage, were recorded. The rutting data from a previous experiment involving similar perpetual pavements in the APLF, with surfaces using Aspha-min WMA and traditional HMA, were compared with the rutting profile data obtained on the HiMA surface. Table 5 presents the maximum rutting depth for APLF and WMA surface mixes under high temperatures.

Table 5. Average Maximum Rut Depth for APLF and WMA Surface Mixes under High Temperature (Khoury et al. 2016)

Number of Passes	HiMA (cm)	HiMA (in)	WMA (cm)	WMA (in)	Control (HMA) (cm)	Control (HMA) (in)
100	0.03	0.0118	0.116	0.0457	0.064	0.0252
300	0.065	0.0256	0.165	0.0649	0.102	0.0402
1,000	0.096	0.0378	0.244	0.0961	0.169	0.0665
3,000	0.137	0.0540	0.348	0.1370	0.267	0.1051
10,000	0.174	0.0685	0.513	0.2020	0.441	0.1736

As shown in Table 5, it was observed that there was minimal rutting in any of the lanes on the HiMA surface. The maximum amount of rutting recorded at the end of the experiment on HiMA surfaces was 0.0685 inch (0.174 cm), which was well below the "low rutting" threshold of 0.126 inch (0.32 cm) set by the Ohio Department of Transportation Office of Pavement Engineering. In contrast, both WMA and traditional HMA surfaces exhibited enough rutting to exceed the ODOT "low rutting" threshold during the experiment.

Zhang et al. conducted an experiment to improve the durability of OGFC by using high-content SBS polymer-modified asphalt binders in the mixture. The authors prepared four SBS modified asphalt samples with SBS contents of 4.5, 6.0, 7.5, and 9.0%, respectively (Zhang et al. 2020). The rheological properties of the asphalt were evaluated through the Brookfield viscosity test and the frequency sweep test. The raveling resistance, moisture susceptibility, rutting resistance, and fatigue cracking resistance of the OGFC mixture were evaluated through the Cantabro test, indirect tensile strength ratio test, Hamburg wheel tracking test, and four-point beam bending test, respectively. The results of the Cantabro test obtained from the experiment are presented in Figure 10.

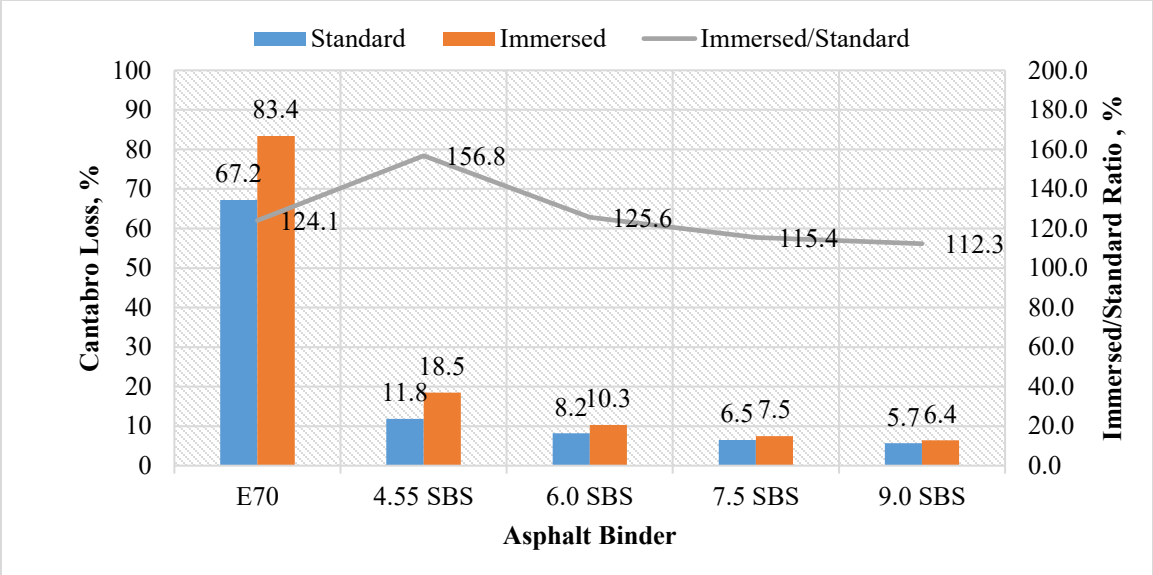

Figure 10. Results of the Cantabro Test for Different Polymer Contents (Zhang et al. 2020)

As shown in Figure 10, the addition of SBS significantly reduced the Cantabro loss of the OGFC mixture. The control mix (E70) exhibited the highest percentage of Cantabro loss. However, as the SBS content was increased, indicating a higher level of asphalt modification, the standard Cantabro loss of the OGFC mixture gradually decreased. In addition, when the SBS content exceeded 6%, the Cantabro loss of the mixture decreased to less than 10%, indicating an effective anti-raveling performance of the HiMA. The immersed Cantabro test were also performed in this experiment to determine the raveling resistance of the OGFC mixture under 60℃ water immersion, which cause asphalt aging and moisture damage. The ratio of immersed Cantabro loss to standard Cantabro loss was used to evaluate the moisture resistance of the OGFC mixture. A smaller immersed/standard ratio corresponds to higher moisture resistance for the mixture. The results of the immersed/standard ratio are shown in Figure 10. As the SBS content increased, the immersed/standard ratio gradually decreased, indicating an improvement in the moisture resistance of the mixture. This study demonstrated that the use of highly modified asphalt in OGFC mix significantly reduced the moisture susceptibility and enhanced the raveling resistance, fatigue cracking resistance, and rutting resistance of the OGFC mixture.

It is important to point out that asphalt mixtures with HiMA behave differently than mixtures with conventional binder (Blazejowski et al. 2021). Therefore, HiMA mixes may require greater compaction effort due to a significant increase in viscosity if stored or conditioned at temperatures above 180°C. Excessive mixing temperatures of the aggregate with the HiMA binder can also lead to workability issues. HiMA asphalt mixtures exhibit optimal compatibility in the temperature range of 145-165°C and achieve better compaction at around 7.0% content (by mass). Considering the compactibility and workability issues of HiMA, special attention needs to be given to limit storage time and control mixing, laydown, and compaction temperatures to ensure the workability and achieve the desired density of the mixture.

Bio-Remediation and Microbial Degradation Mechanisms

In natural soils, microorganisms (primarily bacteria and fungi) mediate the transformation of organic compounds into other compounds in natural systems (Campbell 2020). Biofilms form

within the soil void spaces and organisms grow as they consume target substrate compounds (Figure 11a), as described by established kinetical models based on context, such as the Monod model for population-level dynamics (Figure 11b) or the Michaelis-Menten model for molecular-level interactions. The rate of uptake of a chemical is governed by the uptake capabilities of the microbial cells composing the biofilm as well as by Fickian transport limitations in both the biofilm and the stagnant boundary layer. In a partially penetrated biofilm, the chemical concentration in the biofilm (C_f) would decrease to zero at some point in the biofilm. In a shallow biofilm, C_f would be approximately equal to the chemical concentration in the biofilm immediately adjacent to the stagnant water layer ($C_{f,s}$) throughout the biofilm (Metcalf and Eddy 2014).

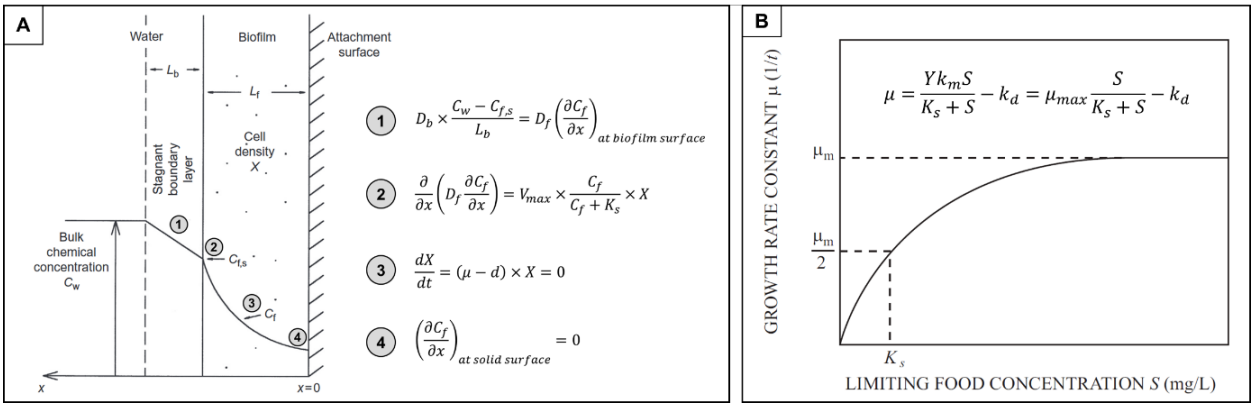

Figure 11. a) Diagram of a Fully Penetrated Biofilm, and B) Monod Kinetics for Substrate-Limited Growth in Continuous Flow Systems Where Growth is Limited by One Substrate (Metcalf and Eddy 2014)

Bioremediation applications, such as hydrocarbon degradation, heavy metal removal, and chemical removal, can benefit from these transformation pathways by promoting biofilm growth in proximity to the target compound and maintaining suitable growth conditions (Bharagava et al. 2022).

Microbial consortia have been developed to effectively treat dye-contaminated and metal-laden wastewater. Examples include bacterial consortia for degrading direct blue 2B dye (Cao et al. 2019), bacteria-algal systems for wastewater remediation (Sepehri et al. 2020), and fungal consortia capable of decolorizing dyes like Acid Blue 161 and Pigment Orange 34 (Mishra et al. 2014). These systems also efficiently remove heavy metals like chromium and copper within 48 hours.

Biochar-based nanocomposites improve heavy metal adsorption by increasing oxygen-containing functional groups (e.g., –COOH, –OH, –C=O) on the biochar surface (Gan et al. 2015). These functional groups enhance adsorption capacity and facilitate strong interactions with metals through surface complexes, cation–π bonding, electrostatic attraction, and ion exchange. This makes biochar nanocomposites highly effective for removing heavy metals like arsenic, cadmium, chromium, copper, mercury, and lead from contaminated environments.

A study comparing porous asphalt (PA) pavements to standard asphalt showed that PA systems efficiently remove particulate stormwater pollutants like sediments (98.7%), total lead (98.4%), and total zinc (97.8%). Removal was attributed primarily to physical processes (i.e., size exclusion based on the pore area being smaller than the particulate diameter), but

discussion indicated the potential for microbial processes to remove dissolved contaminants and hydrocarbons (Jayakaran et al. 2019).

Artificial Neural Networks

Artificial neutral networks are parallel computing schemes that function similarly to the mechanism of the human biological nature of neurons and can model complex problems (Elseifi and Elbagalati 2017). They are effective and accurate tools for solving complex nonlinear problems as they provide robust models that can continuously be updated as new data become available. In addition, they can be used in databases with either large or relatively small amount of data (Plati et al. 2015). The learning ability of genetic flexible training algorithm in ANNs allows it to make decisions based on given inputs (Kim et al. 2014).

The most commonly used ANN structure for both regression analysis and supervised classification is the feed-forward model. This model topology consists of an input layer (i) in which the input independent variables are defined, one or more processing (hidden) layers (j), and a target (output) layer (k) in which the depended variables are implemented (Kim et al. 2014). The network topology is simulating the biological human brain. Each layer consists of processing units called “neurons”, and every neuron in a layer is connected with all neurons in the previous layer (Lawrence et al. 1997). Each of these connections is assigned a “weight”, and each neuron is assigned a “bias.”

The process of calculating the weights and biases of the ANN is called the learning process or the training process. The most commonly used training procedure is the back-propagation error optimization algorithm. In this procedure, random values for weights and biases are assigned to the network connections and neurons, respectively. The network output (y) is then calculated based on the randomly assigned weights and biases and compared with the target value (t) to calculate the error. The process of minimizing the error is an optimization problem that is solved using the Stochastic Gradient Descent (SGD). In the SGD method, the weight parameters are iteratively updated in the direction of the error loss function until a minimum is reached. The process of updating the weight parameters to minimize the error is called backpropagation.

AI Application in Asphalt Pavement Prediction

Artificial Intelligence (AI) can use data sets to develop predictive models, which can serve as tools to identify the optimum component materials and combinations for achieving desired performance characteristics for asphalt mixes. In recent years, Machine Learning (ML) has been extensively applied in the asphalt field. Rahman et al. utilized ML to assist in the design of HMA. Their study involved predicting rut depth from the HWTT and indirect tensile strength (Rahman et al., 2021). The study employed decision tree-based ensemble methods and support vector regression, identifying that recycled asphalt materials and aggregate gradation significantly impact mixture performance.

Ozturk and Kutay applied an ANN model to predict mixture volumetrics, including the percentage of air voids in compacted mixtures for Superpave gyration levels, aggregate gradation, bulk specific gravity, performance grade (PG) of the asphalt binder, and asphalt content (Ozturk et al. 2014). Raza and Sharma's study examined the performance of porous asphalt mixtures through systematic experimentation and modeling techniques, including Response Surface Methodology (RSM) and ANN. Their research aimed to develop efficient, trial-minimizing guidelines to link air voids with permeability exceeding 0.12 cm/sec while maintaining mix stability. The ANN models, calibrated with experimental data, effectively

identified optimal aggregate proportions to achieve desired permeability and stability, thereby reducing the need for trial batches and minimizing material waste (Raza et al. 2024). Gong et al. analyzed data from 78 sections of the Long-Term Pavement Performance (LTPP) program, focusing on metrics such as rutting, cracking, and roughness. They employed random forests to study the impact of various asphalt mixture and structural properties on pavement performance, including aggregate gradation, bulk specific gravity, air voids, asphalt binder viscosity and content, as well as pavement age and thickness (Gong et al. 2020).

Majidifard et al. employed innovative machine learning techniques, including gene expression programming (GEP) and a hybrid artificial neural network/simulated annealing (ANN/SA) approach, to predict the fracture energy of asphalt mixture specimens. The fracture energy was predicted using numerous variables, which were asphalt binder performance grade (PG), asphalt content, aggregate size and gradation, reclaimed asphalt pavement (RAP) content, recycled asphalt shingles (RAS) content, crumb rubber content, and test temperature. This study also provided a calculation procedure to interpret these models and to convert them into practical design equations (Majidifard et al. 2019).

Liu et al. conducted a study to simplify and accelerate the Superpave mixture design process by utilizing machine learning models (Liu et al. 2022). The aim was to develop an automated and efficient method for predicting effective asphalt content and absorbed asphalt content. The inputs for the machine learning models included aggregate gradation, bulk specific gravity of aggregate, blend absorption, air voids content, PG grade of the asphalt binder, and the number of gyrations. A parametric study demonstrated the feasibility of using the proposed mix design method showing that the gradation and optimal asphalt content predicted using a gradient boosting model were consistent with those obtained through traditional Superpave methods and laboratory tests.

Mansour et al. developed AI-based models, including Decision-Tree, XGBoost, ANN, and ensemble learning, to predict Asphalt Concrete (AC) overlay performance up to 11 years, using historical pavement data from Louisiana (Mansour et al. 2024). The study found that ensemble learning provided the most accurate predictions for Pavement Condition Index (PCI) over time, offering a robust alternative to traditional forecasting methods. These AI models support state agencies in more reliably planning pavement maintenance and rehabilitation.

Knowledge Gaps in the Literature

Recent research studies have evaluated the modification of OGFC asphalt mixtures using recycled waste plastic, RAP, steel slag, hydrated lime, and HiMA. However, some research gaps were identified in the literature review as follows:

- The impact of OGFC modification with recycled waste plastic, steel slag, and RAP, as well as hydrated lime as partial replacement for coarse and fine aggregate, has not been evaluated or compared to date.
- Limited studies have evaluated the use of high-polymer asphalt binder in OGFC mixes, and none of these studies were conducted in the south-central United States.
- The cost-effectiveness and constructability of OGFC mixes incorporating recycled plastic waste, steel slag, and high-polymer asphalt binder have not been evaluated to date.
- The evaluation of OGFC mixtures using advanced cracking resistance test methods, such as IDEAL-CT, has not been conducted to date.

- While recent studies have utilized AI in mix performance prediction, no study has considered using AI to assist in the design and performance prediction of OGFC mixes.
- Building on the results of research studies, the developed tool enables the prediction of OGFC mix performance when WMA additives and crumb rubber are incorporated into the mix design.
- Given that advanced asphalt laboratory tests require expensive equipment, such as HWTT, Cantabro test, and moisture susceptibility test, the implementation of the proposed AI tool will benefit low-budget highway agencies and asphalt contractors.

Chapter 3. Research Methodology

The research activities were divided into seven major tasks to achieve the three main objectives of the study. These tasks are outlined in the following sections.

Task 1: Literature Review and Assessment of the Current State of Practice

In this task, research studies detailing global, local, and state practices in the design and performance of OGFC mixes were reviewed, with findings presented in Chapter 2 of this report. The literature review encompassed studies from various countries, including the Netherlands, Japan, the UK, and India, highlighting the global applications of OGFC. Additionally, the review incorporated research studies conducted in the United States including Texas, Louisiana, Florida, Ohio, and the National Center for Asphalt Technology (NCAT).

The literature review placed particular emphasis on regional sources, including the Louisiana Department of Transportation and Development (LaDOTD) specifications, alongside innovative procedures introduced in NCHRP Project 1-55. These resources were carefully reviewed and summarized to serve as key guidelines for the design of OGFC mix in this study. Specific topics covered in the literature review included the following:

- Benefits of OGFC and its global applications;
- Characteristics of OGFC mixtures and durability challenges;
- Effects of aggregate gradation and binder properties on OGFC mix performance;
- Effects of aggregate replacement and asphalt modification on OGFC mix performance;
- Artificial intelligence and its use in asphalt performance prediction.

Task 2: Materials Selection and Development of Experimental Factorial

The primary goal of this task was to select the components of the OGFC mixture that will be included in the experimental factorial design. A state-approved Job Mix Formula (JMF) for an OGFC mix was used to produce the Control Mix (CM). This CM is already in use in Louisiana for OGFC pavement construction and consists of two aggregate types: #78 limestone and #78 sandstone. Asphalt binder PG 76-22 was added at a rate of 6.5% based on the total weight of the mix. This JMF, which is approved by the Louisiana Department of Transportation and Development (LADOTD), has been previously utilized in OGFC pavement construction across the state. The mix design contains 70% #78 limestone and 30% #78 sandstone, with batching conducted in this specific proportion to meet the aggregate gradation requirements. An anti-stripping agent (ASA) known as ZycoTherm was incorporated into all mixes at a dosage of 0.08% by binder weight to prevent moisture damage. To prevent draindown, cellulose fibers were also added at 0.3% of the total mix weight.

In this study, the control mix was modified with several aggregate substitutes - recycled waste plastic (RWP), steel slag (SS), reclaimed asphalt pavement (RAP), and hydrated lime (HL) in an attempt to develop an environmentally-friendly OGFC mix that could improve durability and performance of the asphalt mix while allowing the reuse of waste plastic, steel slag, and RAP into the mixture. The RWP used for this study was recycled from High-Density Polyethylene (HDPE) with the melting point temperature of 165°C and was used to replace 3.75% of the total weight of the dry aggregate in the modified asphalt mix, with the replacement equally distributed between #8 and #16 aggregate. On the other hand, RAP and steel slag each replaced 7% of the dry aggregate (100% of 1/2") by weight. Hydrated lime, used as slurry, replaced 1.5% of the

dry aggregate mix. A highly modified asphalt (HiMA) binder, modified with styrene-butadiene-styrene, was also used in the test factorial in place of PG 76-22 binder. Table 6 presents the aggregate and mixture characteristics and specifications according to the JMF adopted in this study.

Table 6. Job Mix Formula of the Control Mixture

US Sieve / Property	% Passing - #78 Limestone	% Passing - #78 Sandstone	% Passing - Mix Design	JMF Range
3/4 in (19 mm)	100.0	100.0	100.0	96-100
1/2 in (12.5 mm)	91.3	97.2	93.1	90-98
3/8 in (9.5 mm)	67.0	82.3	71.6	67-75
No.4 (4.75 mm)	7.1	25.0	12.4	8-16
No.8 (2.36 mm)	2.5	7.5	4.0	2-8
No.16 (1.18 mm)	1.4	5.7	2.7	2-6
No.30 (0.60 mm)	1.2	5.2	2.4	2-6
No.50 (0.30 mm)	1.1	5.0	2.3	2-6
No.100 (0.15 mm)	0.9	3.9	1.8	-
No.200 (0.075 mm)	0.5	2.4	1.07	0.9-3.9
Bulk specific gravity (Gmb)	2.670	2.640	2.661	-
Apparent specific gravity	2.736	2.719	2.731	-
Absorption	0.9	1.1	1.0	-
Flat and Elongated Ratio	0.5	1.0	0.6	-
Coarse Aggregate Angularity	100%	100%	100%	-

Task 3: Design and Prepare OGFC Mixes According to the Test Factorial

The aim of Task 3 involved preparing the selected OGFC mixes in accordance with the test factorial. The preparation process began by sourcing the aggregate, fibers, and binders from local contractors for laboratory testing and prediction of performance. All of the mixes were formulated and prepared to meet LaDOTD specifications for OGFC. Six OGFC mixes were produced, including a control mix (CM) and five modified mixes, using the materials described in the previous section. Three of the five modified mixes involved partial replacement of aggregate with alternative materials: steel slag (SS), recycled waste plastic (RWP) and reclaimed asphalt pavement (RAP). These mixes were designated as SS, RWP, RAP, respectively. As previously mentioned, aggregate replacements were made based on the weight percentage of the total mix. For the SS, RAP, and RWP modified mixes, the dry mix method was used, where the alternative materials replaced a portion of the limestone and sandstone aggregate used in the control mix.

In one of the modified mixes, hydrated lime was introduced as a slurry and this mix was designated as HL. In the preparation of the HL-modified mix, hydrated lime was first weighed to an amount equal to 1.5% of the total dry aggregate weight. Simultaneously, an equivalent weight of fine aggregate passing through sieve #200 was removed from the dry mix. The weighed HL was then mixed with water in a 1:2 ratio by weight to form a slurry. This slurry was subsequently mixed with the remaining dry aggregate to ensure thorough and even coating. The coated aggregate was then oven-dried at 110°C overnight to prepare them for further use in the mix.

While PG 76-22 binder was used in the control mix and four of the five modified mixes, the fifth modified mixture was prepared by replacing the PG 76-22 binder with Highly Modified Asphalt (HiMA), and this mix was labeled as HiMA. The HiMA used in this study was an asphalt binder product prepared by modifying a base binder, specifically PG 58-28, with 7.5% of Styrene-Butadiene-Styrene (SBS) polymer. The high polymer content is key to improving the asphalt's mechanical properties, enhancing its flexibility and durability.

The production process of HiMA involved creating a concentrated binder by blending the SBS polymer with the base binder using a high-shear mill and heated mixing tanks. This method ensures that the polymer is evenly dispersed, allowing for a highly modified binder that can be diluted to meet the specific concentration required, typically around 7.5%. The following two specifications were met for the HiMA:

- The non-recoverable creep compliance (Jnr 3.2) at 3.2 kPa is less than 0.1, ensuring low deformation under load.
- The percent recovery (% rec) at 3.2 kPa is over 90%, indicating high elasticity.

In both the PG 76-22 and HiMA mixes, ZycoTherm™ was added to the heated binder as an anti-stripping agent to enhance moisture resistance and performance. To incorporate the anti-stripping agent into the binder, the binder was initially heated to the mixing temperature of 165°C. Subsequently, ZycoTherm was added to the asphalt binder at a concentration of 0.08% by weight of the binder. The mixture was then blended using a shear mixer operating at 1,000 rpm for 1 to 2 minutes to ensure the agent was properly blended with the binder.

To minimize binder draindown, cellulose fibers were incorporated into all mixes at a rate of 0.3% by the total mixture weight, utilizing the dry method for every batch. Initially, the dry aggregate was heated to the specified mixing temperature for three hours. The modified mixtures were produced at the same temperature as the CM, with a mixing temperature of 165°C. The cellulose fibers were manually introduced into the heated aggregate, followed by blending with a mechanical mixer for 1 to 2 minutes to ensure even distribution. Afterward, the fiber-aggregate mixture was placed in an oven for 30 minutes to reach the required temperature before blending it with the binder. Asphalt mixes were first prepared at a mixing temperature of 165°C and were then allowed to cool before undergoing short-term aging for 2 to 4 hours, depending on the specific test protocols. Following the aging process, the mixtures were compacted at a temperature of 155°C to prepare the specimens for laboratory testing.

Initial trial asphalt mixes were prepared to satisfy the target air void content. Once the mix designs were finalized based on these trials, specimens were prepared and were used for subsequent laboratory performance and durability testing in Task 4.

Task 4: Laboratory Tests of OGFC Mixes

The aim of this task was to assess the influence of various modifications included in the experimental design on the performance and properties of OGFC mixtures. The experimental factorial was designed to evaluate OGFC performance across the production stage, construction phase, and field performance stage. During the production phase, the draindown test was performed to measure the quantity of binder that drained from a loose OGFC asphalt mix and to evaluate the impact of mix modifications on the draindown of the mix. In the construction phase, the Compaction Energy Index (CEI) was employed to compare the compaction effort needed for various mixtures. CEI is defined as the area under the curve of the

number of gyrations versus the percentage of maximum specific gravity (%G_{mm}), starting from the eighth gyration up to the gyration that reaches 92% G_{mm}. This metric estimates the compaction effort applied by rollers in the field to achieve the necessary density during construction. In this study, compaction data collected during the test specimen preparation stage were used to calculate the CEI for each mix type. Given the higher air void content in OGFC mixtures compared to traditional HMA, the CEI was calculated as the area under the % G_{mm} curve from the eighth gyration to the gyration corresponding to 75% G_{mm} (Abohamer et al. 2022).

Since the primary function of an OGFC layer is to facilitate rainwater drainage, each mixture was evaluated for its air void content and permeability to ensure it maintained the necessary drainage capacity. To assess field performance, a series of tests were conducted, including the Cantabro Test, Hamburg Wheel-Tracking Test (HWTT), Indirect Tensile Cracking Strength (IDEAL-CT) Test at intermediate temperature, and the Modified Lottman Test. These tests evaluated the mix's resistance to raveling, permanent deformation, cracking, and moisture damage, respectively.

The Bitumen Bond Strength (BBS) test was also performed to determine the adhesive strength of the PG 76-22 binder when modified with various fillers, such as steel slag, RAP, hydrated lime, and the control mix filler. Additionally, the adhesive strength of the modified PG 76-22 binder was compared to that of the HiMA binder. Table 7 summarizes the various tests conducted, including the minimum and actual number of test samples prepared for each method.

Table 7. Summary of Tests, Specifications, Purposes, and Minimum Number of Samples

Test	Specification	Purpose	No of Samples Required	No of Samples Used
Bulk Specific Gravity	ASTM D6752	Air void content	03	03
Theoretical Specific Gravity	ASTM D 2041	Air void content	03	03
Permeability	FM 5-565	Permeability coefficient	03	03
Draindown Test	AASHTO T 305-97	Binder draindown	03	03
Cantabro Abrasion Test	AASHTO TP 108-14	Raveling resistance	03	03
Hamburg Wheel-Tracking Test	AASHTO T 324	Rutting resistance	02	04
IDEAL-CT	ASTM D8225-19	Cracking resistance	03	03
Modified Lottman Test	AASHTO T 283	Moisture damage resistance	06	06
Bitumen Bond Strength Test	ASTM D 454	Binder adhesive strength	03	03

As shown in Table 7, the number of samples used for each test met the minimum requirements outlined in the specifications. For the Hamburg Wheel-Tracking Test (HWTT), four samples were produced instead of two. This adjustment was necessary due to the design of the HWTT machine, which simulates both the right and left wheel paths, and each wheel path requires two samples for testing. Thus, a total of four samples were needed to accurately simulate the conditions for both wheel paths. Additionally, preparing four samples allowed for more robust statistical analysis across the different mixtures tested. The test methods presented in Table 7 are discussed in detail in the following sections.

Air Void Content

Air void content is a critical factor separating OGFC from other asphalt mixtures. High air voids enhance the mix's ability to drain rainwater and reduce noise. However, increased air voids also compromise durability, making it essential to accurately calculate and monitor the specified air void content during laboratory tests. Air void is calculated based on the bulk specific gravity (G_{mb}) and theoretical maximum specific gravity (G_{mm}).

The bulk specific gravity is determined according to ASTM D6752 test procedure, which outlines the *Standard Test Method for Bulk Specific Gravity and Density of Compacted Asphalt Mixtures Using Automatic Vacuum Sealing Method* (ASTM D6752, 2018). In this test, three replicates of Superpave Gyratory Compacted (SGC) specimens, each with a diameter of 6 inches (150 mm) and a height of 4.5 inches (115 mm), were compacted. The bulk specific gravity was then calculated using the following equation.

$$\mathbf{G_{mb}} = \frac{\mathbf{A}}{[\mathbf{C} + (\mathbf{B} - \mathbf{A})] - \mathbf{E} - \frac{\mathbf{B} - \mathbf{A}}{\mathbf{F_T}}}$$

Equation 1. Bulk specific gravity calculation

Where,
A = initial weight of the dry sample in air (grams)
B = weight of the dry sample sealed with plastic bag (grams)
C = final weight of the test sample without the plastic bag (grams)
E = weight of the sealed sample under water (grams)
F_T = apparent specific gravity of the plastic bag at 25°C (as provided by the manufacturer)

The theoretical maximum specific gravity (G_{mm}) is determined following ASTM D2041 and AASHTO T 209, *Standard test methods for theoretical maximum specific gravity and density of asphalt mixtures* (ASTM D2041, 2019). Typically, three samples of loose asphalt mix are prepared for each mixture, and the G_{mm} for each mix is determined using the following equation.

$$G_{mm} = \frac{A}{A + \mathrm{B} - \mathrm{C}}$$

Equation 2. Maximum specific gravity calculation

Where,
A = mass of dry sample in air (gram)
B = mass of the container submerged under water (gram)

C = mass of sample and container submerged under water (gram).

Once the theoretical maximum specific gravity (G_{mm}) and the bulk specific gravity (G_{mb}) of the mix were determined, the air void for each test specimen was calculated using the following equation:

$$\text{Air Void } (\%) = \frac{G_{mm} - G_{mb}}{G_{mm}} * 100$$

Equation 3. Air void (%) calculation

After calculating the air void (AV) content of each test sample, the value was assessed to ensure it fell within Louisiana DOTD's acceptable range of AV for OGFC, which is 18 to 24%.

Permeability

The falling head permeability test was conducted to assess the permeability of OGFC mixtures, which is based on FM 5-565, *Florida Method of Test for Measurement of Water Permeability of Compacted Asphalt Paving Mixtures* (FDOT, 2015). First, to ensure the sample was fully saturated, they were submerged in water for one hour before testing. Then, the sample was placed inside the testing device and water was allowed to flow through it for 5 to 10 minutes before the test began. The rate at which water passed through the saturated sample's pores was used to determine its permeability using Equation 4.

$$k = \frac{a * L}{A * t} \ln\frac{h_1}{h_2} * t_c$$

Equation 4. Permeability calculation

Where,
k= coefficient of permeability (cm/sec)
a = inside cross-sectional area of the buret (cm^2)
L = average thickness of the test specimen (cm)
A = average cross-sectional area of the test specimen (cm^2)
t = elapsed time between water head reading h_1 and h_2
h_1 = initial head across the test specimen (cm)
h_2 = final head across the test specimen (cm)
t_c = temperature correction for viscosity of water.

Draindown Test

Draindown characteristics of asphalt mixtures were evaluated by following the test procedure detailed in AASHTO T 305-97, *Draindown Characteristics in Uncompacted Asphalt Mixtures* (AASHTO 2014). Draindown characteristics were determined at a temperature 15℃ higher than the production temperature for each mixture according to the test protocol. Two samples of loose mix (about 1200 grams) were placed on separate wire baskets. The baskets were placed on pans with a known weight in oven for an hour each. The mass of the binder that was drained off in the process was recorded and the draindown percentage was calculated based on Equation (5).

$$\% \text{ Draindown} = \frac{Mf - Mi}{Mt} \; X \; 100$$

Equation 5. Binder draindown calculation

Where,
M_f = Final pan mass
M_i = Initial pan mass
M_t = Initial total sample mass

The average draindown was calculated for each mixture and was compared against the recommended upper limit of binder draindown of 0.3%.

Cantabro Abrasion Test

The Cantabro abrasion test was performed to evaluate the raveling resistance of asphalt mix and was conducted according to AASHTO TP 108-14, *Standard Method of Test for Determining the Abrasion Loss of Asphalt Mixture Specimen* (AASHTO 2021). Three SGC samples of 6 in. (150 mm) diameter and 4.5 ± 0.2 in (115 ± 5 mm) height were prepared for each mix. Test specimens were weighed to the nearest 0.1 gram before running the test. Then, the Los Angeles abrasion test was run on the specimen without the steel balls. Then the test apparatus was run at a speed of 30 to 33 revolutions per minute at a temperature of 25℃ for ten minutes so that the total number of revolutions equaled to 300. In the next step, the test specimen was taken out from the apparatus, loose particles were removed, and the final mass of the test specimen was weighed again to the nearest 0.1 gram. The Cantabro loss of each specimen was then calculated according to the following equation.

$$\% \text{ Abrasion loss of sample} = \frac{W1 - W2}{W1}$$

Equation 6. Cantabro abrasion loss (%)

Where,
W_1 = Initial weight of the test sample
W_2 = Final weight of the test sample

The average abrasion loss of the test specimens was compared to the specification limits to determine the loss of material due to abrasion and durability resistances of the mixes. NCHRP recommends a maximum of 20% abrasion loss for unaged samples (Watson et al. 2018).

Hamburg Wheel Tracking Test

The Hamburg Wheel-Tracking Test (HWTT), performed in accordance with AASHTO T 324, is widely used to assess the resistance of asphalt mixtures to permanent deformation (AASHTO 2019). In this study, four test samples were prepared for each test condition, with dimensions of 6 in. (150 mm) in diameter and 2.36 in. (60 mm) in height. In Louisiana, the criterion for OGFC with PG 76-22 specifies a maximum rut depth of 0.5 in. (12.5 mm) after 5,000 passes (LADOTD 2016). However, according to NCHRP 1-55, the maximum allowable rut depth for OGFC should not exceed 0.5 in. (12.5 mm) after 20,000 passes (Watson et el. 2018). Therefore, the rut

depths at both 5,000 and 20,000 passes for all mixes were compared based on the limits defined by LaDOTD and NCHRP 1-55.

IDEAL-CT

The IDEAL-CT test was performed according to ASTM D8225, Standard Test Method for Determination of Cracking Tolerance Index of Asphalt Mixture Using the Indirect Tensile Cracking Test at Intermediate Temperature, to evaluate the cracking resistance of the asphalt mixtures (ASTM 2019). For each mixture, three specimens were compacted using a Superpave Gyratory Compactor (SGC) with a diameter of 150 ± 2 mm and a thickness of 62 ± 1 mm. Prior to testing, the specimens were conditioned by submerging them in a water bath at 25°C for 2 hours ± 10 minutes. The test was conducted using an InstroTek SmartLoader, which applied a constant displacement rate of 50 mm/min at the target test temperature. The cracking tolerance index (CT_{index}) for each specimen was determined based on the load versus load-line displacement (LLD) curve generated by the SmartLoader Analysis software. The average CT_{index} for each mixture was compared against state specifications. A higher CTindex value signifies greater resistance of the mixture to cracking.

Modified Lottman Test

The resistance of OGFC mixes to moisture damage was assessed using the modified Lottman test, following the procedure outlined in AASHTO T 283 (AASHTO 2014), with adjustments described in ASTM D7064 *Standard Practice for Open-Graded Friction Course* (ASTM 2021). The Tensile Strength Ratio (TSR) was determined in this test by calculating the ratio of the average Indirect Tensile Strength (ITS) of three dry test specimens to that of three conditioned specimens. The conditioned samples underwent one freeze-thaw cycle, and all specimens were submerged in a 25°C water bath for two hours prior to testing. TSR of each mixture was then evaluated in comparison to the minimum ASTM recommended value of 0.8 to predict the moisture resistance performance of the mixtures.

Bitumen Bond Strength Test

The Bitumen Bond Strength (BBS) test was conducted to evaluate the effect of aggregate replacement on the adhesive strength of the binder, following ASTM D4541 standards (ASTM 2022). A pneumatic adhesion tensile testing instrument (PATTI) was used to measure the bond strength of the mastic. The mastic samples were prepared by mixing filler and asphalt binder at a ratio of 0.8 to 0.2 by mass. The PATTI test was conducted under both dry and wet conditions. The bond strength of each mastic was measured by following the test procedure outlined in ASTM D4541. The pull-off tensile strength (POTS) was measured for both dry and wet conditions and the loss of bond strength percentage was calculated based on the pull-off tensile strength under dry and wet conditions, using Equation (7).

$$\% \text{ Loss of bond strength} = \frac{POTSdry - POTSwet}{POTSdry}$$

Equation 7. Loss of binder bond strength (%)

Task 5: Predict Field Performance and Cost-Effectiveness of OGFC

The aim of this task was to analyze the results from Tasks 3 and 4 to identify and quantify the impact of design variables and modifications on the performance and durability of OGFC mixes. Statistical analysis was performed on the test results using Analysis of Variance (ANOVA). The F-statistics and corresponding P-values obtained from ANOVA were employed to determine the statistical significance of the test factorials examined in the study. Tukey's Honest Significant Difference (HSD) test was also conducted in addition to ANOVA to assess whether the performance differences among the various combinations of design variables were statistically significant.

As part of this task, a cost-effectiveness analysis was conducted to evaluate the economic feasibility of the mixture modifications, offering valuable insights into their practical application in road construction. This analysis was centered on the unit costs of each mixture and the performance of each modification in the laboratory tests. The resulting ranking based on cost-effectiveness indicated the relative effectiveness of the mixes compared to one another.

Task 6. Analyze Bio-Remediation and Microbial Degradation Mechanisms

To evaluate the retention of environmental contaminants and microbes within OGFC samples, a modular trickling-flow showerhead reactor (up to ~10 L) was constructed to enable the exposure of asphalt samples to contaminants at varying concentrations and flowrates (up to 1.7 L min^{-1}). The reactor (see Figure 12), which is intended to simulate natural rainfall and infiltration in roadway environments, maintains a recycle-type flow of well-mixed feed solution such that aqueous samples can be extracted periodically to explore temporal variations in contaminant concentration. Feed solutions comprised of sediments, salts, and hydrocarbons were prepared to explore the contaminant removal capability for total suspended solids (TSS), heavy metals, and motor oil, respectively. TSS was quantified according to EPA Method 160.2 (gravimetric, dried at 103-105 °C), heavy metals (lead, copper, zinc, and cadmium) were quantified using inductively coupled plasma mass spectrometry (ICP-MS), and motor oil removal was quantified as the volume fraction of oil remaining in the recycled feed solution after successive exposure cycles.

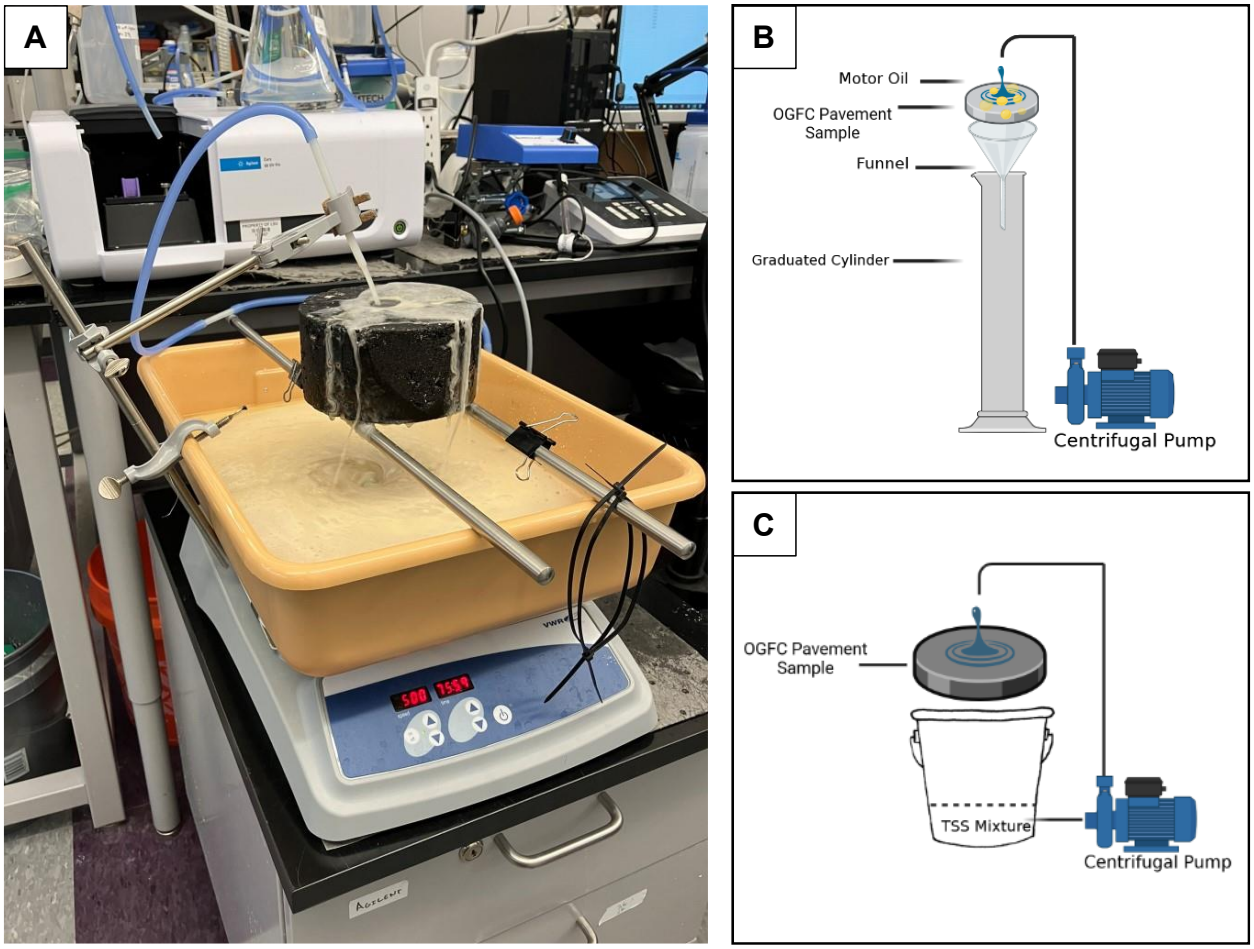

Figure 12. a) Photograph of an Iteration of the Trickling-Flow Showerhead Reactor for Exposure Experiments. Pictured is an Experiment involving a 10 vol% Motor Oil Solution Cycling through a Low-Porosity (DGHMA). Setup Schematics for Filtering b) Suspensions of Motor Oil and c) Suspended Solids Mixtures through OGFC

Task 7. Development of ANN Tool for OGFC Performance Prediction

The objective of Task 7 was to develop an AI-based design tool, which by integrating the OGFC mix volumetric characteristics and the design parameters, will enable designers to predict mix performance without the need for extensive laboratory testing. To develop the AI-based design tool, data were mined from the laboratory test results of this study and other multiple sources and test results available in the literature. Collected data were then used to train and validate a set of Artificial Intelligence (AI) models that can be used in mix performance prediction.

The general workflow of the methodology followed for this task is illustrated in Figure 13. Four main subroutines define the proposed methodology, where the first is based on data collection, and the subsequent three occur as part of the data analysis and design tool pipeline. Each of these subroutines is described in the following paragraphs.

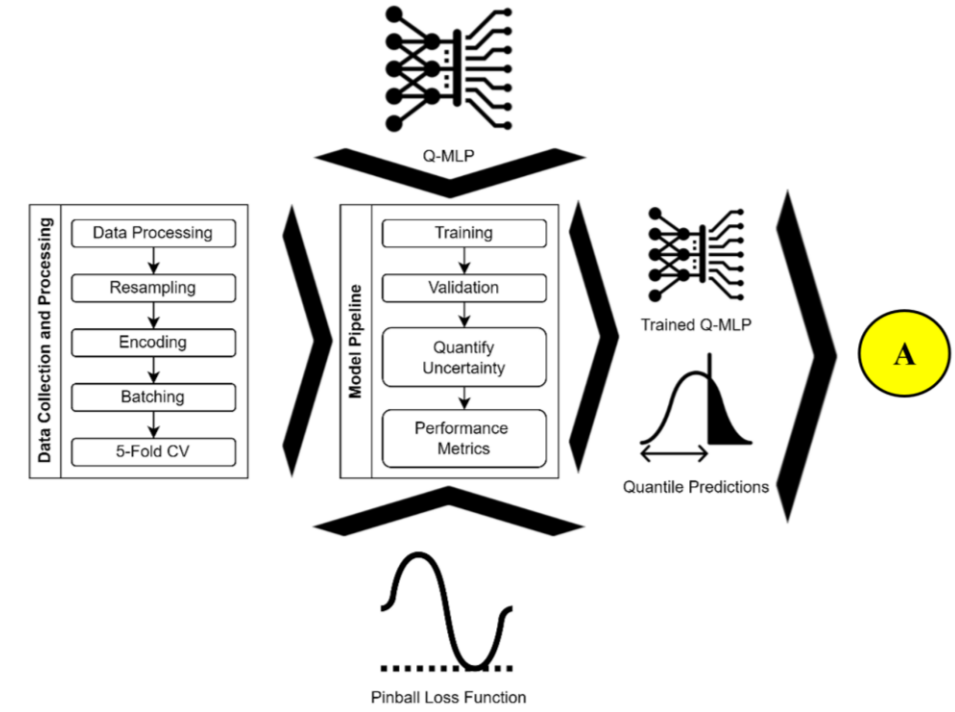

(a)

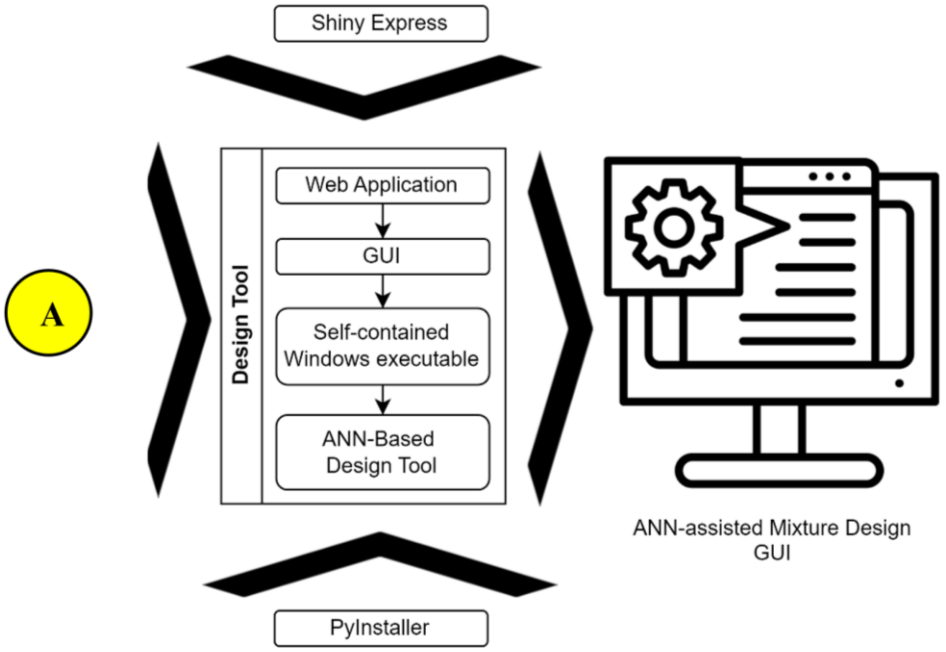

(b)

Figure 13. General Outline of the Research Methodology in Task 7: (a) Development of ANN Model and (b) Development of Design Tool

Data Collection: The first phase involved collecting performance and volumetric properties of OGFC mixes from various sources in the literature as well as from the experimental program of the present study (Tasks 4 and 5). This included gathering information about the design variables to be used in the ANN models. Given the inherent variability, multiple factors can affect the final results and predictions. Most of the performance data collected in this study were obtained from the present study, a recent research study conducted in Louisiana by the research team, and data collected as part of NCHRP 1-55 (Watson et al., 2018). However, additional data can be included in the future to increase the size of the dataset. From these studies, the relevant variables related to OGFC mixtures were used for both design configuration and performance metrics. This extraction process will be explained in detail in a subsequent section. The output of this phase is a dataset containing the relevant configuration metrics that characterize the individual mixes and the independent performance metrics for each measure of the OGFC mixes.

Data Pipeline: This phase encompassed all the data preparation tasks required to transform the collected data into data containers that are enabled to be processed by the ANN training subroutine. The first step, *Preprocessing*, involves processing the raw data and turning it into the appropriate data types for each variable. The second step, *Resampling*, is a necessity born out of the small sample size and the independent specimens for each of the metrics of interest. Resampling involves the creation of all the possible combinations of the individual samples that purposefully quantify the marginal distributions of the metrics of interest for each set of mixture characterization variables. For this, an outer product merging of independent samples in the dataset is performed. This preserves the relative frequency of each of these observations in their underlying independent, identically parameterized (conditional on the inputs) generator distributions.

The next step, **Encoding**, is the translation from the original data to processable variable ranges and formatted into tensor data types, which are to be used in combination with the Deep Learning (DL) library in Python (Ansel et al. 2024). In this step, categorical data is one-hot encoded into binary tensors, with ones corresponding to the presence of a given category and zero to its absence. Continuous data is mapped to floating-point tensors, capable of representing an extensive range of real numbers.

The second to last step, **Batching**, refers to creating mini-batches of data samples that will be used to update the parameters of the ANN by taking the loss function and finding the corresponding gradient for each mini-batch. This process will be repeated for all mini-batches and all training epochs.

The *5-fold CV* refers to randomly splitting the dataset into five subsets of equal size to validate the ANN model and quantify the specified model performance metrics on an unobserved data subset; this will be detailed in the following subroutine about model training.

Model Training: This phase encompasses the model development and training processes. The inputs for this subroutine are three main types. First, the 5-fold data subsets for cross-validation. Second, the designed model for data prediction, the Quantile Multilayer Perceptron (Q-MLP), a DNN model conformed by stacked layers of interconnected neurons that take the input variables and map them to three specified quantiles in the distributions of the output variables: the 2.75% quantile, the 50% quantile, and the 97.5% quantile. Essentially, this configuration allows predictions to be generated for the 95% variation interval and the median of each of the variables of interest.

The last input for this subroutine is the chosen loss function that enables the generation of quantile predictions: The Pinball (quantile) loss function. The details corresponding to the formulation of this loss function and the QMLP model will be presented in a subsequent section. The training process was repeated for each of the five folds by withholding each of them for validation; therefore, the model does not use it for parameter updates. The remaining four folds were used for training, where the model and parameters that observe the output variables' actual values are updated according to the gradients of the loss function. The performance metrics on each validation subset were computed, and an estimate of their variance was generated, thus estimating the uncertainty for model performance on out-of-sample data.

The output of this subroutine is the trained and validated Q-MLP model capable of generating quantile predictions for each output variable. This was the engine that drives the design tool as it allowed for generating credible ranges for the OGFC performance metrics of interest for a given combination of mixture design parameters.

Design Tool: The last subroutine corresponds to the creation of the self-contained, interactive Graphic User Interface (GUI) for the ANN-assisted design tool. The first input to this subroutine is the trained model, used to create predictions for the OGFC metrics of interest based on the mixture design specifications dictated by the target users. The second input, the Shiny Express Python library (Posit 2024), is the framework used to create the interactive and responsive GUI, enabling the users to tune the categorical and continuous options that characterize a hypothetical OGFC sample.

Finally, the last input is the **PyInstaller library** (Cortesi 2024), the framework that enables packing the design tool into a single Windows executable program, allowing users to run the tool by just clicking the executable and interacting with the GUI. This encapsulated all the code running in the background, effectively removing the need for users to interact with any Python code or DL models directly and exposing only the interactive and intuitive tool for assisted OGFC design.

Data Collection and Categorization

The data collected included volumetric properties, design parameters, and OGFC mixture performance metrics. The regression problem of interest involves predicting the performance of an OGFC mixture given a set of volumetric and design parameters in a data-driven fashion while quantifying the uncertainty in the variation of the predictions. The following section describes the input and target variables, resampling, and cross-validation schemes.

The input variables can be represented by $X = \{x_1 \dots x_p\}$ where each x_p is one of the P design characteristics of interest after encoding. For the categorical variables, a one-hot encoding scheme is adopted, resulting in input tensors of size $P = 29$. Denote the number of sets of different design characteristics by N indexed by $i = \{1, \dots, N\}$. In this study, 33 OGFC mixes were collected (N = 33). The set of volumetric properties and design variables (x_p) were as follows:

a. AC: Asphalt Content. Type: Numerical. Units: percentage;
b. Additive: warm mixture additive used. Type: categorical. Categories: None, Zycotherm, Evotherm, Sasobit;
c. Special Materials: filler or other materials used in mixture. Type: Categorical. Categories: None, Sandstone and Limestone, Traprock, Granite, Hydrated Lime, Crumb Rubber;

d. NMAS: Nominal Maximum Aggregate Size. Type: Categorical. Categories: 9.5, 12.5;
e. s_<p>: Passing sieve percentages, where "<p>" represents the size of a given sieve. There are ten variables containing the percentage passing sieves of different sizes. Type: Numerical. The sizes are: 19mm, 12.5mm, 9.5mm, 4.75mm, 2.36mm, 1.18mm, 0.6mm, 0.3mm, 0.15mm, 0.075mm.

These variables can be represented by $Y = \{y_1 \dots y_m\}$ where each y_m is one of the M performance metrics. For this study, $M = 5$, all being numerical, continuous, and non-negative. Each of these variables has n_{im} collected independent data points, potentially varying for each design configuration. For each variable, $n_m = \sum_{i=1}^{N} n_{im}$ represents the total number of samples available across all design subsets. The data samples collected the following performance metrics of interest (y_m):

a. AV: Air Voids. Type: numerical. Units: percentage. $n_m = 171$;
b. Cantabro: Cantabro Loss (Unconditioned). Type: numerical. Units: percentage. $n_m = 99$;
c. TSR: Tensile Strength Ratio. Type: numerical. Units: ratio. $n_m = 99$;
d. Rut5k: Rut Depth at 5,000 passes. Type: numerical. Units: inches. $n_m = 120$;
e. Rut20k: Rut Depth at 20,000 passes. Type: numerical. Units: inches. $n_m = 120$.

Development of Artificial Intelligence Models

The created model, Quantile Multilayer Perceptron (Q-MLP), is a feed-forward, fully-connected ANN with five layers. The input layer had 29 neurons, one for each variable in the input tensor. Then, there were three hidden layers of size 32 and, finally, three parallel output layers of size 5. Each of these parallel layers creates the predictions corresponding to each of the quantiles of interest. All neurons used a Leaky Rectified Linear Unit (LeakyReLU) as their non-linearity, selected by its empirically tested good performance in previous projects.

The selected loss function, the Pinball Loss *(Chung et al., 2021)*, is designed to create predictions for quantiles in the observed target data. In the following equation, adjusted from the original for multiple target variables and quantiles and averaging them uniformly, Q is the set of different quantiles represented by τ_{mq} for $q \in Q$, to be predicted.

$$\mathcal{L}_{Pinball} = \frac{1}{|Q|} \cdot \frac{1}{M} \sum_{m=1}^{M} \sum_{q=1}^{Q} (\hat{y}_{mq} - y_m)(I\{y_m \leq \hat{y}_{mq}\} - \tau_{mq})$$

Equation 8. Pinball loss calculation

The difference in the predicted value, $\hat{y}_{mq}$, and the actual value, y, is signed and weighted depending on whether the predicted value exceeds or not the actual value in that quantile. For this study, the quantiles selected were 2.5%, 50%, and 97.5%. The 50% is the median, our surrogate for point estimates, and the other two complete the 95% confidence interval.

Chapter 4. Results and Analysis

This section presents and interprets the laboratory test results obtained in this study. The performance of the selected mixes was evaluated at the mix production, pavement construction, and field performance stages, with the corresponding results discussed in this section. A description of the fabricated mixtures evaluated in this study is presented in Table 8.

Table 8. Description of the Evaluated Mixes

Mixture ID	Mixture Description
CM	Standard OGFC mix prepared with PG 76-22
RAP	OGFC mix with PG 76-22 binder and partial aggregate replacement using 7% RAP
SS	OGFC mix with PG 76-22 binder and partial aggregate replacement using steel slag
RWP	OGFC mix with PG 76-22 binder and partial aggregate replacement using RWP
HL	OGFC mix with PG 76-22 binder and partial aggregate replacement using HL
HiMA	OGFC mix prepared with highly-modified asphalt binder

The results of the laboratory experiment were analyzed using ANOVA and Tukey's HSD grouping, both at a 95% confidence level. This approach was used to test the null hypothesis that performance indicators for each mix were statistically equivalent. A significance value (α) of 0.05 was assumed indicating a maximum probability of 5% failing to detect real differences.

In the analysis, statistical differences between mixtures were identified by assigning letters (A, B, C, etc.) to represent distinct performance groups. A mixture labeled with "A" represents the best-performing group. If mixtures are labeled with different letters (e.g., A, B, C), it indicates that these groups are statistically different from each other in performance, with later letters (B and C) indicating progressively lower performance rankings. While the mixtures labeled with the same letter (e.g., "A") are not significantly different in their performance, mixtures labeled with two letters (e.g., A/B, B/C) indicate that these groups do not have significant differences from either of the adjacent groups (A and B, or B and C). Therefore, an A/B group is not significantly different from both group A and group B, while a B/C group is not significantly different from both group B and group C. Laboratory results were compared and grouped using this approach to highlight significant performance differences among the mixes.

Air Void Content

Figure 14 presents the air void considered for the six OGFC mixes evaluated in this study. The incorporation of RAP and SS increased the air void content, while replacing aggregate with HL and RWP reduced the air void content. Substituting the PG 76-22 binder with HiMA also led to a decrease in air void content, though the reduction was not very significant. Among all the mixes, the OGFC mix with RAP exhibited the highest air void content (23.5%), whereas the mix with RWP had the lowest (20.7%). Despite these variations, all the mixes met the air void limits specified by LaDOTD (18 to 24%) and NCHRP guidelines (≥15%) (Watson et al. 2018).

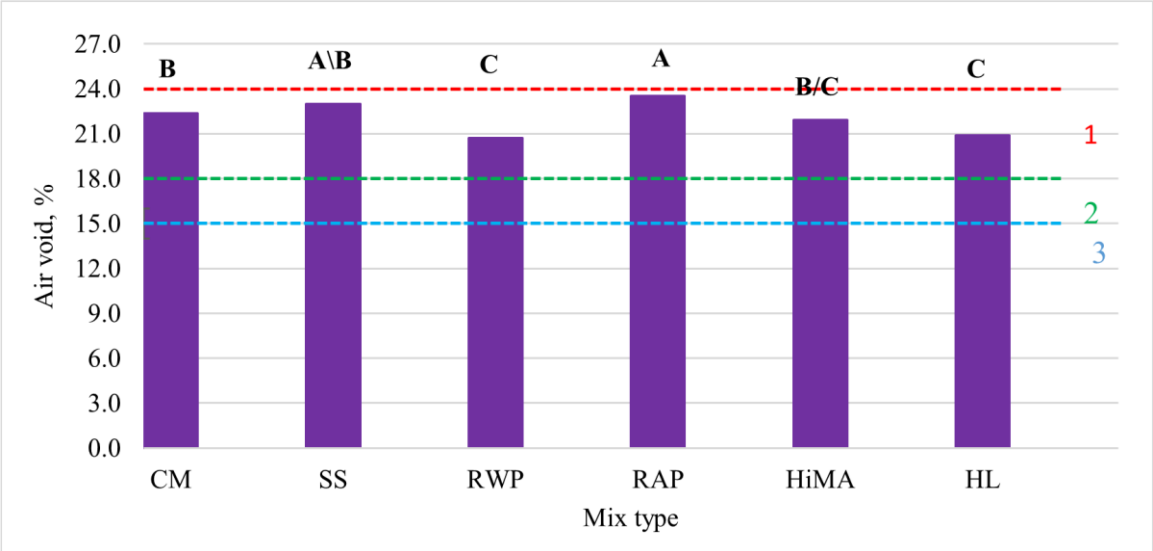

[1] Maximum LaDOTD requirement; [2] Minimum LaDOTD requirement, [3] Minimum NCHRP requirement

Figure 14. Air Void Content of the Evaluated OGFC Mixes

Permeability

Figure 15 presents the permeability coefficients (k) for the various OGFC mixes. While the incorporation of SS and RAP as aggregate replacement increased the permeability, the addition of HL, RWP, and HiMA resulted in reduced permeability. The OGFC mix modified with RAP exhibited the highest permeability at 380 ft/day, while the mix with HL slurry showed the lowest permeability at 234 ft/day. Despite the variations, all the permeability values met the NCHRP requirements. According to NCHRP Report 1-55, a minimum permeability value of 164 ft/day is sufficient for OGFC to function effectively (Watson et al. 2018). It is also worth noting that the permeability coefficient values aligned with the trend of air void contents presented in Figure 14.

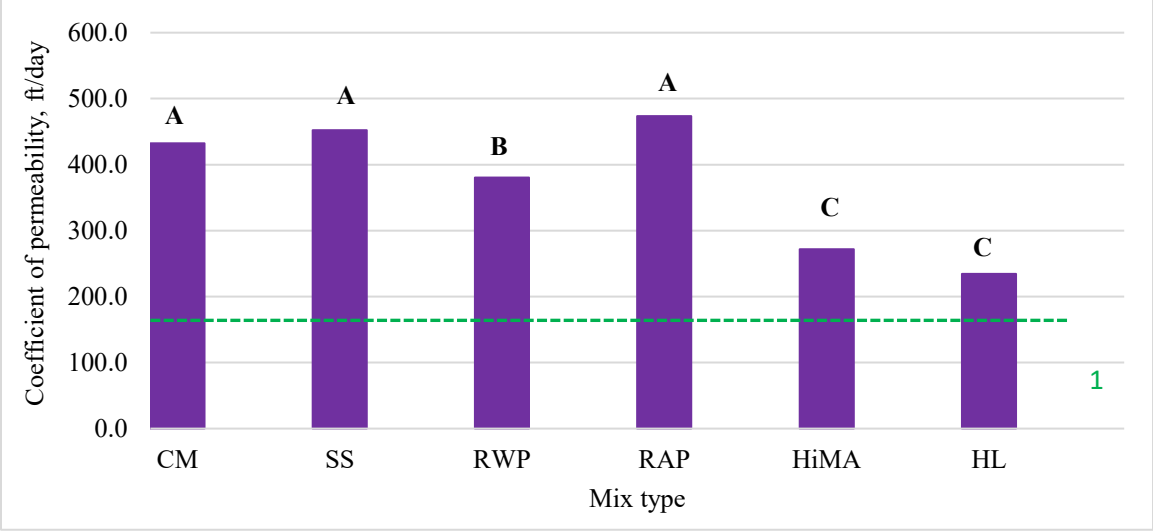

[1] Minimum NCHRP requirement

Figure 15. Permeability Coefficient of the Evaluated OGFC Mixes

Draindown Test Results

Figure 16 presents the results of the draindown test for the evaluated OGFC mixtures. The results show that although the incorporation of HiMA and RWP did not result in significant changes in binder draindown percentages, draindown slightly increased compared to CM for these two modifications, even though the values remained well within the maximum allowable limit of 0.3%. On the other hand, binder draindown significantly decreased for SS, RAP, and HL-modified mixes, indicating that these modifications enhanced binder viscosity and adhesion to the aggregate. This improvement promotes better binder retention within the mix and minimizes the likelihood of draindown.

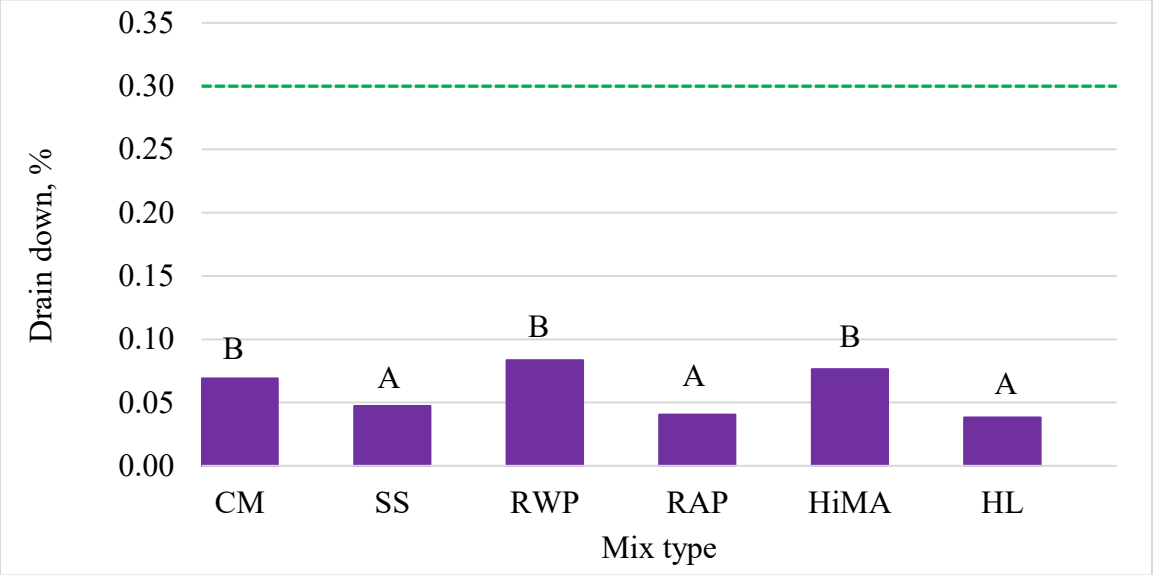

Figure 16. Draindown Test Results for the Evaluated OGFC Mixes

Compaction Energy Index

Figure 17 presents the compaction energy indices for the evaluated OGFC mixtures. The CM had the highest compaction energy index among all the evaluated mixtures, which indicates that the control mix would require more compaction effort and energy consumption during the compaction stage as compared to the modified mixes. In contrast, RAP, HL and HiMA-modified OGFC mixes required significantly lower compaction energy, likely due to the binder characteristics of these modifications. The compaction energy index for the SS and RWP-modified OGFC did not differ significantly from the CM, indicating that these modifications had a minimal impact on the compaction effort.

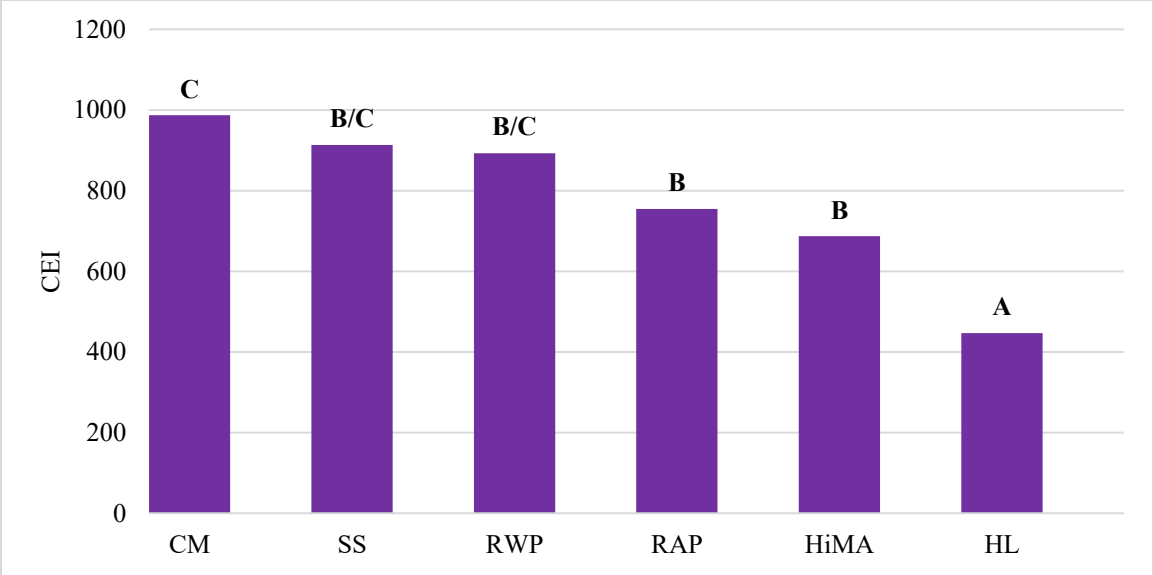

Figure 17. Compaction Energy Index (CEI) for the Evaluated OGFC Mixes

Cantabro Abrasion Test Results

Figure 18 presents the results of the Cantabro loss test, which was conducted to evaluate the raveling resistance and durability of the OGFC mixtures. The findings reveal that RAP and HiMA-modified OGFC mixes exhibited substantially lower Cantabro loss compared to the CM, indicating improved durability and resistance to raveling. On the other hand, the OGFC mixes incorporating SS, RWP and HL did not exhibit a significant change in Cantabro loss relative to the control mix. Only the RAP and HiMA-modified OGFC mixes achieved Cantabro losses below the 20% limit set by the NCHRP. As shown in Figure 18, HiMA-modified OGFC showed excellent performance with only 4.7% aggregate loss, while the RAP-modified OGFC had an aggregate loss of 6.7%, both within the allowable limit. Conversely, RWP demonstrated a Cantabro loss of 23.0%, which was almost the same as the control mix, 23.3%. The steel slag-modified mix exhibited the highest loss at 24.4%, slightly higher than the control mix, but the difference was not significant according to ANOVA and Tukey's HSD test. The hydrated lime-modified OGFC had a Cantabro loss of 21.5%, which is lower than the control mix but above the NCHRP limit of 20%. Despite the reduction in Cantabro loss observed in the RWP and HL-modified mixes, only HiMA and RAP performed within the NCHRP limits for OGFC mixtures.

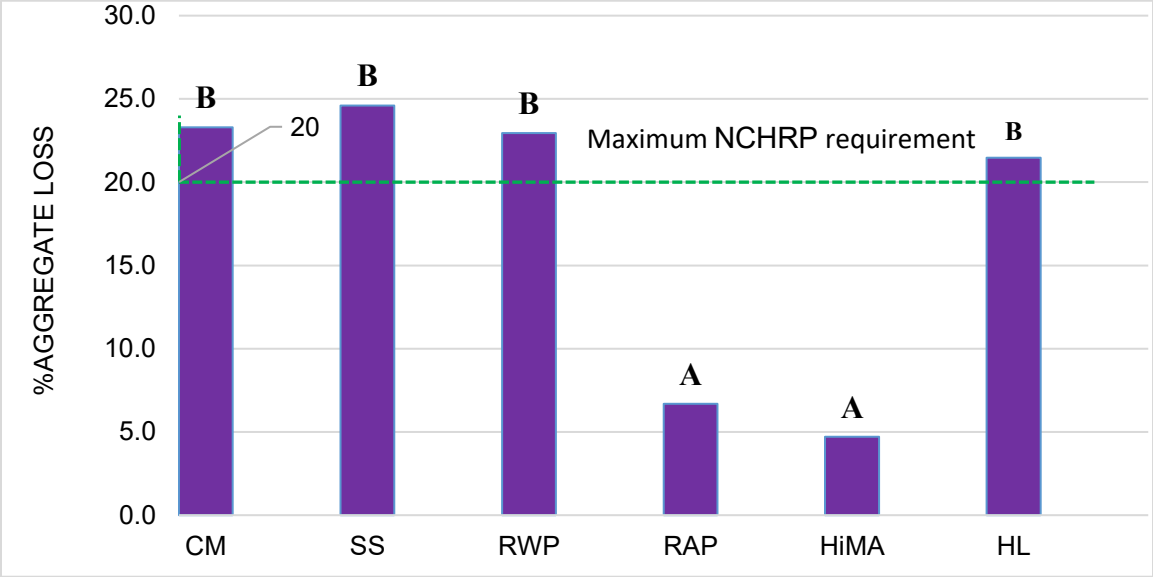

Figure 18. Cantabro Abrasion Test Results for the Evaluated OGFC mixes

Hamburg Wheel Tracking Test Results

Figure 19 summarizes the results of the rutting performance test using the Hamburg Wheel Tracking Test (HWTT). In general, compared to the CM, all of the modified OGFC mixes exhibited better rutting performance. However, steel slag and hydrated lime significantly improved the rutting resistance. This enhancement can be attributed to the higher polishing resistance of steel slag and the enhanced adhesion strength provided by the hydrated lime between the binder and the aggregate of the OGFC mix.

Figure 19(a) shows the rut depth results of the OGFC mixes at 5,000 passes. While the SS-modified mix achieved the lowest rut depth of 6.55 mm, the CM exhibited the highest rut depth of 8.70 mm. All the modified mixes improved the rutting resistance compared to CM and met the LaDOTD criterion of less than 12 mm rut depth after 5,000 passes. Figure 19(b) presents the rut depth of the evaluated mixes after 20,000 passes. SS and HL showed improved rut resistance, both achieving rut depths below the NCHRP limit of a maximum of 12.5 mm rut depth after 20,000 passes. Both RWP and HiMA-modified mixes also met the NCHRP rutting performance criteria after 20,000 passes. While RAP failed to meet the NCHRP limit after 20,000 passes, all the modified mixes including RAP performed comparatively better than the CM. These results indicate that the modified OGFC mixtures provided enhanced resistance to rutting compared to the control mix, making them viable candidates for asphalt pavement applications.

Figure 19(c) displays the rut depth vs. number of passes for all the mixes, illustrating the trend in rut depth as the number of passes increases. As observed, none of the mixes reached the tertiary creep region, which is characterized by a rapid and significant increase in rut depth over a relatively short number of passes. Yet, both the CM and RAP mixes exhibited excessive rut depth after 20,000 passes.

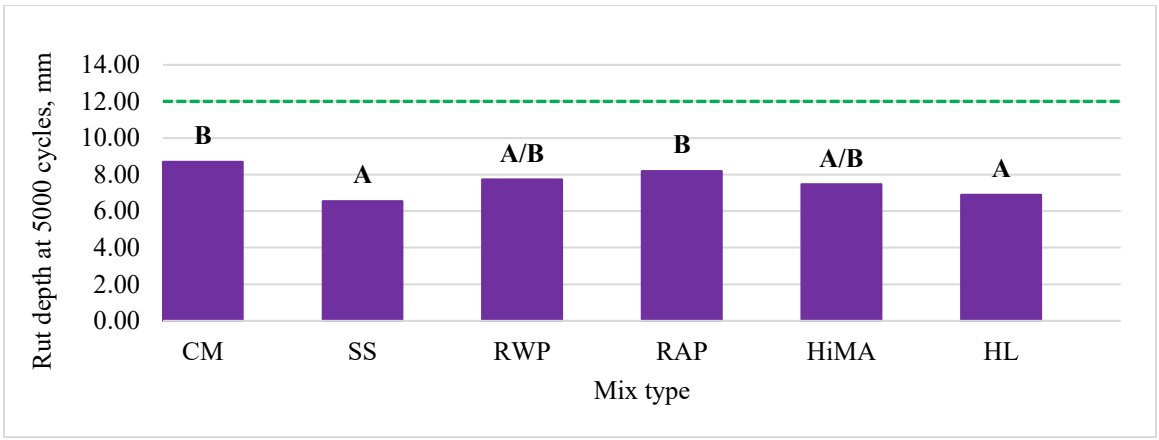

(a)

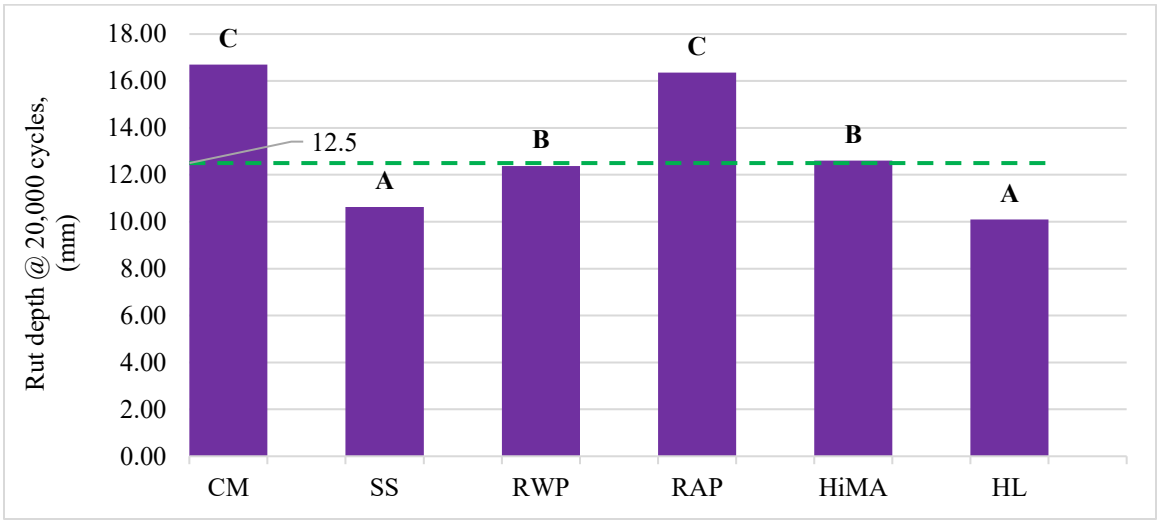

(b)

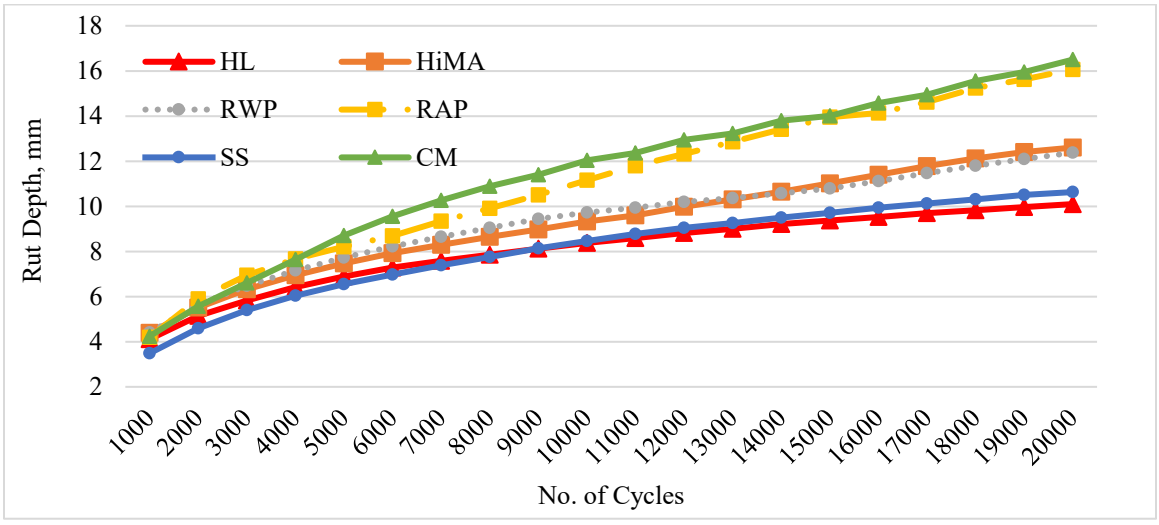

(c)

Figure 19. HWTT Test Results for the Evaluated OGFC Mixes: (a) Rut Depth at 5,000 Passes; (b) Rut Depth at 20,000 Passes; and (c) Rut Depth versus Number of Passes

IDEAL-CT

Figure 20 illustrates the IDEAL-CT test results, which were conducted to evaluate the cracking resistance of the OGFC mixtures at intermediate temperatures. The findings demonstrate that the mixes incorporating SS, RWP, RAP and hydrated lime exhibited significantly higher CT indices compared to the CM, suggesting improved resistance to cracking.

Among the tested mixes, the HL-modified and HiMA-modified OGFC mixes achieved the highest CT index of 450 and 395, indicating superior resistance to cracking. These results highlight the added strength and durability provided by the HL in the mix and the highly-modified asphalt binder. Although there is currently no consensus on a CT index threshold for OGFC mixes, the Virginia Department of Transportation (VDOT) has recommended a minimum CT index value of 70 for short-term aged asphalt surface mixes to mitigate cracking susceptibility (Habbouche et al. 2021), while the Tennessee Department of Transportation (TDOT) set the minimum requirement for CT index at 100 (Le et al. 2024) and Texas has recommended a minimum CT index of 65 for dense-graded asphalt mixtures (Mogawer 2019). All the modified OGFC mixtures in this study exceeded or met these thresholds, signifying their potential to offer enhanced cracking resistance in field applications.

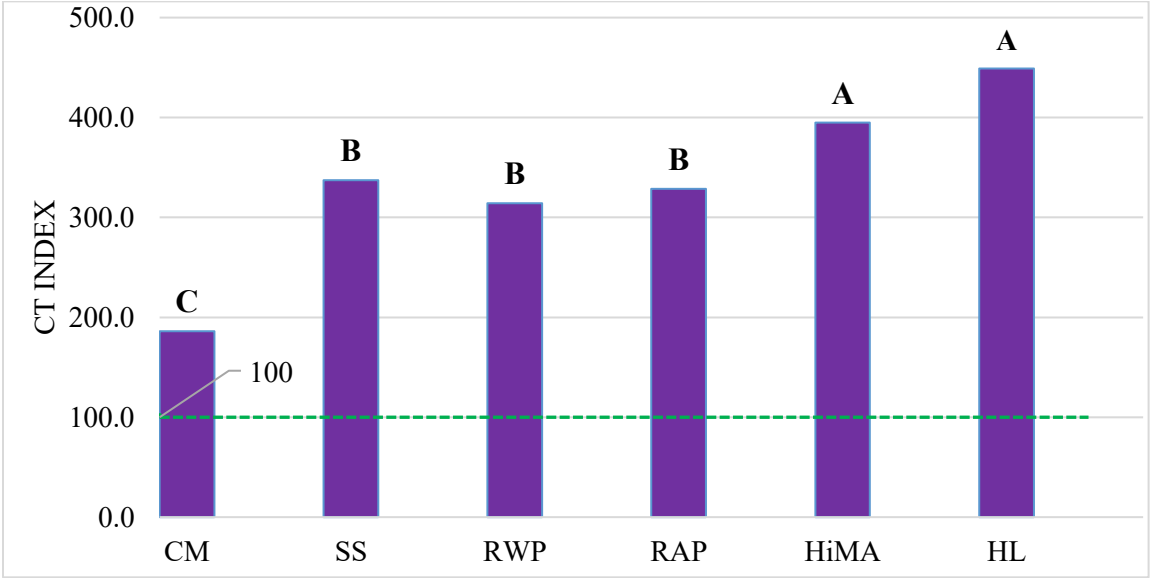

Figure 20. Test Results of IDEAL-CT for the Evaluated OGFC Mixes

Modified Lottman Test Results

Figure 21 illustrates the results from the Modified Lottman test, which was used to assess the moisture susceptibility of the OGFC mixtures by evaluating the Tensile Strength Ratio (TSR), which was calculated as the ratio between the conditioned Indirect Tensile Strength (ITS) and unconditioned ITS. Figure 21(a) shows the results for unconditioned ITS. RAP and hydrated lime-modified OGFC mixtures exhibited a significant increase in dry ITS, surpassing the NCHRP minimum limit of 70 psi, while steel slag-modified OGFC also improved dry ITS, though just meeting the threshold. Although HiMA and RWP modified mixes demonstrated higher dry ITS values compared to the CM, neither of these modifications met the NCHRP minimum requirement.

Figure 21(b) presents the conditioned (wet) ITS values. In this case, the OGFC mixtures modified with RAP, HL, SS, and RWP exhibited substantial improvements in wet ITS, with all three modifications surpassing the NCHRP minimum requirement of 50 psi. HiMA-modified mixes also improved the wet ITS, satisfying the NCHRP minimum value. Figure 21(c) presents the TSR, a critical parameter for evaluating moisture resistance. All the modified OGFC mixes met the ASTM minimum requirement of 0.80. However, among the modified mixtures, RWP and HL demonstrated the highest improvements in moisture resistance, performing better than the control mix and the other modifications in this test.

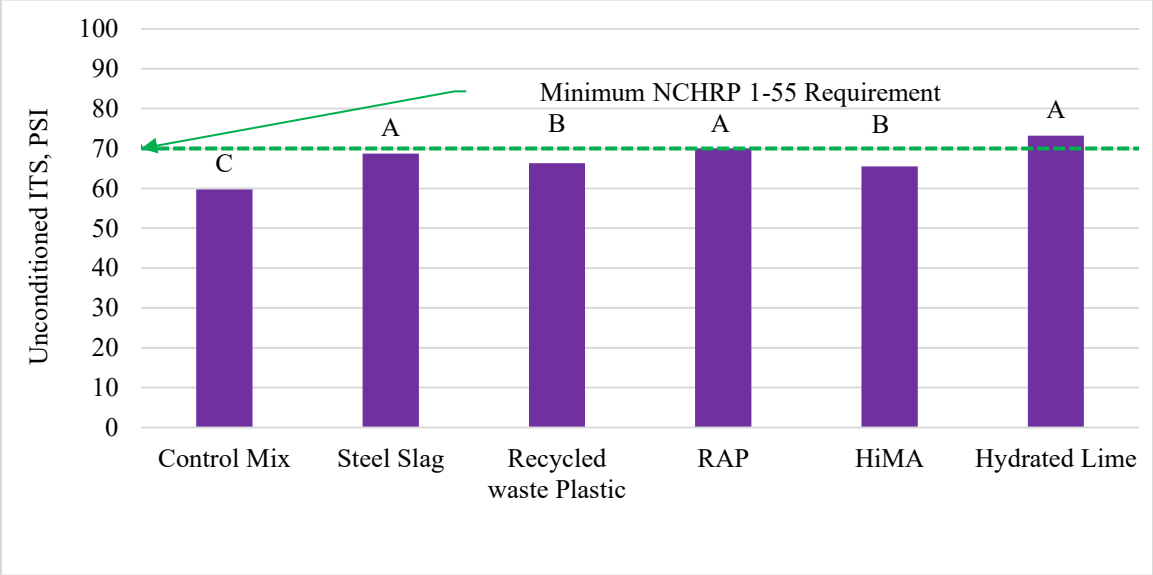

(a) Unconditioned ITS

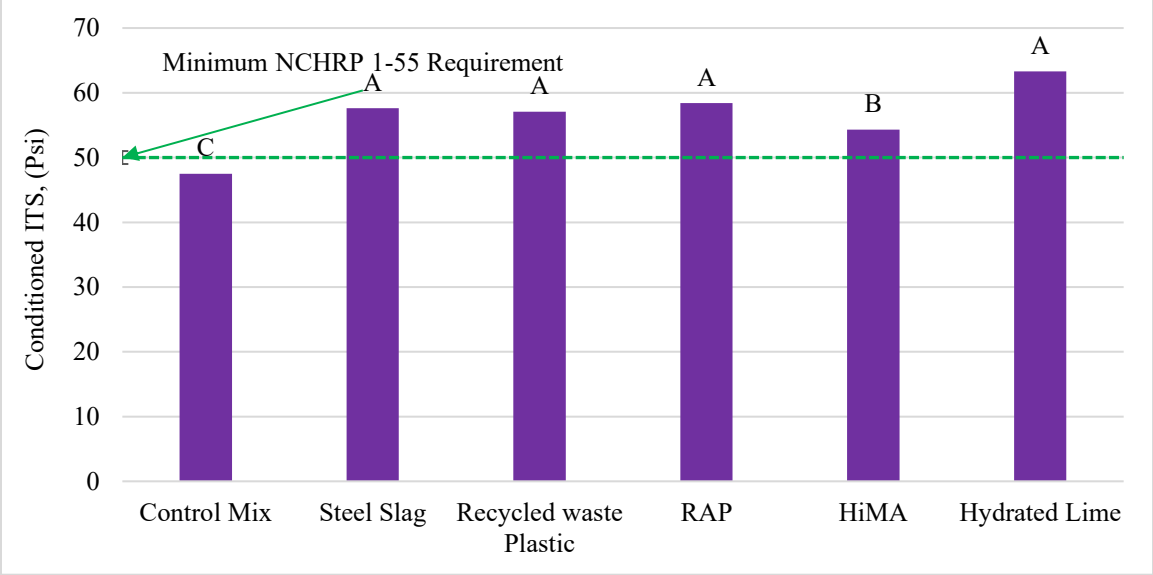

(b) Conditioned ITS

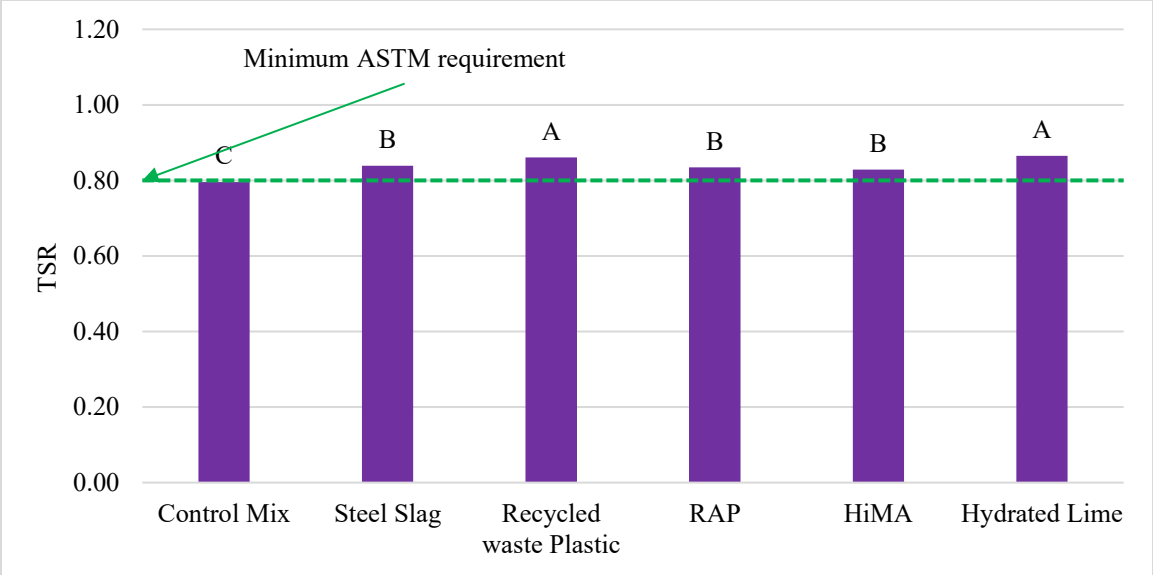

(c) Tensile strength ratio

Figure 21. Modified Lottman Test Results for the Evaluated OGFC Mixes

Bitumen Bond Strength Test Results

Figure 22 illustrates the measured adhesive strength across different filler materials under both dry and wet conditions, using the BBS test. The BBS test evaluates the percentage loss in pull-off tensile strength between these two conditions, providing insights into the impact of filler materials on binder adhesive strength. Figure 22(a) compares the pull-off tensile strengths of the various mixes in both dry and wet conditions. As shown in this figure, HiMA had the highest pull-off tensile strength for both conditions, highlighting its superior binder adhesion capacity. This was followed by RAP, which also showed strong adhesive properties. HL offered a moderate improvement in pull-off tensile strength, though the increase was only marginal compared to RWP, which showed minimal effect. SS, however, did not demonstrate any significant improvement over the control mix for either dry or wet conditions.

Figure 22(b) presents the percentage loss in pull-off tensile strength, a key measure of binder bond strength. HiMA, HL, and RAP all showed significant improvements in binder bond strength, with reduced % loss in tensile strength, indicating better moisture resistance. However, steel slag slightly deteriorated the % loss in pull-off tensile strength, showing a small decrease in bond strength compared to the CM, though results were not statistically significant.

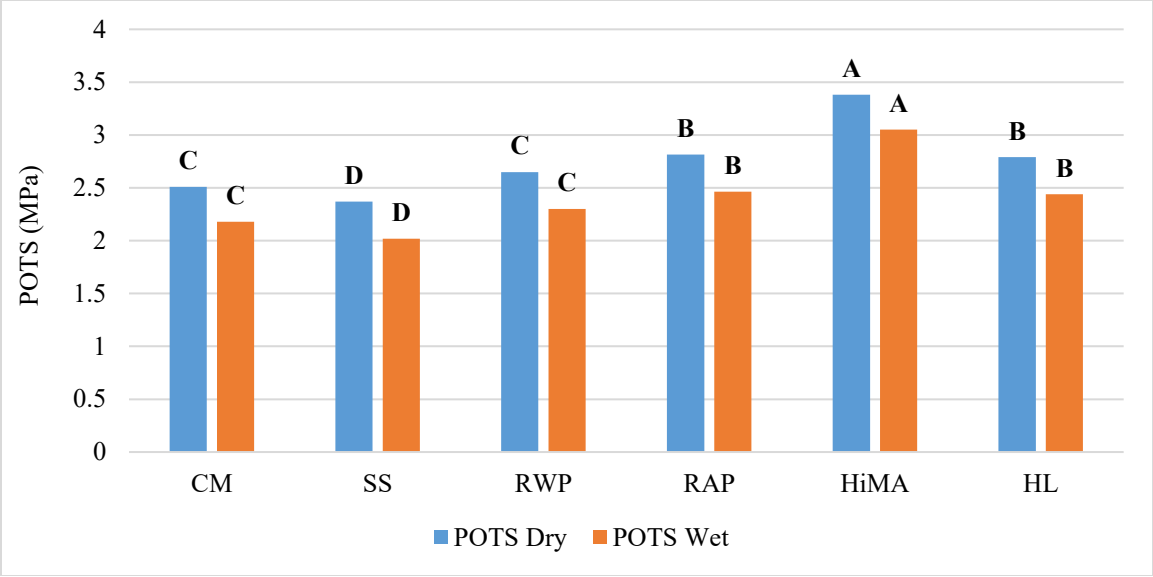

(a)

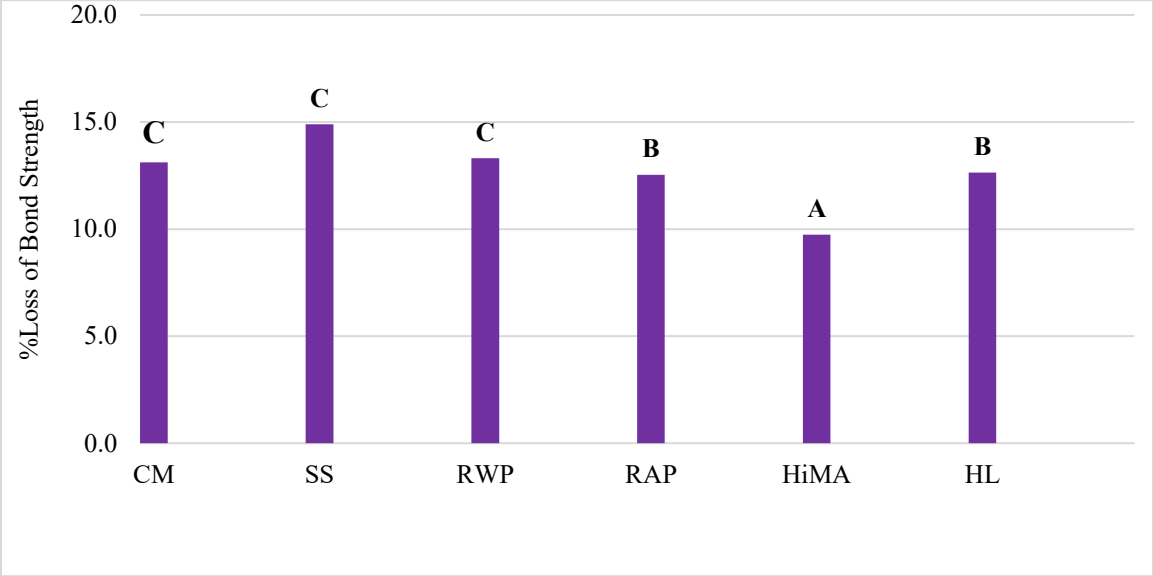

(b)

Figure 22. Pull-Off Tensile Strength Test Results; (a) Pull-Off Tensile Strength under Dry and Wet Conditions (b) Loss of Bond Strength

Bio-Remediation and Microbial Degradation Mechanisms

Figure 23 presents the comparative water retention results, which were obtained diagnostically to evaluate the interconnectedness of the sample pore network. As shown in this figure, OGFC exhibits a high capacity to host biofilms, which can be leveraged for bioremediation applications. This is primarily due to the large pore spaces present in the sample when compared to traditional asphalt. These pore spaces are irregular in shape and size, thereby presenting an

opportunity for the formation and growth of smaller, independent biofilm colonies as well as larger networks throughout the material.

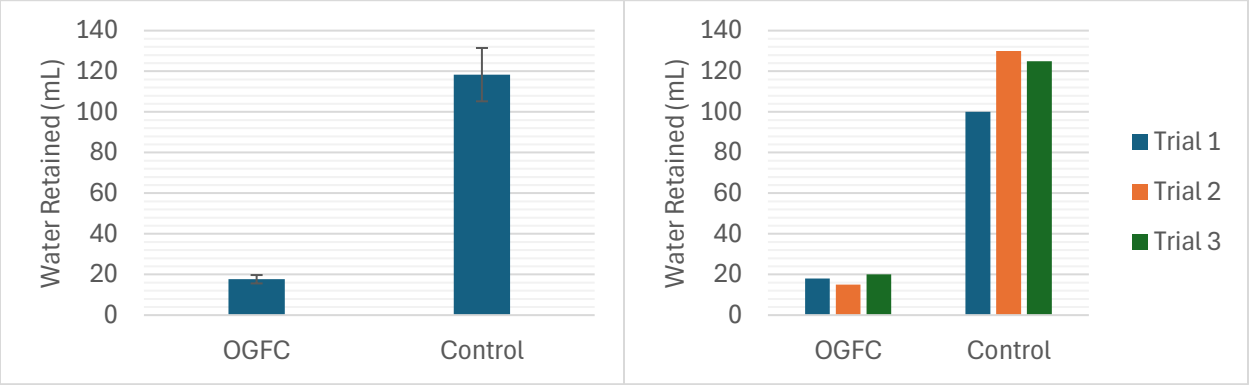

Figure 23. Water Retention Testing Results with an Indirect Comparison of the Porosity and Hydrophilicity OGFC and Dense-Graded Mix

Figures 24 and 25 show the analysis of metals removal by OGFC samples during trickling flow exposure experiments. Over a 4-hour period, aqueous solutions of metal chloride salts were filtered through the samples to simulate natural rainfall and infiltration in roadway environments. Of the four metals analyzed (lead, copper, zinc, and cadmium), zinc showed the largest reduction in relative concentration. However, the rate of metal removal over time shows that while the relative concentration reduction was higher for zinc, the largest mass reduction was observed for copper. These differences are likely due to variations in metal adsorption affinity based on the chemical functional groups present on the sample surface.

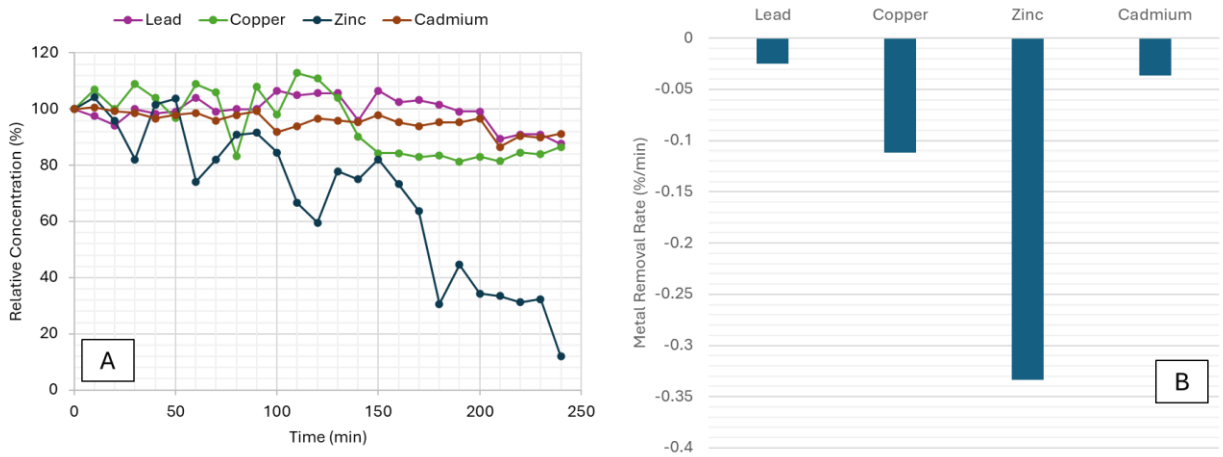

Figure 24. A) Analysis of Metals Removal by OGFC Samples during Trickling Flow Exposure Experiments, and B) the Rate of Metal Removal over Time

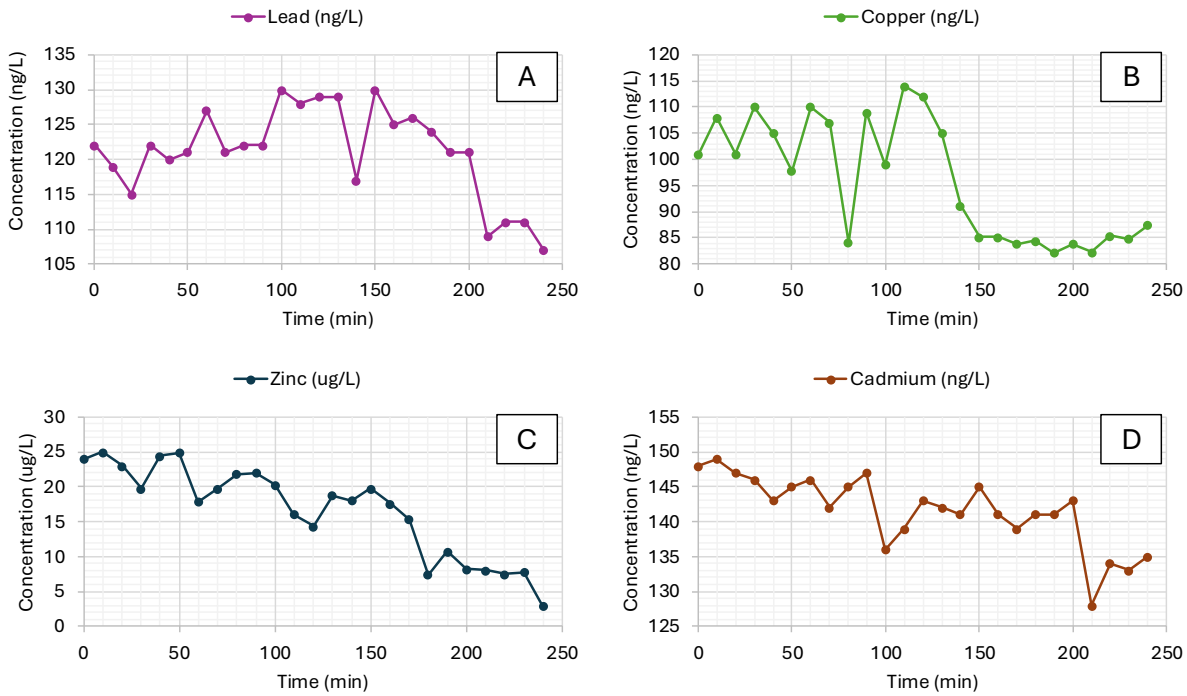

Figure 25. Concentrations of Metals Analyzed during a 4-hour Trickling-Filter Exposure Test to Analyze the Potential for Adsorbing A) Lead, B) Copper, C) Zinc, and D) Cadmium to OGFC Samples

Figure 26 shows the total suspended solids (TSS) retention analysis results. It was observed that the concentration of TSS (300 µm average particle size) within the reactor for the OGFC and control sample are reduced by more than 70% and 80%, respectively within a 1-hour test. This further confirms the influence of porosity and pore size on the contaminant removal prospects of porous asphalt.

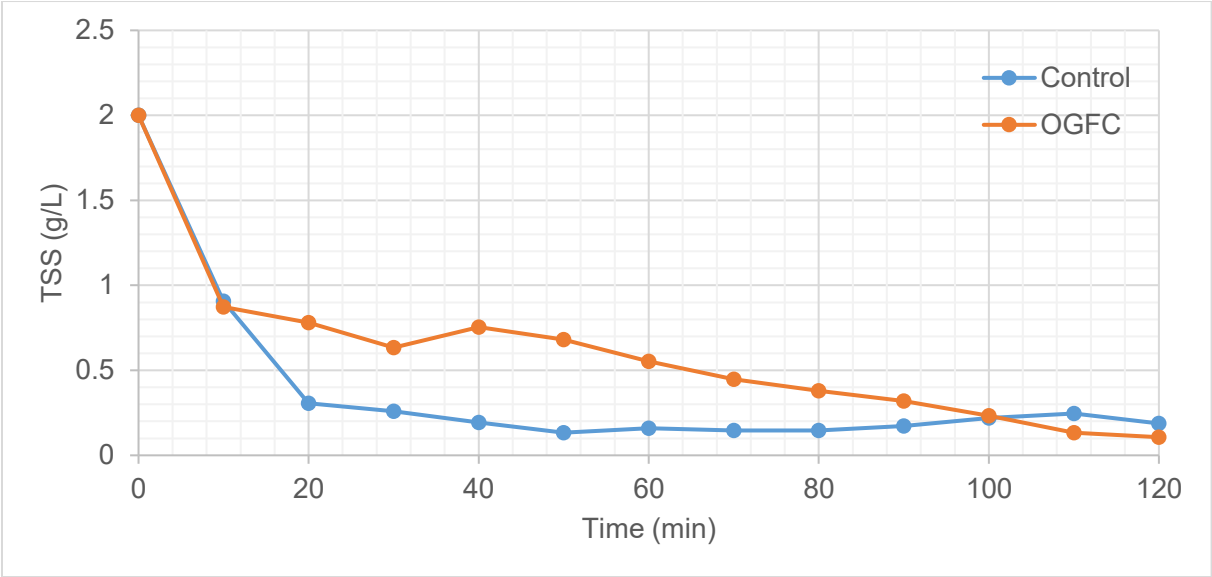

Figure 26. Total Suspended Solids (TSS) Concentration over time for a 2-hour Looped-exposure Trial for Each Sample.

Figure 27 shows the large variation in motor oil retention when comparing the OGFC to the control sample. Due to the much tighter pore structure of the control sample, no oil was able to penetrate through the control sample to be collected as effluent when 0.045 vol% oil/water emulsion was used as feed solution. Therefore, the OGFC sample will be a much more suitable candidate for hydrocarbon degradation once biofilm formation takes place within the sample pores.

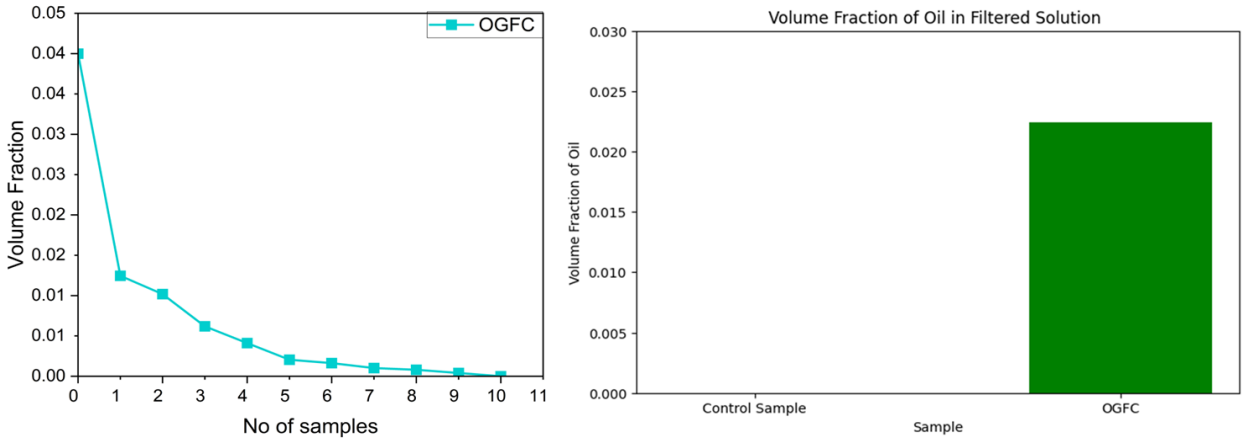

Figure 27. Motor Oil Removal Results for Control and OGFC Samples

Cost Effectiveness Analysis

A cost-effectiveness analysis was conducted to evaluate the economic feasibility of the mixture modifications, offering valuable insights into their practical application in road construction. This analysis was based on the unit costs of each mixture and the performance of each mixture in the experimental program. The resulting ranking based on cost-effectiveness indicates the relative cost-effectiveness of the mixes compared to one another. This study opted for a simple approach where the production cost of the mixture was divided by its expected performance. Because this study focused on key performance factors such as cracking, rutting, durability, and moisture resistance; the results of the CT index, rutting depth, % Cantabro loss, and TSR were used as performance indicators to estimate the cost-effectiveness of the evaluated mixtures. The following equation was used to calculate the cost-effectiveness (CE) of a given mixture:

$$CE_i = \frac{E_i}{C_i} x100$$

Equation 9. Cost-effectiveness calculation

Where,
E_i = Expected effectiveness
C_i = Unit cost of the mixture (per ton)

The expected effectiveness (performance) of a given mix, Ei, was determined using the following equation:

$$E_i = \frac{CT_i}{CT_{max}} + \frac{\frac{1}{Rut\ Depth_i}}{\frac{1}{Rut\ Depth_{max}}} + \frac{\frac{1}{\%\ Cantabro\ loss_i}}{\frac{1}{\%\ ACantabro\ Loss_{\max}}} + \frac{TSR_i}{TSR_{\max}}$$

Equation 10. Effectiveness calculation method

Where,
CT_i = mixture CT-index value
CT_{max} = maximum CT-index value observed among all the mixes
Rut $Depth_i$ = mixture rut depth value
Rut $Depth_{max}$ = maximum rut depth value observed among all the mixes
% Cantabro $Loss_i$ = mixture Cantabro loss value (%)
% Cantabro $Loss_{max}$ = maximum Cantabro loss value (%) observed among all the mixes;
TSR_i = mixture TSR value
TSR_{max} = maximum TSR value observed among all the mixes

Based on Equation (9), the asphalt mixture, which provides the highest CE value i.e., the highest ratio of performance to cost, as compared to other mixtures, is the most cost-effective mixture. The cost of OGFC can vary significantly due to factors such as material sourcing, production processes, and transportation. For this study, the estimated initial costs per ton for various modified OGFC mixes were derived from data available through different sources (Vargas-Nordcbeck and Musselman 2021; Elnaml et al. 2024). The initial estimated costs for the modified OGFC mixes were as follows: OGFC with steel slag at $140.00 per ton, OGFC with RWP at $160.00 per ton, OGFC with RAP at $138.00 per ton, OGFC with HiMA at $165.00 per ton, and OGFC with hydrated lime at $152.00 per ton. On the other hand, the initial production cost of the control mix was $150.00 per ton.

Figure 28 provides a comparison of the cost-effectiveness results for all OGFC mixtures alongside the control OGFC mix. The analysis revealed that the OGFC prepared with HiMA demonstrated the best cost-effectiveness, significantly outperforming all other mixes. While RAP emerged as the second most cost-effective modification for OGFC, partially replacing aggregate with SS and RWP, using HL as slurry for OGFC modification also resulted in significantly higher cost-effectiveness compared to the control mix. Overall, the cost-benefit analysis confirmed that all the proposed modification approaches are viable solutions to enhance OGFC performance with RAP and highly-modified asphalt binder (HiMA) being the most effective.

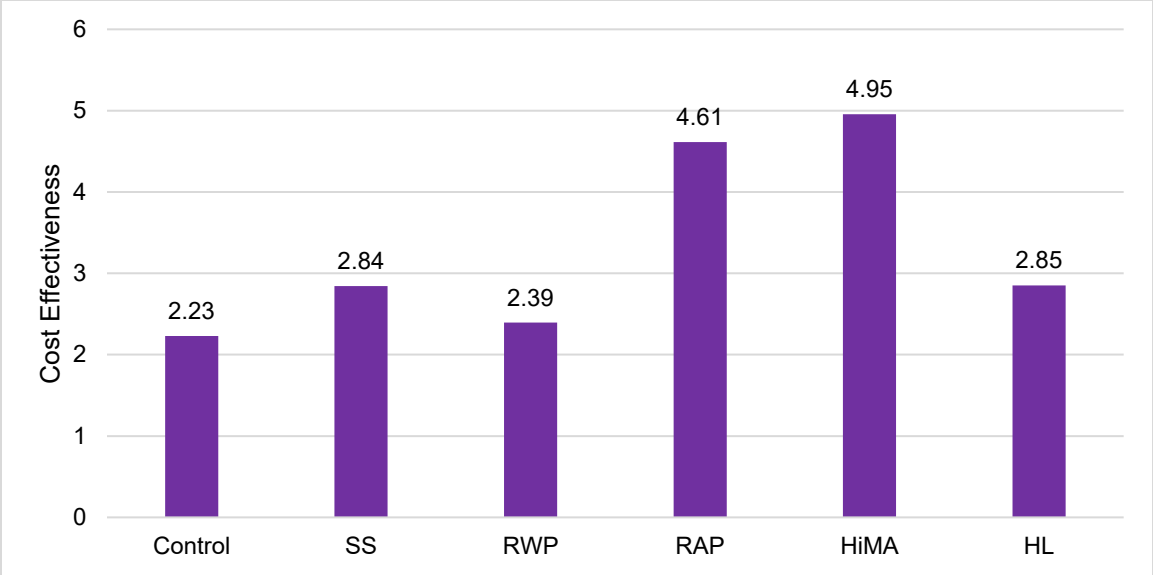

Figure 28. Cost Effectiveness of the Evaluated OGFC Mixtures

Development of ANN Tool for OGFC Performance Prediction

AI Model Accuracy

The Q-MLP model was implemented using PyTorch and validated using a 5-fold cross-validation approach. In this process, at each iteration, four folds were used for training (parameter updates), while the fifth fold was reserved as the validation set to compute performance metrics. A run of 50 epochs was performed for each fold. During each epoch, the model processed the entire training set in mini-batches of size 128. After completing training on a fold, the validation metrics were computed before proceeding to the next fold.

The Pinball Loss function was used as the objective to optimize parameter updates, applied uniformly across five target variables and three quantiles. The Adam optimizer was employed with a learning rate of 1×10^{-4}. The learning rate scheduler was configured to halve the learning rate exponentially every ten epochs. To prevent data leakage and ensure reliable results, the optimizer parameters, scheduler, initial random weights of the network, and gradient computations were reset at the start of each fold.

Four metrics were used to evaluate model performance on the validation folds, with uniform weighting across the five target variables. The first metric, R-squared, quantified the proportion of variance in the actual values explained by the predicted values, where higher scores indicated better performance. The second metric, Root Mean Squared Percent Error (RMSPE), assessed the average absolute percentage difference between predicted and actual values, with lower scores being preferable. The third metric, the 95% Confidence Interval (CI) Coverage, evaluated the percentage of observations included in the confidence interval, ideally achieving a value close to 95%. The fourth metric, Pinball Loss, measured the quantile regression loss, where lower values indicated better model performance. For each metric, the

average and standard deviation were computed across all folds to assess consistency. Table 9 summarizes the cross-validation results after training the model for 50 epochs.

As shown in Table 9, the average R-squared was 0.9, consistent across folds. This shows good predictive capabilities. The RMSPE shows an average error of 10.83% across all target variables. The standard deviation, 0.09%, also indicates good consistency across folds. The coverage of the Confidence Intervals (CI) suggests that the prediction intervals are successful as, even in the cross-validation folds, 95.14% of the data is contained between the predicted bounds. Finally, the Pinball loss is, on average, 0.032 across all target variables and generally consistent across folds.

Table 9. Cross-validation Model Performance Metrics

Fold	R-squared (ŷ=median)	RMSPE (ŷ=median)	95% CI Coverage	Pinball Loss
1	0.9008	10.70%	95.21%	0.032
2	0.9025	10.87%	95.25%	0.032
3	0.9041	10.94%	95.07%	0.032
4	0.9039	10.78%	95.08%	0.031
5	0.9059	10.88%	95.09%	0.032
Avg.	0.9034	10.83%	95.14%	0.032
Std. Dev.	0.0019	0.09%	0.08%	0.0003

Overall, the results show good predictive power, as the cross-validation variances in the metrics are low, and the performance averages move in the desired direction—however, more efforts to avoid overfitting need to be explored for future work. For example, applying batch normalization or dropout layers is a future alternative. Improving the resampling and cross-validation schemes are also valid directions as, in the current approach, more solid guarantees are needed to avoid data-leakage across resampling combinations. Another future direction includes the optimization of hyperparameters, both in the model architecture and the training scheme. Finally, while this ANN model has shown promising results, more sophisticated methods such as Generative Adversarial Networks (GANs) augment data samples could also be explored in the future.

Design Tool Development

The developed GUI for the design tool is based on a web application that runs its backend using Python. It was built on a Shiny Express framework integrated with Python and uses the trained ANN model to generate predictions based on user inputs. This self-contained application includes all the required Python libraries to execute as a standalone desktop application, using PyInstaller to generate a single executable file. The user can select to generate performance predictions for different combinations of inputs, as shown in Figure 29. The input values are specified using radio buttons and sliders. The latter is used for continuous inputs, and the former is used for categorical inputs. This GUI is designed so that a practitioner or contractor does not need to interact with the underlying code or models to conduct an ANN-assisted design process.

The passing sieve percentages have been configured such that the passing percentage of a larger sieve affects the actionable upper limit of a smaller sieve in a sequence defined by the order of sizes. In this way, the selection of the 19 mm sieve affects the upper limit of the 9.5

sieve, the 9.5 sieve affects the limit of the 4.75mm sieve, and so on consecutively. These inputs respond to the observed pattern in the mixture. The inputs for these variables can be observed in Figure 30.

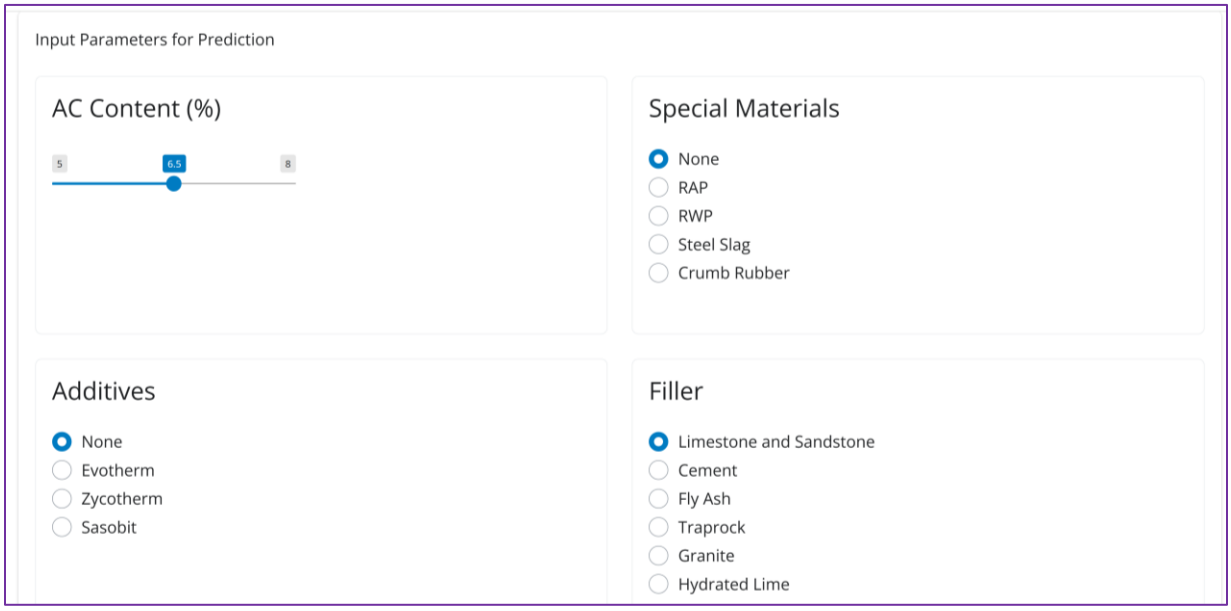

Figure 29. GUI Input Selection

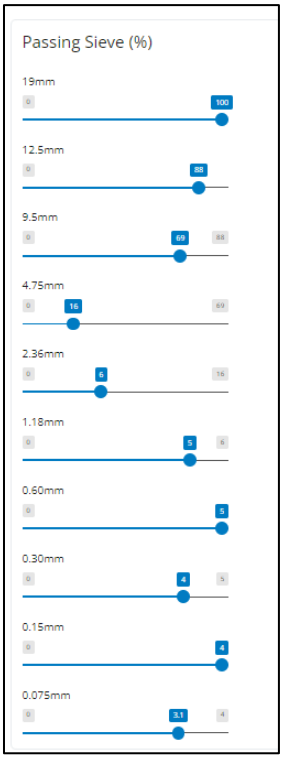

Figure 30. GUI Passing Sieve Inputs

After specifying the desired input values, a user must click the "Predict" button to generate performance values from the ANN model; as shown in Figure 31. The predictions are generated for the five metrics of interest, with three percentiles for each: the median, the lower, and the upper bound of the 95% variation interval. A comparison with specified acceptance criteria is carried out, and values within the specifications are shown with a green text color, while values out of specification are shown in red. The user may then modify the selected design input criteria to address any predicted failure in performance. This tool allows the designer to preliminarily predict the mix performance without the need for extensive laboratory testing, resulting in significant savings in time and money.

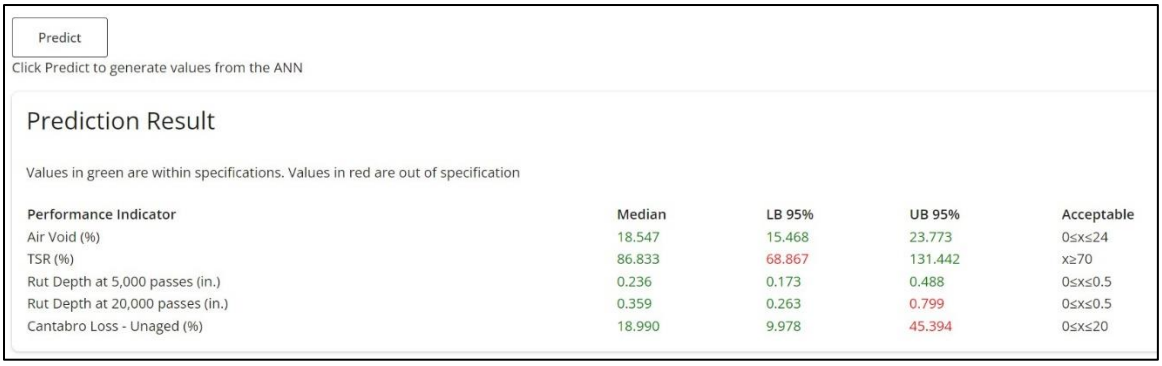

Figure 31. GUI Prediction Button and Results

The developed tool was structured as a standalone Windows program with a standalone launcher executable file. This program runs all the Python code in a self-contained package to deploy a local web server (not accessible from outside of the local machine) and generate the web application. The web application is accessible in the local host IP of the computer in use, and a hyperlink titled "OGFC Tool" is provided for convenience. To execute the program, then, a user needs to click once on "controller.exe," wait until the message displayed shows that the deployment was successful, and then click on "OGFC Tool" to access the ANN with any web browser. The tool has been successfully tested and executed using Google Chrome on different machines.

Chapter 5. Conclusion and Recommendations

This study was conducted with the aim of developing a next-generation OGFC mix that enhances durability, incorporates materials like SS, RWP, and RAP, and offers a cost-effective solution. Based on the results presented in this study, the following conclusions may be drawn.

Laboratory Performance of Modified OGFC Mixes

Based on the results of the experimental program, the following conclusions may be drawn:

- The incorporation of HiMA, RAP, and HL significantly improved the raveling resistance of OGFC mixes compared to the control mix. These modifications are expected to result in enhanced durability and surface wear resistance.
- All evaluated OGFC mixes met the maximum allowable permanent deformation requirement at 5,000 passes, including the CM. In addition, all the mixes met at 20,000 passes except the RAP and control mix.
- IDEAL-CT test results showed that the mixes incorporating SS, RWP, RAP, HiMA, and hydrated lime exhibited significantly higher CT indices compared to the CM, suggesting improved resistance to cracking. Among the tested mixes, the HL-modified and HiMA-modified OGFC mixes achieved the highest CT index of 450 and 395, indicating superior resistance to cracking.
- Results of the modified Lottman test indicated that all the OGFC mixes exhibited acceptable moisture damage resistance. Notably, the mixes modified with RAP, SS, RWP, HiMA, and HL showed significant improvements in moisture damage resistance compared to the CM.
- The cost-effectiveness analysis revealed that all proposed modifications to the OGFC mixtures demonstrated significantly higher cost-effectiveness in comparison with CM. In addition, the mixes with RAP and highly-modified asphalt binder were the most cost-effective.

Bio-Remediation and Microbial Degradation Mechanisms

To evaluate the retention of environmental contaminants and microbes within OGFC samples, a modular trickling-flow showerhead reactor was constructed to enable the exposure of asphalt samples to contaminants at varying concentrations and flowrates. Based on the results of the analysis, the following conclusions may be drawn:

- OGFC exhibits a high capacity to host biofilms, which can be leveraged for bioremediation applications. This is primarily due to the large pore spaces present in the sample when compared to traditional asphalt. These pore spaces are irregular in shape and size, thereby presenting an opportunity for the formation and growth of smaller, independent biofilm colonies as well as larger networks throughout the material.
- OGFC demonstrates excellent effectiveness in hydrocarbon degradation, such as motor oil. In contrast, the much tighter pore structure of dense-graded asphalt prevents oil from penetrating the surface of the sample. As a result, motor oil on dense-graded asphalt is likely to drain into water streams, leading to water runoff contamination.

AI-Based Design Tool

While numerous research studies were successful in addressing the durability of OGFC, highway agencies are still considering these modifications on a case-by-case basis. This study aimed to address this issue by developing an AI-based tool that may be used by mix designers and contractors to predict the performance of OGFC mixtures without the need to conduct extensive laboratory testing. Based on the results of this analysis, the following conclusions may be drawn:

- The artificial neural networks model was successfully trained and validated based on Quantile Multilayer Perceptron (Q-MLP) method. The accuracy of the model was validated based on four statistics metrics with a predicted average percentage error of 10.83%.
- A Windows-based interface tool was successfully developed to allow mix designer and contractors to use the ANN model and to interact with the underlying code and models to conduct an ANN-assisted design process.
- In the developed computer tool, after specifying the desired input values, a user can predict the performance of the mix without the need for extensive laboratory testing. The predictions are generated for the five metrics of interest, with three percentiles for each: the median, the lower, and the upper bound of the 95% variation interval.

Chapter 6. Implementation of Project Outputs

The following impacts and benefits are anticipated from the implementation of the study outputs.

Enhanced Durability of OGFC Mixes and Extended Service Life

The proposed modifications to OGFC mixtures significantly enhance their performance and durability, ensuring better resistance to raveling, cracking, and deformation while maintaining the functional properties of the mix, such as permeability and drainage capacity. Furthermore, the modified OGFC mixes demonstrated superior cost-effectiveness compared to conventional mixes, offering a more optimal and economically viable solution for road construction and maintenance. These improvements collectively contribute to extending the service life of pavements, reducing the frequency and costs associated with repairs and rehabilitation.

Reduction in Disposal and Environmental Impact of Waste Materials

The incorporation of recycled waste materials, such as plastic waste, steel slag, and RAP, into OGFC mixtures exhibited excellent laboratory performance, meeting key engineering criteria. Recycling and reusing these materials not only mitigate waste disposal challenges but also significantly reduce the adverse impact of road construction by diverting waste from landfills and decreasing the demand for virgin materials. This approach aligns with optimal construction practices, offering a dual benefit of preservation and resource conservation.

Biodegradation of Contaminants and Conditions Protection

This study confirmed OGFC's exceptional capacity to support biofilms, enabling its potential application in bioremediation. OGFC's open pore structure facilitates the degradation of hydrocarbons, such as motor oil, reducing contamination risks. In contrast, dense-graded asphalt's tight pore structure prevents oil penetration, increasing the likelihood of hydrocarbon runoff entering water streams and contaminating water supplies. Leveraging OGFC for biodegradation can significantly improve stormwater quality, making it a viable option for conscious road construction.

AI-Assisted Design and Predictive Analysis

The development of an AI-based predictive tool allows engineers to estimate the performance of OGFC mixes, such as their durability and drainage properties, using minimal input variables. This tool minimizes the need for extensive laboratory testing in the initial design phase, saving considerable time and financial resources. By simplifying the mix design process, this AI-driven approach empowers engineers, particularly in small communities, to make informed, data-supported decisions regarding pavement construction and maintenance. The tool is available as an executable file ready for use by any DOTs or researchers.

Chapter 7. Technology Transfer and Community Engagement and Participation (CEP) Activities

The following technology transfer and community engagement, and participation activities are reported:

Conference presentations (asterisk indicates graduate students).

Azucena, J.C, S.M. Tanvir*, M.A. Elseifi, H. Liao, and N. Kumar*. (2025). Development of an Artificial Intelligence (AI)-Based Tool for the Design of Open-Graded Friction Course. Paper presented at the 104th Transportation Research Board (TRB) Annual Meeting, Washington, D.C.

Webinars

Elseifi, M.A. (2025). Performance Evaluation of OGFC Mixes with Waste Plastic, Reclaimed Asphalt Pavement, and Steel Slag. SPTC Webinar Series, January 15th, 2025.

Chapter 8. Invention Disclosures and Patents, Publications, Presentations, Reports, Project Website, and Social Media Listings

The following publications and presentation activities are reported.

Publications (asterisk indicates graduate students).

Tanvir*, S.M., M.A. Elseifi, and H. Liao. (2025). Enhancing Durability and Cost-Effectiveness of Open-Graded Friction Course Using Recycled Materials and Highly-Modified Binder. Paper submitted to the Journal of Road Materials and Pavement Design (RMPD), Under Review.

Tanvir*, S.M. (2024). Next Generation Permeable Pavement for Enhanced Durability and Functionality. MSc. Thesis, Louisiana State University, LSU Scholarly Depository.

Azucena, J.C., S.M. Tanvir*, M.A. Elseifi, H. Liao, and N. Kumar*. (2025). AI-Powered Design Framework for Open-Graded Friction Course (OGFC) Mixtures. Paper submitted to the International Journal of Pavement Engineering, Under Review.

Tanvir*, S.M., M.A. Elseifi, H. Liao, K.S.S. Christie, J.C. Azucena, and N. Kumar*. (2025). Advancing Durability, Affordability, and Environmental Performance of Open-Graded Friction Course Using Waste Materials. Paper to be submitted to the Association of Asphalt Paving Technologists (AAPT), In Preparation.

References

Abohamer, H., Elseifi, M. A., Mayeux, C., Cooper, S. B., III, and Cooper, S. (2022). "Laboratory evaluation of warm-mix asphalt open graded friction courses." *Transportation Research Record: Journal of the Transportation Research Board*, 2676(10), Washington, D.C.,https://doi.org/10.1177/03611981221090239.

Abohamer, H., Elseifi, M. A., Mayeux, C., Cooper, S. B., III, and Cooper, S. (2023). "Effects of air void content, crumb rubber, and pozzolanic fillers on OGFC laboratory performance." *Transportation Research Record: Journal of the Transportation Research Board*, Washington, D.C., https://doi.org/10.1177/03611981231165756.

Abohamer, H., Elseifi, M. A., Mayeux, C., Cooper, S. B., III, and Cooper, S. (2023). "Investigating the seepage characteristics of open graded friction course using finite element modeling." *Transportation Research Record: Journal of the Transportation Research Board*, Washington, D.C., https://doi.org/10.1177/03611981231168103.

Abdullah, W. S., Obaidat, M. T., and Abu-Sa'da, N. M. (1998). "Influence of aggregate type and gradation on voids of asphalt concrete pavements." *Journal of Materials in Civil Engineering*, 10(2), 76-85.

Ahmedzade, P., and Sengoz, B. (2009). "Evaluation of steel slag coarse aggregate in hot mix asphalt concrete." *Journal of Hazardous Materials*, 165(1), 300-305.

Airey, G. D., Collop, A. C., and Thom, N. H. (2004). "Mechanical performance of asphalt mixtures incorporating slag and glass secondary aggregates." *Proceedings of the 8th Conference on Asphalt Pavements for Southern Africa (CAPSA'04)*, South Africa.

Al-Busaltan, Shakir, Al-Yasari, Rand, Aljawad, Ola, and Saghafi, B. (2020). "Durability assessment of open-graded friction course using a sustainable polymer." International Journal of Pavement Research and Technology, 13(6), 645-653. https://doi.org/10.1007/s42947-020-6013-6.

Aljbouri, H., and Albayati, A. (2024). "The effect of nano-hydrated lime on the durability of hot mix asphalt." *Journal of Engineering*, 30, 143-158.

Al-Shabani, Z., and Obaid, I. (2023). "Investigate the effect of using reclaimed asphalt pavement (RAP) and polymer-modified bitumen on the moisture damage of hot mix asphalt*." E3S Web of Conferences*, 427, 03019.

American Association of State Highway and Transportation Officials. (2014). *Standard method of test for determining the draindown characteristics in uncompacted asphalt mixtures* (AASHTO T305). Washington, D.C.: AASHTO

American Association of State Highway and Transportation Officials. (2021). *Standard method of test for abrasion loss of asphalt mixture specimens* (AASHTO TP 108-14). Washington, D.C.: AASHTO

American Association of State Highway and Transportation Officials. (2019). *Hamburg wheel-track testing of compacted hot mix asphalt (HMA)* (AASHTO T 324). Washington, D.C.: AASHTO

American Association of State Highway and Transportation Officials. (2014). *Standard method of test for resistance of compacted asphalt mixtures to moisture-induced damage* (AASHTO T 283). Washington, D.C.: AASHTO.

Anderson, K. W., Uhlmeyer, J. S., Sexton, T., Russell, M., & Weston, J. (2012). Evaluation of long-term pavement performance and noise characteristics of open-graded friction courses (WA-RD 683.2). Washington State Department of Transportation, Materials Laboratory. https://www.wsdot.wa.gov/research/reports/fullreports/683.2.pdf.

Ansel, J., Yang, E., He, H., Gimelshein, N., Jain, A., Voznesensky, M., ... & Chintala, S. (2024). PyTorch 2: Faster machine learning through dynamic Python bytecode transformation and graph compilation. In Proceedings of the 29th ACM International Conference on Architectural Support for Programming Languages and Operating Systems (Vol. 2, pp. 929–947).

Anusha, T., Huskur, J., and Sunil, S. (2019). "Experimental investigation of open graded mixes using reclaimed asphalt pavement*." IOP Conference Series: Materials Science and Engineering*, 561. https://doi.org/10.1088/1757-899X/561/1/012025

Aschenbrener, T. (1995). "Evaluation of Hamburg wheel-tracking device to predict moisture damage in hot-mix asphalt." *Transportation Research Record*, (1492), 193-201

Asi, I. M., Qasrawi, H. Y., and Shalabi, F. I. (2007). "Use of steel slag aggregate in asphalt concrete mixes." *Canadian Journal of Civil Engineering*, 34(8), 902-911.

ASTM International. (2018). *Standard test method for bulk specific gravity and density of compacted asphalt mixtures using automatic vacuum sealing method* (ASTM D6752/D6752M-18). https://www.astm.org/d6752_d6752m-18.html

ASTM International. (2019). *Standard test method for theoretical maximum specific gravity and density of asphalt mixtures* (ASTM D2041/D2041M-19). https://doi.org/10.1520/D2041_D2041M-19

ASTM International. (2019). *Standard test method for theoretical maximum specific gravity and density of asphalt mixtures (*ASTM D2041-03a). https://www.astm.org/d2041-03a.html

ASTM International. (2021). *Standard practice for open-graded friction course* (ASTM D7064). https://www.astm.org/d7064_d7064m-21.html

ASTM International. (2019). *Standard test method for determination of cracking tolerance index of asphalt mixture using the indirect tensile cracking test* (ASTM D8225-19). https://www.astm.org/d8225-19.html

ASTM International. (2022). *Standard test method for pull-off strength of coatings using portable adhesion testers* (ASTM D4541-22). https://www.astm.org/d4541-22.html

Bernhard, R., Wayson, R. L., Haddock, J., Neithalath, N., El-Aassar, A., Olek, J., and Weiss, W. J. (2005). "An introduction to tire/pavement noise of asphalt pavement." *Institute of Safe, Quiet and Durable Highways*, Purdue University, 26.

Bharagava, R. N. (Ed.). (2022). *Bioremediation: Green approaches for a clean and sustainable environment* (First edition). CRC Press. https://doi.org/10.1201/9781003181224

Blazejowski, K., Ostrowski, P., Baranowska, W., and Wójcik-Wiśniewska, M. (2021). "Compactibility of asphalt mixtures with highly polymer modified bitumen (HiMA)." *Proceedings of the 7th E&E Congress—Eurasphalt & Eurobitume*, ORLEN Asfalt, Poland.

California Department of Transportation. (2020). Open graded friction course design guidance. https://dot.ca.gov/programs/design/hydraulics-stormwater/treatment-bmp-design guidance.

Campbell, N. A., & Reece, J. B. (2020). *Biology* (Twelfth edition). Pearson.

Cao, J., Sanganyado, E., Liu, W., Zhang, W., & Liu, Y. (2019). Decolorization and detoxification of Direct Blue 2B by indigenous bacterial consortium. *Journal of Environmental Management*, *242*, 229–237. https://doi.org/10.1016/j.jenvman.2019.04.067

Chen, X., Zhu, H., Dong, Q., and Huang, B. (2017). "Case study: Performance effectiveness and cost benefit analyses of open-graded friction course pavements in Tennessee." *International Journal of Pavement Engineering.*

Chen, J., Tang, T., and Zhang, Y. (2017). "Laboratory characterization of directional dependence of permeability for porous asphalt mixtures." *Materials and Structures*, 50, 1–11.

Chung, Y., Neiswanger, W., Char, I., & Schneider, J. (2021). Beyond pinball loss: Quantile methods for calibrated uncertainty quantification. *Advances in Neural Information Processing Systems*, 34, 10971–10984.

Coomarasamy, A., and Walzak, T. (1995). "Effects of moisture on surface chemistry of steel slags and steel slag-asphalt paving mixes." *Transportation Research Record*, (1492).

Copeland, A. (2011). *Reclaimed asphalt pavement in asphalt mixtures: State of the practice* (Report No. FHWA-HRT-11-021). Office of Infrastructure Research and Development, Federal Highway Administration.

Cortesi, D. (2024). PyInstaller manual - PyInstaller 6.9.0 documentation. https://pyinstaller.org/

Crisman, B., Ossich, G., Bevilacqua, P., and Roberti, R. (2019). "Degradation prediction model for friction of road pavements with natural aggregates and steel slags." *Applied Sciences*, 10(1), 32. https://doi.org/10.3390/app10010032

D. Watson, N. H. Tran, C. Rodezno, A. J. Taylor and T. M. James, "Performance-Based Mix Design of Porous Friction Courses," *National Academy of Sciences, Transportation Research Board*, NCHRP Report 877, Project 01-55, 2018.

Dell'Acqua, G., De Luca, M., and Lamberti, R. (2011). "Indirect skid resistance measurement for porous asphalt pavement management." *Transportation Research Record*, 2205(1), 147 154.

Donavan, P. R., and Crocker, M. (2007). *Handbook of noise and vibration control*. M. Crocker, Ed., John Wiley and Sons.

Eck, B., Klenzendorf, B., Charbeneau, R., and Barrett, M. (2010). "Permeable friction course for sustainable highways." Proc., *2010 International Low Impact Development Conference: Redefining Water in the City*, 389, 201-212. https://doi.org/10.1061/41148(389)17.

Elnaml, I., Liu, J., Mohammad, L., Cooper, S., and Cooper, S. Jr. (2023). "Developing sustainable asphalt mixtures using high-density polyethylene plastic waste material." *Sustainability*, 15(13). https://doi.org/10.3390/su15139897.

Elnaml, I., Mohammad, L. N., Baumgardner, G., Cooper, S. III, & Cooper, S. Jr. (2024). Sustainability of asphalt mixtures containing 50% RAP and recycling agents. *Recycling*, 9(5), 85. https://doi.org/10.3390/recycling9050085

Elseifi, M. A., & Elbagalati, O. (2017). Assessment of continuous deflection measurement devices in Louisiana-rolling wheel deflectometer (Final Report No. FHWA/LA. 17/581). Louisiana Transportation Research Center.

Fay, L., and Akin, M. (2014). "Snow and ice control on porous and permeable pavements: Literature review and state of the practice." *Transportation Research Board 93rd Annual Meeting, Transportation Research Board*, Paper No. 14-2839.

FHWA. (1990). "Technical Advisory T 5040.31 Open Graded Friction Courses." Federal Highway Administration. Available at: https://www.fhwa.dot.gov/pavement/t504031.cfm [Accessed Aug. 19, 2024].

FHWA. (2011). "Reclaimed asphalt pavement in asphalt mixtures: State of the practice." Publication No. FHWA-RD-97-148, U.S. Department of Transportation. Available at: https://www.fhwa.dot.gov/publications/research/infrastructure/pavements/97148/046.cf [Accessed Aug. 19, 2024].

FHWA. (2016). "User guidelines for waste and byproduct materials in pavement construction." Publication No. FHWA-RD-97-148, Federal Highway Administration Research and Technology.

Florida Department of Transportation. (2015). *Florida method of test for measurement of water permeability of compacted asphalt paving mixtures* (FM 5-565). State Materials Office.

Gan, C., Liu, Y., Tan, X., Wang, S., Zeng, G., Zheng, B., Li, T., Jiang, Z., & Liu, W. (2015). Effect of porous zinc–biochar nanocomposites on Cr(vi) adsorption from aqueous solution. *RSC Advances*, *5*(44), 35107–35115. https://doi.org/10.1039/C5RA04416B

Genet, M. B., Sendekie, Z. B., and Jembere, A. L. (2021). "Investigation and optimization of waste LDPE plastic as a modifier of asphalt mix for highway asphalt: Case of Ethiopian roads." *Case Studies in Chemical and Environmental Engineering*, 4, 100150.

Gilliland, A., Mohanraj, K., & Taghavi Ghalesari, A. (2022). *Open-graded friction course: How to document* (Report No. FHWA-HIF-23-015). Federal Highway Administration.

Gong, H., Sun, Y., Dong, Y., Han, B., Polaczyk, P., Hu, W., & Huang, B. (2020). Improved estimation of dynamic modulus for hot mix asphalt using deep learning. *Construction and Building Materials*, 263, 119912.

Gu, F., Zhang, W., Li, H., and Wang, C. (2018). "Evaluation of the benefits of open graded friction course: Case study." *Construction and Building Materials*, 189, 131-143.

Habbouche, J., Hajj, E., and Sebaaly, P. (2019). *Structural coefficient of high polymer modified asphalt mixes*. Report No. WRSC-UNR-FDOT-BE321-DEL6.

Habbouche, J., Boz, I., Diefenderfer, S., & Bilgic, Y. (2021). Round robin testing program for the indirect tensile cracking test at intermediate temperature: Phase I. *International Journal of Pavement Engineering.* https://doi.org/10.1080/10298436.2021.1894982

Hajj, E. Y., Sebaaly, P. E., and Shrestha, R. (2009). "Laboratory evaluation of mixes containing recycled asphalt pavement (RAP)." *Road Materials and Pavement Design*, 10(3), 495-517.http://dx.doi.org/10.1080/14680629.2009.9690211

Hassan, K., Attia, M., Reid, M., and Al-Kuwari, M. (2021). "Performance of steel slag aggregate in asphalt mixtures in a hot desert climate." *Case Studies in Construction Materials*, 14, e00534. https://doi.org/10.1016/j.cscm.2021.e00534

Hasan, M., Rosli, M., Eng, J., Hamzah, M., and Voskuilen, J.L.M. (2013). "The effects of break point location and nominal maximum aggregate size on porous asphalt properties." *Construction and Building Materials*, 44, 360–367. https://doi.org/10.1016/j.conbuildmat.2013.02.053

Hassani, A., Ganjidoust, H., and Maghanaki, A.A. (2005). "Use of plastic waste (polyethylene terephthalate) in asphalt concrete mixture as aggregate replacement." *Waste Management & Research*, 23(4), 322–327.

Hemond, H. F., & Fechner, E. J. (2015). Chapter 3—The Subsurface Environment. In H. F. Hemond & E. J. Fechner (Eds.), *Chemical Fate and Transport in the Environment (Third Edition)* (pp. 219–310). Academic Press. https://doi.org/10.1016/B978-0-12-398256-8.00003-7

Heydari, S., Hajimohammadi, A., Javadi, N., and Khalili, N. (2021). "The use of plastic waste in asphalt: A critical review on asphalt mix design and Marshall properties." *Construction and Building Materials,* 309, 125185. https://doi.org/10.1016/j.conbuildmat.2021.125185

Jayakaran, A., Knappenberger, T., Stark, J., & Hinman, C. (2019). Remediation of Stormwater Pollutants by Porous Asphalt Pavement. *Water*, *11*(3), 520. https://doi.org/10.3390/w11030520

Kabir, M.S. (2008). "Effect of hydrated lime on the laboratory performance of Superpave mixtures." M.S. thesis, Department of Civil and Environmental Engineering, Louisiana State University and Agricultural and Mechanical College.

Kandahl, P.S., and G.L. Hoffman. (1982). "The use of steel slag as bituminous concrete fine aggregate." Pennsylvania Department of Transportation, Materials Evaluations Group.

Kar, D., Panda, M., and Jena, S. (2024). "Utilization of Waste Polyethylene in Open Graded Friction Course." *Proceedings of the International Conference on Transportation Planning and Implementation Methodologies for Developing Countries*, pp. 121-132. doi:10.1007/978-981-99-6090-3_11.

Khoury, I., Sargand, S., Green, R., Jordan, B., and Cichocki, P. (2016). "Rutting Resistance of Asphalt Mixes Containing Highly Modified Asphalt (HiMA) Binders at the Accelerated Pavement Load Facility in Ohio." *Proceedings of the Transportation Research Board*, pp. 28. Springer. https://doi.org/10.1007/978-3-319-42797-3_28.

Kim, M., Burton, Y. M., Prozzi, J. A., & Murphy, M. (2014). Maintenance and rehabilitation project selection using artificial neural networks. Transportation Research Board 93rd Annual Meeting (No. 14-3620).

King, W., Kabir, S., Cooper, S. B., and Abadie, C. (2013). *Evaluation of open graded friction course (OGFC) mixtures* (No. FHWA/LA. 13/513). Louisiana Dept. of Transportation and Development.

Kneller, W. A., Tew, A., and C. D. (1994). "Determination of original free lime content of weathered iron and steel slags by thermogravimetric analysis." *Transportation Research Record*, (1434), 1-9.

Kwon, O., Choubane, B., Greene, J., and Sholar, G. (2018). "Evaluation of the performance of high-SBS modified asphalt binder through accelerated pavement testing." *Research Report FL/DOT/SMO/18-588*. Florida Department of Transportation.

Lawrence, S., Giles, C. L., & Tsoi, A. C. (1997). Lessons in neural network training: Overfitting may be harder than expected. In AAAI/IAAI Proceedings (pp. 540–545).

Lesueur, D., Petit, J., and Ritter, H.-J. (2012). "The mechanisms of hydrated lime modification of asphalt mixtures: A state-of-the-art review." Road Materials and Pavement Design, 14, 1 16.

Liu, J., Liu, F., Zheng, C., Zhou, D., & Wang, L. (2022). Optimizing asphalt mix design through predicting effective asphalt content and absorbed asphalt content using machine learning. *Construction and Building Materials*, 325, 126607.

Louisiana Department of Transportation and Development. (2016). *Louisiana standard specifications for roads and bridges*. Baton Rouge, LA.

Majidifard, H., Jahangiri, B., Buttlar, W. G., & Alavi, A. H. (2019). New machine learning-based prediction models for fracture energy of asphalt mixtures. Measurement, 135, 438–451

Mansour, E., Dhasmana, H., Mousa, M. R., & Hassan, M. (2024). Machine learning-based technology for asphalt concrete pavement performance decision-making in hot and humid climates. *Construction and Building Materials*, 442, 137625. https://doi.org/10.1016/j.conbuildmat.2024.137625

Mazouz, M., and M'Hammed, M. (2019). "The effect of low-density polyethylene addition and temperature on creep-recovery behavior of hot mix asphalt." *Civil Engineering Journal*, 5, 597.

Metcalf & Eddy, Tchobanoglous, G., Stensel, H. D., Tsuchihashi, R., Burton, F. L., Abu-Orf, M., Bowden, G., & Pfrang, W. (2014). *Wastewater Engineering: Treatment and Resource Recovery* (5). McGraw-Hill Education; WorldCat.org. http://catdir.loc.gov/catdir/enhancements/fy1501/2014415848-t.html

Mensching, D., Sias, J., Bennert, T., Medeiros, M., Elwardany, M., Mogawer, W., Hajj, E., and Alavi, Z. (2014). "Low temperature properties of plant-produced RAP mixtures in the Northeast." *Road Materials and Pavement Design*, 15, 10.1080/14680629.2014.926617.

Mishra, A., & Malik, A. (2014). Novel fungal consortium for bioremediation of metals and dyes from mixed waste stream. *Bioresource Technology*, *171*, 217–226. https://doi.org/10.1016/j.biortech.2014.08.047

Mitchell, T. (2000), WesTrack Track Roughness, Fuel Consumption, and Maintenance Costs, Fed. Highw. Adm. Tech. Br. RD-00-052

Mogawer, W. S. (2019, March 19). *Balanced mix design (BMD) for asphalt mixtures*. 62nd Annual New Jersey Asphalt Paving Conference. University of Massachusetts Dartmouth. https://www.umassd.edu/hsrc

Mohammad, Louay N., Altinsoy, Rana (2002). Evaluation of the Fundamental Engineering Properties of Bituminous Mixtures containing Hydrated Lime. Louisiana Transportation Research Center.

Motz, H. and J. Geiseler (2001), Products of steel slags an opportunity to save natural resources. *Waste management*, 21(3): p. 285-293.

Nicholls, J. (1999), *Review of UK porous asphalt trials*. Vol. 264. 1999: Thomas Telford

Ozturk, H. I., & Kutay, M. E. (2014). An artificial neural network model for virtual Superpave asphalt mixture design. *International Journal of Pavement Engineering*, 15, 151–162

Pattanaik, M., Choudhary, R., Kumar, B., & Kumar, A. (2019). Mechanical properties of open graded friction course mixtures with different contents of electric arc furnace steel slag as

an alternative aggregate from steel industries. *Road Materials and Pavement Design*, 125. https://doi.org/10.1080/14680629.2019.1620120

Pathak, S., Choudhary, R., Kumar, A., & Shukla, S. (2020). Evaluation of benefits of open-graded friction courses with basic oxygen furnace steel-slag aggregates for hilly and high-rainfall regions in India. *Journal of Materials in Civil Engineering*, 32(6), 04020356:1-14. https://doi.org/10.1061/(ASCE)MT.1943-5533.0003445

Plati, C., Georgiou, P., & Papavasiliou, V. (2015). Simulating pavement structural condition using artificial neural networks. Structure and Infrastructure Engineering, 1–10.

Posit. (2024). *Shiny for Python*. https://shiny.posit.co/py/

Preti, F., Accardo, C., Gouveia, B., Romeo, E., & Tebaldi, G. (2020). Influence of high-surface area hydrated lime on cracking performance of open-graded asphalt mixtures. *Road Materials and Pavement Design*, 22(1), 1-7. https://doi.org/10.1080/14680629.2020.1808522

Punith, V., Subbarao, S., Raju, S., Bose, S., & Amirthalingam, V. (2011). Laboratory investigation of open-graded friction-course mixtures containing polymers and cellulose fibers. *Journal of Transportation Engineering,* 138(1), 67-74. https://doi.org/10.1061/(ASCE)TE.1943 5436.0000304

Radeef, H., Hassan, N., Razin, A., Zainal Abidin, A. R., Zul, M., Mahmud, M. Z. H., Md Yusoff, N. I., Yusoffa, M., Khairul, M., Satar, I., Naqiuddin, M., & M. Warid, M. N. (2021). Enhanced dry process method for modified asphalt containing plastic waste. *Frontiers in Materials*, 8, 247. https://doi.org/10.3389/fmats.2021.700231

Rahman, W. M. N. W. A., & Wahab, A. F. A. (2013). Green pavement using recycled polyethylene terephthalate (PET) as partial fine aggregate replacement in modified asphalt. *Procedia Engineering,* 53, 124-128.

Rahman, S., Bhasin, A., & Smit, A. (2021). Exploring the use of machine learning to predict metrics related to asphalt mixture performance. *Construction and Building Materials,* 295, 123585.

Rand, D. (2004). Permeable friction courses TxDOT experiences. *In Proceedings of the Southeastern Asphalt User/Producer Group (SEAUPG),* Arkadelphia.

Raza, M. S., & Sharma, S. K. (2024). Optimizing porous asphalt mix design for permeability and air voids using response surface methodology and artificial neural networks. *Construction and Building Materials*, 442, 137513. https://doi.org/10.1016/j.conbuildmat.2024.137513

Rungruangvirojn, P. and K. Kanitpong (2010), Measurement of visibility loss due to splash and spray: porous, SMA and conventional asphalt pavements*. International Journal of Pavement Engineering,* 11(6): p. 499-510.

Sepehri, A., Sarrafzadeh, M.-H., & Avateffazeli, M. (2020). Interaction between *Chlorella vulgaris* and nitrifying-enriched activated sludge in the treatment of wastewater with low C/N ratio.

Journal of Cleaner Production, *247*, 119164. https://doi.org/10.1016/j.jclepro.2019.119164

Shimeno, S., A. Oi, and T. Tanaka (2010). Evaluation and further development of porous asphalt pavement with 10 years experience in Japanese expressways. *in Proceedings of the 11th International Conference on Asphalt Pavements*, Nagoya.

Song, Weimin & Shu, Xiang & Huang, Baoshan & Woods, Mark. (2015). "Factors affecting shear strength between open-graded friction course and underlying layer". *Construction and Building Materials.* 101. 527-535. 10.1016/j.conbuildmat.2015.10.036.

Takahashi, S. (2013), "Comprehensive study on the porous asphalt effects on expressways in Japan: Based on field data analysis in the last decade". *Road Materials and Pavement Design*, 14(2): p. 239-255.

You, Zhanping & Mills-Beale, Julian & Fini, Elham & Goh, Shu Wei & Colbert, Baron. (2011). "Evaluation of Low-Temperature Binder Properties of Warm-Mix Asphalt, Extracted and Recovered RAP and RAS, and Bioasphalt". *Journal of materials in Civil Engineering*. 23. 1569-1 574. 10.1061/(ASCE)MT.1943-5533.0000295.

Van der Zwan, J. (2011), "Developing porous asphalt for freeways in the Netherlands: Reducing noise, improving safety, increasing service life". *TR News*, (272).

Vargas-Nordcbeck, A., & Musselman, J. A. (2021). *Highly modified asphalt Florida case study* (Report No. FHWA-HIF-22-044). The National Center for Asphalt Technology. https://rosap.ntl.bts.gov/view/dot/61114

Volcovici, V. (2022), How is the growing plastic waste problem impacting America?, in *World Economic Forum.*

Walker, T.R. (2017), China's ban could curb plastic waste. *Nature*, 551: p. 427-431.

Wu, H., Yu, J., Song, W., Zou, J., Song, Q., & Zhou, L. (2020). "A critical state-of-the-art review of durability and functionality of open-graded friction course mixtures". *Construction and Building Materials*, 237, 117759. https://doi.org/10.1016/j.conbuildmat.2019.117759

Xie, Zhaoxing & Tran, Nam & Watson, Donald & Blackburn, Lyndi. (2019). "Five-Year Performance of Improved Open-Graded Friction Course on the NCAT Pavement Test Track". *Transportation Research Record: Journal of the Transportation Research Board*. 2673. 036119811982757. 10.1177/0361198119827577.

Yildirim, I. Z., and Prezzi, M. (2011). "Chemical, Mineralogical, and Morphological Properties of Steel Slag." *Advances in Civil Engineering*, 2011, 1-13. https://doi.org/10.1155/2011/463638

Zhang, Y., and Leng, Z. (2017). "Quantification of Bituminous Mortar Ageing and Its Application in Ravelling Evaluation of Porous Asphalt Wearing Courses." *Materials & Design*, 119, 1-11.

Zhang, Jiawei & Huang, Weidong & Hao, Gengren & Yan, Chuanqi & Lv, Quan & Cai, Qi. (2020). “Evaluation of open-grade friction course (OGFC) mixtures with high content SBS polymer modified asphalt”. *Construction and Building Materials.* 270. 121374. 10.1016/j.conbuildmat.2020.121374.

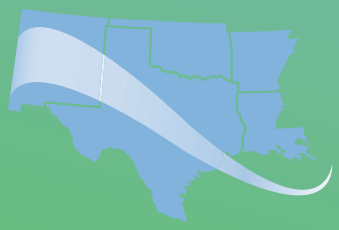

SOUTHERN PLAINS
TRANSPORTATION CENTER

The University of Oklahoma | OU Gallogly College of Engineering
202 W Boyd St, Room 213A, Norman, OK 73019 | (405) 325-4682 | Email: sptc@ou.edu